Max-Planck-Institut
für Meteorologie

MAX-PLANCK-GESELLSCHAFT

International Max Planck Research School
on Earth System Modelling

A stochastic parameterization of shallow cumulus convection for high-resolution numerical weather prediction and climate models

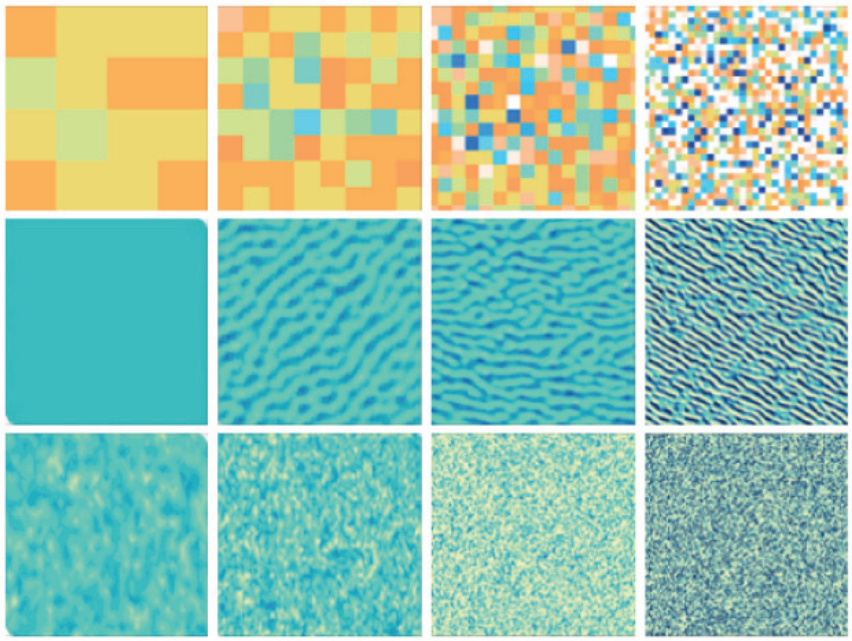

Mirjana Sakradžija

Hamburg 2015

Berichte zur Erdsystemforschung
Reports on Earth System Science

171
2015

Hinweis

Die Berichte zur Erdsystemforschung werden vom Max-Planck-Institut für Meteorologie in Hamburg in unregelmäßiger Abfolge herausgegeben.

Sie enthalten wissenschaftliche und technische Beiträge, inklusive Dissertationen.

Die Beiträge geben nicht notwendigerweise die Auffassung des Instituts wieder.

Die "Berichte zur Erdsystemforschung" führen die vorherigen Reihen "Reports" und "Examensarbeiten" weiter.

Notice

The Reports on Earth System Science are published by the Max Planck Institute for Meteorology in Hamburg. They appear in irregular intervals.

They contain scientific and technical contributions, including Ph. D. theses.

The Reports do not necessarily reflect the opinion of the Institute.

The "Reports on Earth System Science" continue the former "Reports" and "Examensarbeiten" of the Max Planck Institute.

Anschrift / Address

Max-Planck-Institut für Meteorologie
Bundesstrasse 53
20146 Hamburg
Deutschland

Tel./Phone: +49 (0)40 4 11 73 - 0
Fax: +49 (0)40 4 11 73 - 298

name.surname@mpimet.mpg.de
www.mpimet.mpg.de

Layout

Bettina Diallo and Norbert P. Noreiks
Communication

Copyright

A stochastic parameterization of shallow cumulus convection for high-resolution numerical weather prediction and climate models

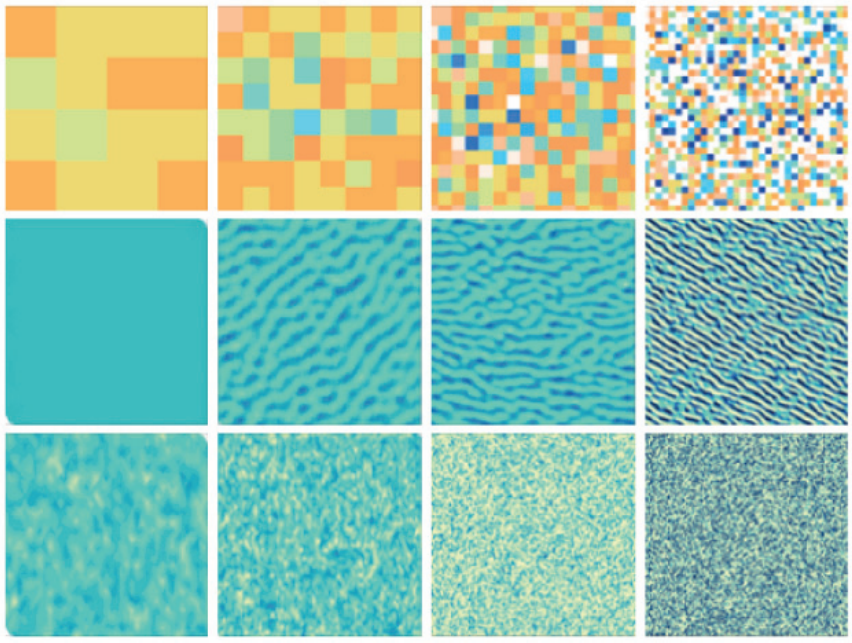

Mirjana Sakradžija

Hamburg 2015

Mirjana Sakradžija

Max-Planck-Institut für Meteorologie
Bundesstrasse 53
20146 Hamburg

Als Dissertation angenommen
vom Fachbereich Geowissenschaften der Universität Hamburg

auf Grund der Gutachten von
Prof. Dr. Valerio Lucarini
und
Dr. Axel Seifert

Hamburg, den 6.7.2015
Professor Dr. Christian Betzler
Leiter des Departments Geowissenschaften

Berichte zur Erdsystemforschung / Max-Planck-Institut für Meteorologie 171
Reports on Earth System Science / Max Planck Institute for Meteorology 2015

ISSN 1614-1199

Abstract

All conventional cloud parameterization schemes rely on a quasi-equilibrium assumption, which defines the relation between the subgrid cloud processes and the grid scale model flow. However, the quasi-equilibrium assumption is valid in a limited number of model applications on the relatively coarse model grids and in slowly varying convective environments.

In this thesis, a stochastic parametrization of shallow cumulus clouds is developed to simulate a shallow cumulus cloud field over the ocean across a range of model grid resolutions. A theory of fluctuations in a shallow convective ensemble is developed by combining the canonical ensemble theory applied to convection and large eddy simulations (LES) of the convective case over the ocean. The main purpose of this theory is to represent fluctuations of the convective states within model grid columns around the statistical equilibrium. Such a representation provides the distribution of all possible subgrid convective states for the given synoptic situation, instead of delivering an ensemble average response like in a conventional parameterization approach, and thus provides a way to quantify the uncertainty of subgrid convection in numerical models.

In a parametrization based on a mass flux approach, the upward transport of mass and other conserved quantities is controlled by the convective mass flux through the cloud base, which is the main variable to be defined by the model closure. Based on LES and findings from cloud tracking, we define the cloud mass flux distribution of a shallow convective cloud ensemble as a bimodal distribution, with the two modes separated by the buoyancy criterion. This distribution is a generalization of the exponential distribution to the Weibull distribution function by accounting for the change in the distribution shape due to diversity of cloud lifetimes.

First, a stochastic stand alone model is constructed based on the developed shallow convective ensemble framework. It is formulated as a compound random process, with a number of convective elements drawn from the Poisson distribution, and the cloud mass flux sampled from the mixed Weibull distribution. The convolution of these two functions results in a scale-aware compound distribution, with the variance and skewness increasing with resolution. The convective memory is accounted for through the diversity of cloud lifetimes, making the model formulation consistent with the choice of the Weibull cloud mass flux distribution function, which is required to capture the correct convective variability.

Second, the stochastic model is coupled to the eddy-diffusivity mass-flux parameterization scheme in the ICON model. The closure assumption that the cloud area fraction is much smaller than one is retained over the large-scale region around a model column, for which the statistical quasi-equilibrium is still valid under stationary conditions. The total convective mass flux within model grid columns represents the random cloud subensembles, whose spatial variability increases with resolution. The variability of the cloud subensembles combined with the stochastic cloud layer vertical structure improves the modeled average thermodynamic structure and evolution of the boundary layer over the ocean in the shallow cumulus cloud field.

On the model grids with resolution below approximately 10 km that falls into the convective gray zone, grid-scale dependent secondary circulations develop and influence the distribution of cloud field properties by increasing the variance and by increasing and reversing the distribution skewness. In the deterministic model simulations, the gray zone circulations are prone to develop into strongly organized cloud streets with artificial features, while the stochastic model is acting to break down the spurious convective organization.

Zusammenfassung

Konventionelle Wolkenparameterisierungen basieren auf der Annahme eines Quasi-Gleichgewichts, wobei eine direkte Beziehung zwischen subskaligen Wolkenprozessen und den aufgelösten Prozessen angenommen wird. Ein solches Gleichgewicht ist jedoch nur für eine begrenzte Zahl von Modellanwendungen, insbesondere für grobe Gitterauflösung und schwach veränderliche konvektive Prozesse, gültig.

In dieser Doktorarbeit wird eine stochastische Parametrisierung zur Simulation von flachen Cumuluswolken entwickelt und für Wolkenfelder über dem Ozean unter verschiedenen Auflösungen getestet. Eine Theorie für Fluktuationen in einem Ensemble mit flacher Konvektion wird entwickelt, indem die kanonische Ensembletheorie für Konvektion angewandt und mit Large Eddy Simulationen (LES) für den konvektiven Fall über dem Ozean kombiniert wird. Die Hauptaufgabe dieser Theorie ist es, konvektive Fluktuationen innerhalb einer Modellgitterzelle um das statistische Gleichgewicht darzustellen. Die neue Theorie nutzt eine Verteilung für alle realisierbaren subskaligen konvektiven Zustände bei einer bestimmten synoptischen Situation, anstelle des Ensemblemittels wie in konventionellen Parametrisierungsansätzen. Das neue Verfahren stellt damit ein Mittel zur Quantifizierung der Unsicherheiten von subskaliger Konvektion in numerischen Modellen zur Verfügung.

In einer Parametrisierung, die auf dem Massenflussansatz basiert, sind der vertikale Massentransport und andere Erhaltungsgrößen abhängig von dem konvektiven Massenfluss durch die Wolkenbasis, welches die wichtigste Variable ist, die von der Schließungsbedingung im Modell definiert wird. Basierend auf Erkenntnissen aus LES und Wolkenverfolgung definieren wir die Massenflussverteilung von einem Ensemble flacher konvektiver Wolken als eine bimodale Verteilung, wobei die beiden Moden anhand des Auftriebskriteriums unterschieden werden. Die Verteilungskurve ändert sich von einer Exponentialverteilung zu einer gemischten Weibull-Verteilung, weil die Diversität der Wolkenlebenszeit berücksichtigt wird.

In dem ersten Teil der Doktorarbeit wird ein eigenständiges stochastisches Modell konstruiert, das auf der Ensembletheorie für flache Konvektion basiert. Es ist formuliert als ein zusammengesetzter Zufallsprozess, wobei zum Einen die Anzahl der konvektiven Elemente aus einer Poisson-Verteilung bestimmt werden, und zum Anderen der Massenfluss in den Wolken aus einer gemischten Weibull-Verteilung entnommen wird. Die Überlagerung dieser beiden Funktionen ermöglicht eine skalenabhängige zusammengesetzte Verteilung, wobei Varianz und Schiefe bei besserer Auflösung ansteigen. Das konvektive Gedächtnis wird durch die Diversität der Wolkenlebenszeiten und durch explizite Wolkenlebenszyklen berücksichtigt, wodurch die Modellformulierung konsistent ist mit der Wahl der Weibullverteilung von konvektiven Massenflüssen. Dies ist nötig, um die korrekte konvektive Variabilität widerzugeben.

In dem zweiten Teil der Doktorarbeit wird das stochastische Modell mit einem Eddy-Diffusivity Mass-Flux (EDMF) Parametrisierungsschema kombiniert und im ICON Modell getestet. Die Schließungsannahme, dass der Bedeckungsgrat sehr klein ist, wird in dem großskaligen Gebiet

um eine Gitterbox, für die das statistische Quasi-Gleichgewicht noch unter stationären Bedingungen gültig ist, erfüllt. Der gesamte konvektive Massenfluss in den Modellsäulen repräsentiert einen quasi-zufälligen Teil des Wolkenensembles mit der räumlichen Variabilität, die bei besserer Auflösung zunimmt. Durch die Variabilität der Teilensembles in Kombination mit der stochastisch ermittelten vertikalen Struktur der Wolkenschichten wird die modellierte mittlere thermodynamische Struktur der Grenzschicht verbessert. Dies zeigt sich insbesondere für den Fall von flachen Cumuluswolken über dem Ozean.

Auf Modellgittern mit einer horizontalen Auflösung unter 10 km, auch konvektive Grauzone genannt, entwickeln sich von der Auflösung abhängige Sekundärzirkulationen, die die Verteilung der Wolkenfelder beeinflussen. Dadurch steigt die Varianz der Verteilung und die Verteilungsschiefe kann sowohl steigen als auch umgekehrt werden. In den deterministischen Modellsimulationen neigen die Zirkulationen innerhalb der Grauzone dazu, sich zu gut organisierten Wolkenstraßen mit künstlichen Merkmalen zu entwickeln, während das stochastische Modell diese unechte Organisation von Konvektion abzubauen versucht.

Contents

Chapter 1

Introduction

The purpose of parameterizations in numerical atmospheric modelling is to account for the small-scale processes that are cut off from a solution of the dynamical equations that describe the atmosphere by discretization of the model equations onto a numerical grid of a finite size. A conventional parameterization of boundary layer clouds is a statistical-physical representation of the average collective effect of cumulus clouds within a model grid column based on the known grid-scale quantities. In a parameterization of subgrid cloud processes, simplified statistical parametric relations are employed instead of applying the exact and complete set of physical equations, which would be huge in number and uncertain even if it would be possible to solve them. These parametric relations carry a number of unknown parameters, thus every cloud parametrization relies on one or more closure assumptions that are in principle based on some physical process that determines the convective intensity and control mechanisms on convection by the grid-scale flow. The closure assumption, as a physical aspect of parameterization, places a physical constraint on an ensemble average property of the subgrid cloud system.

From the statistical point of view, every parameterization relies on the statistical equilibrium assumption, which results from the law of large numbers (Williams, 2005; Yano and Plant, 2012). If the number of events within the model grid column is large, then the average outcome of the subgrid-scale processes will be predictable and uniquely determined by the known large-scale quantities. In the numerical atmospheric models, the statistical equilibrium is practically never fulfilled, because the number of events within the model grid column is limited, but also because a clear separation between the small-scale and the large-scale processes in the continuous spectrum of atmospheric flows can not be assumed and justified (Nastrom and Gage, 1985; Williams, 2005; Yano and Plant, 2012). This signifies that the fluctuations around the statistical equilibrium are in theory always present. In practice, these fluctuations can be assumed negligible in the coarse-resolution models (coarser than 50-100 km, depending on the case) applied to a convective field in a slowly changing environment, in which case the statistical quasi-equilibrium is assumed valid, and convection is in principle parameterizable (Xu

et al., 1992). Otherwise, the fluctuations around the statistical equilibrium can be substantial, as in a fast changing convective environment or in the convective cases modelled on high-resolution model grids (finer than 10-50 km), where the assumption of quasi-equilibrium is no longer applicable and the average value loses its statistical significance (Arakawa and Jung, 2011).

Given the fact that there is always some spread of the subgrid convection outcomes around the statistical equilibrium, an important question to ask is which outcome of subgrid convection should be provided as the tendency for updating the grid-scale thermodynamic fields. This question is very similar to one asked by Jaynes (1957) - whether it is the most probable rather than the average outcome of a probability distribution that maximizes the entropy of a physical system that should be compared with observations. If the maximum-entropy distribution of the system has a single, well defined and sharp peak, then the answer to this question is obvious: the average over the distribution represents the most probable outcome at the same time. However, in the case where the available physical information does not infer the sharp-peaked distribution, or simply in the case which carries large uncertainty, the distribution of possible outcomes can be very broad, and can have a non-Gaussian shape, thus it is no longer justifiable to compare the distribution average with observations. Furthermore, this distribution can possibly have two or more peaks and the distribution average can differ significantly from the most probable outcome (Jaynes, 1957). If we translate this to the question of parameterization of clouds and validity of the statistical equilibrium, we expect that in the coarse-resolution simulations of a quasi-stationary convective case, the average of the distribution can represent the subgrid convection correctly, while on the high resolution grids or in the fast varying convective conditions, the fluctuations around the equilibrium average become substantial. Thus, in the latter case, in order to represent the uncertainty of parameterization schemes in numerical models, the distribution of all possible states should be defined in a parameterization. A physical constraint on the system, formulated as a closure of the parametric relations, should determine the spread and the shape of the distribution of all possible subgrid convective outcomes. This distribution will be scale-dependent, meaning that as the model resolution becomes finer, the spread around the equilibrium will become broader (e.g. Xu et al., 1992). Therefore, the parameterization development should also be guided towards a scale-dependent formulation.

Once the statistical quasi-equilibrium is assumed valid to provide the basic parameterizability criterion, the physical aspect of parameterization is brought forward on the large scale that is assumed predictable. In most of the boundary layer cumuli parameterizations, the main closure assumption that brings the physical aspect into the parameterization is some form of the boundary layer equilibrium, by which cumuli are related to processes that control the development and maintenance of the convective boundary layer (CBL).

The topic of this thesis revolves around these two aspects of closure in cumulus parameterization, the statistical and the physical closure aspect, the scales at which these assumptions are valid and their interplay across scales. In the remainder of this introduction we describe the thermodynamic structure of a typical cloudy boundary layer over the ocean, and through the historical recapitulation of parameterization development, we emphasize the importance of parameterizing shallow convection in numerical models. As a further motivation for this thesis research, an overview of convection

treatment in the convective-scale-resolution models is given, after which we define the thesis goals and its structure.

1.1 Thermodynamic structure of moist convective boundary layers

In order to understand the principles of parameterization of shallow clouds and convective boundary layers, it is important first to learn about the vertical thermodynamic structure and mechanisms that lead to a typical marine shallow cumulus boundary layer.

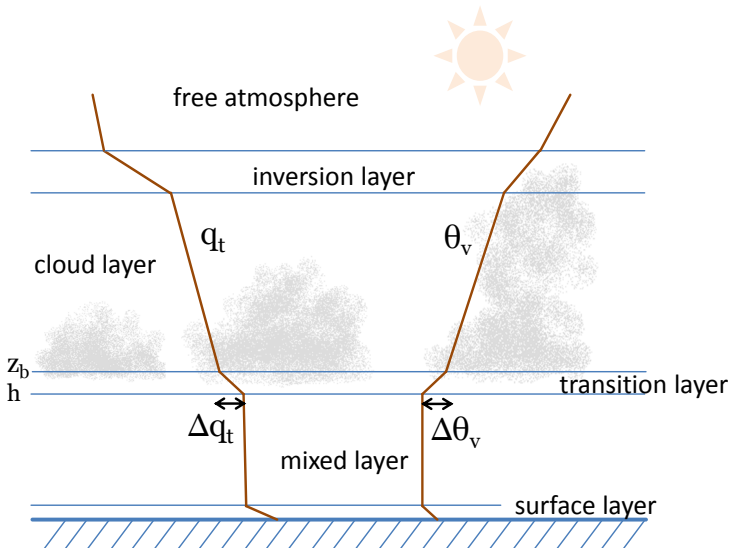

Figure 1.1: A sketch of the cloudy CBL thermodynamic structure. Based on the vertical profiles of total water mixing ratio q_t and virtual potential temperature θ_v, several well defined layers can be recognized: a thin surface layer with large q_t and θ_v gradients, a mixed layer extending to the height h, a transition layer of depth δ_{tr} between the top of the mixed layer h and cloud-base height z_b, and a cloud layer capped by an inversion.

The convective boundary layer (CBL) develops when the underlying Earth's surface is heated by the incoming solar radiation and becomes warmer than the overlying air, or when colder air is advected over the warmer surface. The surface that is warmer than the air atop transports heat to the lowest layer of the atmosphere, a shallow surface layer spanning up to $\sim$ 100 m, where heat, moisture and momentum are transported upwards via turbulent motion and where thermodynamic properties of air change rapidly with height (Fig. 1.1). Thermally induced convective instability initiates narrow organized updrafts, which rise and transport heat, moisture, momentum and pollutants from the surface layer upwards, while dense colder air sinks in the surrounding area to compensate for the upward mass transport. These organized updrafts are a source of the turbulent kinetic energy in the CBL. The turbulent kinetic energy is generated by the largest turbulent eddies or convective thermals in the CBL, and is passed to smaller eddies in a cascade down to the smallest eddies which dissipate energy by molecular viscosity. The energy cascade and turbulent mixing develop a well-mixed layer that can be easily recognized by the typical, nearly constant vertical profiles of thermodynamic quantities, like virtual potential temperature θ_v and total water mixing ratio q_t (Fig. 1.1).

The rising updraft can be thermodynamically described as a parcel of moisture-containing air that is being lifted adiabatically. As the air parcel rises it expands and cools adiabatically following the dry adiabatic lapse rate (around -10 K/km). At the top of the mixed layer, the rising parcel overshoots into a weakly stable transition layer, and if it contains enough water vapor it will become saturated at some height and will begin to condense its water. Those parcels that don't have enough energy to overcome the inhibition by the weakly-stable transition layer terminate their ascent within this layer and detrain their mass into the environment. The height where the parcels become saturated is called the lifting condensation level (LCL), which is recognized as the base of the transition layer. The transition layer spans between the mixed layer top and the height of maximum liquid water content at the cloud-base level. As the parcel rises above the LCL, it releases latent heat due to condensation, which partly compensates the adiabatic cooling, so the temperature of the parcel now drops following the moist adiabatic lapse rate (around -4 to -6 K/km).

If the parcel, now representing the cloudy updraft, has enough inertia it will reach the height level where it will become positively buoyant again, and this level is recognized as the level of free convection (LFC). Those clouds in which latent heating is not sufficient to overcome the stable transition layer and thereby do not reach the LFC are the forced clouds, and they will live as long as they are forced by their convective updrafts. Clouds that can reach the LFC are considered the active clouds, and their further evolution above the LFC is determined by their own dynamics and mixing with the environment. These active clouds can develop to large heights and vent the boundary layer air into the free atmosphere. Passive clouds are classified as old decaying active clouds which no longer transport the mixed layer air upwards. This classification of boundary layer clouds is defined in Stull (1985). Vertical growth of active cumuli is limited by the temperature inversion at the top of the boundary layer. Cumuli towers that reach the top of the CBL, overshot into the inversion and entrain the dry and warm air from the free atmosphere down into the CBL to compensate for the upward outflow. Thus, the inversion layer is also called the entrainment zone.

1.2 Background on parameterization of shallow convective clouds

The purpose of parameterization schemes extends further from numerical modelling applications in weather prediction and climate studies. Theoretical parametric and conceptual models of physical processes are very useful tools for gaining knowledge and understanding of the atmospheric phenomena (Arakawa, 2004). Thus, the early shallow convection conceptual models helped in understanding the structure of the boundary layer and the role that shallow convection plays in the large-scale circulation of the atmosphere. The parameterization schemes that are developed for use in large-scale models are mostly relying on these early parametric studies of cloud-topped boundary layers. Here we review the background on parameterization of shallow clouds by separating the topic into three stages: the early parametric studies, the parameterization schemes used in large-scale models, and the relevance of parameterizing shallow cumulus clouds in numerical models. In the following, we review only the most influential and relevant parameterization studies for the scheme developed in this thesis.

1.2.1 Early parametric studies of cloud-topped boundary layers

One of the first parametric models developed for studying the vertical transport of heat and moisture by nonprecipitating cumulus convection is the model of Betts (1973). It consists of a mixed layer model that represents the turbulent transport in the subcloud layer and a lapse rate model for the cumulus cloud layer. The transition layer below the cloud base is parameterized as well to determine the convective activity by controlling the convective mass flux into the cloud layer. A detailed description of a mass flux approach for shallow convection is given in Chapter 3 of this thesis, thus we will not provide the extensive description here. The closure of Betts (1973) model is based on an adjustment of the cloud layer lapse rate structure towards a characteristic quasi-equilibrium stratification of the moist CBL. This adjustment is usually realized during a defined adjustment timescale or during a single model time step. This model predicted a destabilizing effect of cumulus clouds by warming the lower part of the cumulus cloud layer and cooling the upper part of the CBL, which corresponds to the inversion layer. This destabilization by cumulus convection together with the radiative cooling near the CBL top maintains the trade inversion against the warming and drying effects of the large-scale subsidence by counteracting its stabilizing effects (Betts, 1973, 1975). This mechanism had been confirmed in numerous observational studies, as for example in Holland and Rasmusson (1973) during the Barbados Oceanographic and Meteorological Experiment (BOMEX) measurement campaign.

The interaction of a cloud ensemble with its environment is studied by Yanai et al. (1973) who developed an entraining-detraining model for cumulus clouds of different types. The closure of this model is based on the statistical equilibrium by which an activity of the cloud ensemble is controlled by the imposed large-scale flow. The model is based on a mass flux approach, where clouds are classified into separate groups based on their cloud top heights, but the bulk representation of the cloud ensemble is retained by averaging the outcome over all cloud types. This model, as well as a parallel study of Gray (1973), revealed that the re-evaporation of liquid water and large amounts of water vapor detrained from clouds are responsible for balancing the drying and heating of environmental air due to compensating downward motion between active cumulus clouds. The shallower, nonprecipitating cumulus clouds are thus essential in supporting the growth of deep precipitating cumulus towers by supplying and maintaining the moisture in the lower part of the cloud layer against the heating effects of subsiding air (Yanai et al., 1973; Esbensen, 1978).

The scheme of Yanai et al. (1973) was developed in parallel to the perhaps most famous cloud scheme, the Arakawa and Schubert (1974) scheme. The Arakawa and Schubert (1974) cloud scheme is a spectral, multiple cloud type, mass flux parameterization based on the theory of the interaction of a cumulus ensemble with the large-scale environment. The basic parameter in the model is the cloud work function, which is an integral measure of the buoyancy force of the cumulus clouds defined for each cloud type. By transporting the mass out of the mixed layer, clouds decrease the mixed layer depth and warm and dry the environment above. Such modification in the environment will produce a smaller buoyancy force in the clouds and therefore will lower the cloud work function, which is an act of stabilization. Large-scale forcing is counteracting the warming and drying of the environment thus controlling the convective activity by increasing the cloud work function as an act of destabilization. So, the cumulus activity will act to stabilize the atmosphere by equilibrating the

cloud ensemble against the destabilization effect of the large-scale forcing. This is the main closure assumption of this model named “the convective quasi-equilibrium assumption”. This assumption is twofold, it assumes statistical equilibrium and the large number of convective clouds within a model column, and it assumes that the convective activity is fully controlled by the large-scale flow.

The importance of a different interpretation between lateral entrainment and detrainment effects and between their timescales was recognized in a diagnostic study of Betts (1975). In this study, a single cloud type conceptual model for trade wind cumulus is developed, as an entraining-detraining bulk cloud model with adjustment type closure. Detrainment acts on the longer timescale that is characteristic for the effective changes caused in the environment, while entrainment acts on shorter cloud timescales and represents the cloud dilution with height. This model was used to interpret BOMEX fluxes in terms of moistening and cooling of the environment due to detrainment and warming and drying due to cumulus-induced subsidence. The success of this scheme and the one from Yanai et al. (1973) in representing the mean properties and thermodynamic structure of the CBL, supported the argument that a single mass flux profile is sufficient in representing the thermodynamic fluxes for some cases equally well but more simple than the spectral cloud models.

The interaction between the subcloud layer and shallow cumulus layer was modelled by Betts (1976), where the mixed layer model of Betts (1973) is coupled to the cumulus parameterization of Betts (1975). The coupling between these two CBL layers involves two important parameters: the ratio of the model heat flux just below the cloud base to the surface heat flux and the ratio of the depth of the model transition layer to the depth of the subcloud layer. These two parameters relate the cloud-base mass flux and mass flux gradient to the subcloud layer parameters, and they also determine the moisture budget of the subcloud layer and the rate of change of the cloud-base height. A similar approach to coupling between the subcloud and the cloud layer is further developed in the parameterization study of Neggers et al. (2006, 2009).

Another model that couples the trade wind cumulus clouds with their subcloud thermals was developed by Esbensen (1978) by extending the Arakawa and Schubert (1974) cloud scheme, where the same budget equations for the moist conserved variables are applied to the subcloud and the cloud layer. This study revealed that the buoyancy of shallow cumuli is an order of magnitude lower than the buoyancy of deeper clouds, so the effects of shallow clouds on the temperature stratification in the CBL are much smaller compared to radiative cooling and subsidence warming due to deep clouds. This implies a much longer adjustment timescale in the case of a shallow cumuli ensemble until the ensemble reaches the quasi-equilibrium state compared to the adjustment timescale of deep convective clouds. This adjustment timescale of shallow cumuli ensembles towards the quasi-equilibrium stratification can be of the order of one day, so the conclusion of this study is that these two cloud types should be parameterized using different approaches.

These early parametric studies leave us with several dilemmas about the cloud parameterization formulation. Until today there is no common approach to parameterization related to the questions of whether a spectral parameterization of clouds is necessary or a bulk scheme would suffice, whether a single-cloud-type model can represent the cloudy layers well or multi-cloud-type models are necessary, and whether to develop parameterizations with a unified or separate treatment of subcloud and

cloud layers. Recently, more and more studies are revising the spectral and unified approaches to parameterization, and some of them are listed in the following subsection.

1.2.2 Parameterization schemes for shallow convection in large-scale models

Early parametric models for cumulus clouds served as a basis for development of the parameterization schemes that are applied in present day numerical weather prediction and climate models. The scheme of Betts (1976) is applied in the adjustment-type cloud scheme of Betts and Miller (1986) in a single column model setup. The novelty of this parameterization scheme is that it uses the observational data in tropical areas to define the reference quasi-equilibrium profiles towards which the cumulus cloud ensembles are being adjusted. The scheme of Yanai et al. (1973) was developed further by Tiedtke (1989) to serve a practical purpose in the ECMWF (European Centre for Medium-Range Weather Forecasts) forecasting model. In this scheme deep convection is controlled by the moisture convergence in the large-scale flow, while shallow clouds are effectively controlled by the subcloud layer turbulence. Thus Tiedtke (1989) recognized the importance of separating between various types of convection because of different mechanisms controlling deep penetrative and mid-level clouds compared to shallow cumulus clouds. However, Tiedtke (1989) also concluded that it is sufficient to apply the bulk approach to model the effects of a cloud ensemble on the environment and large-scale flow. Another bulk parameterization scheme for representing different cloud types, deep, mid-level and shallow clouds, as well as dry convection was developed by Gregory and Rowntree (1990). The closure of this model connects the initial convective mass flux to the initial buoyancy of a cloudy rising parcel. This bulk model takes into account the differences in cloud heights within an ensemble through the lateral detrainment at all levels bellow the cloud top.

More dependence of cloud profiles on the environmental conditions is introduced in a buoyancy-sorting entraining-detraining model of Kain and Fritsch (1990). Mixing between clouds and their environment is represented by defining mixtures of cloudy and environmental air in different proportions. If it is positively buoyant, a mixture will entrain a fraction of environmental air into the cloud, or if it is negatively buoyant, a mixture will detrain a fraction of cloudy air into the environment. Bechtold et al. (2001) used the buoyancy sorting mixing scheme in a bulk parametrization based on the convective available potential energy (CAPE) mass flux closure. This scheme includes deep and shallow convection parameterizations. Another scheme based on the buoyancy-sorting approach is the scheme of Bretherton et al. (2004) where the buoyancy sorting mechanism is used to represent detrainment of cloudy air into the environment, while the dilution of cloud properties is parameterized by an entraining model as in Betts (1973). Cloud-base mass flux is controlled by a convective inhibition based scheme, which is similar to the transition layer control on the cloud-base mass flux in the Betts (1973) scheme.

From all above mentioned studies it is evident that the representation of mixing of the cloudy air with the environment is among the most uncertain aspects of cloud parameterizations. Based on LES of the BOMEX shallow cumulus case, Neggers et al. (2002) developed a model formulated as the ensemble of rising parcels to examine the relaxation timescale for lateral mixing in shallow cumulus clouds. In this study, it is found that the timescale of mixing is not dependent on the cloud depth, but

the dependence of cloud dilution on the updraft property comes from the entrainment rate, which is inversely proportional to the vertical velocity. Such a multi-parcel model was able to represent the typical variability in a cumulus ensemble and to reproduce the joint distribution of conserved variables in the cloud layer. Neggers et al. (2002) emphasize that the previous bulk models were not able to represent the convective variability properly because of uncertain or inadequate parameterizations of mixing with the environment. The importance of diversity of convective plumes for an accurate description of lateral mixing with the environment was also noted by Cheinet (2004), who developed a multiple mass flux parameterization for the surface generated convection. This parameterization is extended to include the cloud layer parametrization, by unifying the convective mixed layer and cloud layer transports, where the same surface-generated convective plumes are used to represent the subcloud updrafts and clouds.

One of the first unified parameterization frameworks for moist convection that combines a high order planetary boundary layer (PBL) turbulence scheme with a mass flux cloud scheme was developed by Lappen and Randall (2001). In this scheme a joint probability density function (PDF) of moist conserved quantities is assumed and integrated to derive the equations that are then used in the high order closure of the PBL turbulence scheme. Soares et al. (2004) developed a unified description of turbulent transport in the cloud-topped boundary layer within the eddy-diffusivity mass-flux (EDMF) framework previously proposed by Teixeira and Siebesma (2000). The EDMF scheme unifies local turbulent mixing and nonlocal convective mixing, while the same budget equations of surface-generated convective updrafts are used to represent the subcloud and cloud layer updrafts. Strong updrafts are modelled by using a mass flux approach and an entraining parcel model similar to Betts (1973) with an extension to the cloud layer, while the small-scale turbulent transport is modelled by an eddy-diffusivity approach. The unified framework of EDMF is further developed in work of Neggers et al. (2009) and Neggers (2009) where the scheme is extended by allowing a gradual transition and partitioning between the dry and moist bulk updrafts as a least complex scheme that can represent a smooth coupling between the shallow convective cloud layer and subcloud mixed layer. This scheme is described in detail and developed further in Chapter 3 of this thesis.

An updraft multiple-mass-flux scheme of Sušelj et al. (2012) is a further development of EDMF by introducing the branching updraft approach based on a PDF of moist updraft properties. In this scheme, a single updraft originates at surface and as it ascends it branches with height into multiple dry and moist updrafts. Sušelj et al. (2012) favor the multi-mass-flux approach to realistically represent the thermodynamic structure of a steady case over the ocean and a time-varying convective case over the land. Sušelj et al. (2013) further developed EDMF in a single-column model by implementing two stochastic processes into the scheme, one to represent the variability in the number of plumes and second to represent the uncertainty in lateral mixing. Sušelj et al. (2013) argue that a stochastic method is necessary to represent the vertical thermodynamic structure of various shallow convective cases. A stochastic parameterization of shallow convection can as well be a good approach to represent the ensemble spread of temperature and humidity in the convective gray zone, though the range where a stochastic approach is required extends beyond the gray zone up to 10 km of grid spacing (Dorrestijn et al., 2013). This stochastic parameterization uses a lattice type model for sampling the pairs of turbulent heat and moisture fluxes, whose states are pre-calculated using LES on different

coarse-grained resolutions. Another lattice type model of convective states is used in the multi-cloud parameterization of Khouider et al. (2010) for application in coarse-resolution climate models (on the 100 km scales). They define three types of cloud elements of different heights that interact with each other within the model grid column and with the convective environment to represent the subgrid variability due to convective organization. The novelty of the stochastic approach developed in this thesis is mostly related to the physical aspects that control the variability in a convective ensemble on high-resolution grids and to nonlocality and scale-dependence of the distribution of subgrid-convective states, and will be outlined in Section 1.4.

1.2.3 Importance of shallow cumuli in weather and climate modelling

As it was already mentioned in this chapter, shallow cumulus clouds play an important role in shaping the thermodynamic structure of the CBL by transporting heat, momentum and moisture within the lower part of the troposphere and thus influencing the hydrological and energy cycles of the atmosphere. The importance of parameterizing shallow convection in numerical models is further emphasized by the work of Tiedtke et al. (1988), where shallow convection was recognized as a necessary mechanism to maintain a realistic trade wind inversion, which is in line with previous studies of Betts (1973, 1975) and Holland and Rasmusson (1973). Shallow convection dries the subcloud layer, so more moisture can be supplied to the atmosphere via turbulent fluxes by evaporation from the subtropical oceans. The increased moisture being supplied to the boundary layer by the effects of shallow convection parameterization is transported into the tropics by the trade winds thus increasing the moisture source for deep cumulus convection. Through this connection, shallow clouds influence the general circulation patterns, and are responsible for the enhancement of the Hadley cell and a more realistic intertropical convergence zone (ITCZ, Tiedtke et al., 1988; Zhu and Bretherton, 2004; Neggers et al., 2007a). Tiedtke et al. (1988) further demonstrated that the shallow convection parameterization and the improved model physics were more important than the resolution increase for reducing the model systematic errors in the tropics.

Over the land, the shallow convection parameterization included into the model configuration improves the simulation of the diurnal cycle of convection and preconditioning of deep convection (Zhu and Bretherton, 2004). On the larger scales, by moistening and preconditioning the lower troposphere for deep convection, shallow clouds are essential for simulation of the Madden-Julian oscillation (MJO) in global climate models (GCMs, e.g. Zhang and Mu, 2005; Zhang and Song, 2009). The role of shallow convection in the low-level heating in GCMs is also critical for initial strengthening and maintenance of the MJO (e.g. Li et al., 2009; Lappen and Schumacher, 2014).

In the modelling studies of tropical cyclones, parameterization of shallow convection can influence the intensification rate of the cyclone vortex during the early stage of cyclone development, by lowering the buoyancy within the vortex core (Zhu and Smith, 2002). Shallow convective clouds influence not only the tropical cyclone intensity but also the tropical cyclone tracks (Torn and Davis, 2012). In the study of Torn and Davis (2012), the forecast of the tropical cyclone tracks using a cloud-permitting model was significantly improved when the parametrization of shallow cumulus clouds was included into the model configuration.

Another example of interaction of shallow cumuli with other types of clouds in a GCM is the role of shallow cumulus clouds in decreasing the stratocumulus cloud amounts in the lower subtropical atmosphere over the oceans (von Salzen et al., 2005). An important role of shallow convection parameterization is to transport moisture from the CBL into the free atmosphere, thus when shallow convection is not parameterized this transport becomes inefficient. This results in an enhanced development of stratiform cloudiness, which strongly perturbs the global radiative balance. Due to the shallow cumulus effects, the change in the global mean shortwave forcing at the top of the atmosphere can be of the order of -11 Wm^{-2} (von Salzen et al., 2005).

All the above mentioned mechanisms through which shallow clouds influence the atmospheric circulation and atmospheric moisture and energy budgets indicate the importance of shallow cloud parameterization in climate modelling. Due to a limited understanding of these interaction processes and due to inadequate representation of shallow clouds in global and regional climate models, shallow clouds are one of the largest sources of uncertainty in climate sensitivity studies (Bony and Dufresne, 2005; Wyant et al., 2006; Medeiros et al., 2008; Bony et al., 2015)

1.3 Convection on the meso-γ-scale grids

The target resolution range for the shallow cumulus scheme developed in this thesis extends down to the atmospheric meso-γ scales (2-20 km). So, in this subsection, we briefly review the status of numerical modelling of convection on the meso-γ-scale resolutions.

A common approach to atmospheric modelling at the kilometer-scale resolution is to permit deep convection to develop on the model grid instead of applying a subgrid deep convection parameterization. A benefit of this approach is that the meso-α- (20-200 km) and meso-β-scale (200-2000 km) convective systems are effectively resolved, and uncertainties and deficiencies of the convective parameterization for these processes are avoided. Another benefit of models on high resolutions is the ability of using the high-resolution input data such as orography and land use data or assimilation of high-resolution radar or satellite data (e.g. Lean et al., 2008). Even though deep clouds are not effectively resolved on the kilometer-scale grids, there is a number of studies that show a better representation of mesoscale convective systems and convective organization when simulations and forecasts are performed without a parameterization scheme for deep convection (e.g. Weisman et al., 1997; Speer and Leslie, 2002; Steppeler et al., 2003; Knippertz et al., 2009; Baldauf et al., 2011). This improvement results from more physical processes that are explicitly resolved when the resolution of models is increased, however objective scores of forecasts do not necessarily get higher and the point-specific accuracy of forecasts can not be achieved on kilometer scales (Mass et al., 2002; Done et al., 2004).

The length of a useful numerical forecast depends on the scale of the modelled flow, so at the mesoscales the predictability limit is reached faster than on the synoptic scales (Lorenz, 1969). To assess the sensitive dependence on initial conditions and model uncertainty, ensemble prediction systems are developed for atmospheric modelling on convective scales (e.g. Kong et al., 2007; Gebhardt et al., 2008, 2011; Clark et al., 2011; Migliorini et al., 2011; Romine et al., 2014). This is a relatively

new area of research, and although the ensemble techniques are commonly applied on the synoptic scales, the methods of constructing an ensemble on the synoptic scales can not be translated directly to the convective scales. The main reason for this is the mechanism of error growth on convective scales, which differs from the mechanisms on synoptic scales. Moist convection is the leading process that controls the forecast skill of a convective-scale resolution model and the fast error growth at mesoscales is associated with the moist-convective instability (Zhang et al., 2003, 2006; Tan et al., 2004; Hohenegger et al., 2006; Selz and Craig, 2015). A well known fact from the convective-scale ensemble studies is that the ensemble spread is underestimated, and a great deal of the underestimation comes from the lacks in representation of the model uncertainty (e.g. Romine et al., 2014). Furthermore, techniques used to account for the model uncertainty in current ensemble systems, such as the stochastic kinetic energy back-scatter scheme (Shutts, 2005) or the stochastically perturbed parameterization tendencies (Buizza et al., 1999), improve the ensemble spread, but reduce the forecast value of the individual ensemble members (e.g. Romine et al., 2014). Given that moist convection is causing the fast error growth at the mesoscales and that the ensemble spread lacks variability due to the model uncertainty, the focus should be in developing a stochastic parameterization of convection, in which the perturbation distribution is based on the physical principles, and the system is constrained in the mean so that the performance of the individual ensemble members is not degraded.

Another difficulty for atmospheric modelling on the kilometer scales results from under-resolved convection developed on the model grid. These under-resolved circulations are overenergetic and their spatial overturning scales are much larger than natural convective scales (Bryan et al., 2003; Bryan and Rotunno, 2005; Petch, 2006). The reason for this behavior is in the interruption of the turbulent energy cascade, which is not explicitly resolved because the simulated flow does not become turbulent unless the grid scale is less than 100 m. So, the energy accumulates at the large scales controlled by the model grid scale (Bryan and Rotunno, 2005). Overenergetic, under-resolved flows lead to problems in forecasts such as over-prediction of rainfall amount and delayed convective activity (Lean et al., 2008; Roberts and Lean, 2008). Furthermore, on the kilometer-scale grids, as a result of introducing numerical fluctuations from imperfect numerical schemes into the statically unstable layers in atmosphere, unnatural and spurious organization can develop, such as a regular pattern of convective cells 3 km above ground in the simulation of a squall-line at the kilometer-scale resolution of Takemi and Rotunno (2003) and Bryan (2005). The atmospheric free convection on the gray zone grids is another processes that can form spurious organization, as a combination of numerical artifacts and under-resolved convective circulations (Piotrowski et al., 2009; Zhou et al., 2014; Ching et al., 2014). The spurious organization can be removed by increasing the model diffusivity (like in Takemi and Rotunno, 2003), but this approach is case dependent and requires tuning with no physical basis. A better solution to this problem would be to develop a parameterization scheme that introduces controlled fluctuations and is able to dissolve the spurious organized structures. It is an open question whether the convective scheme should completely take over the convective transport and prevent the under-resolved convective circulations from developing on the grid scale.

On top of all the above listed examples of model performance when deep convection is permitted on the kilometer-scale-resolution grids, shallow cumulus convection is far from being resolved, but at the same time it is in the gray zone for an effective parameterization. The gray zone for shallow

convective clouds is approximately between hundreds of meters and ten kilometers of grid spacing in numerical models, which intersects with the meso-γ scales. In some of the above cited studies about the convective-scale modelling, shallow convection is not considered separately from deep convection and is parameterized at resolutions coarser than 4 km and explicitly modelled on higher resolutions (Weisman et al., 1997; Speer and Leslie, 2002; Steppeler et al., 2003; Done et al., 2004). In other studies, shallow convection is accounted for by using modified cloud schemes with reduced convective activity, by limiting the cloud-base mass flux. The reasoning behind this approach is to allow the model to explicitly represent the mesoscale convective structures, but also to include the parameterization of weaker convective clouds that are not resolved at all at these resolutions (Lean et al., 2008). If the shallow clouds are parameterized in the convection-permitting simulations, (e.g. like in Knippertz et al., 2009), the scheme will work in the gray zone regime, which is not an adequate approach. So, obviously, the situation is far from being solved and the best strategy for treatment of convection at these high-resolution scales is still not agreed upon. Thus, there is a need for a parameterization scheme that can perform adequately in the gray zone for shallow convection.

1.4 Thesis objective

The goal of this thesis is to develop a stochastic parameterization of shallow cumulus clouds that is equally adequate for coarse and for high-resolution scales of atmospheric models. The purpose of this stochastic parameterization is to model the fluctuations of convective subgrid states around the equilibrium state of the cloud ensemble embedded in a slowly changing large-scale environment. The research here focuses on the RICO (Rain In Cumulus over the Ocean) case, which is modified for the purpose of this study by suppressing precipitation in order to limit the level of mesoscale organization of convection and shallow clouds. The reason for this choice is to isolate the intrinsic variability of convection emerging from the subgrid scales from the variability originating in cloud organization.

As a first step towards parameterization development, a theory of fluctuations in a shallow convective cloud ensemble is developed by generalization of the convective ensemble of deep clouds (Craig and Cohen, 2006). The formulation of the generalized convective ensemble is supported by the numerical large eddy simulation (LES) and cloud tracking of individual clouds of the RICO case. This theoretical-empirical shallow cumulus ensemble framework defines the scale-dependent probability distribution of possible convective states in the model grid columns. By randomly sampling the individual realizations of this distribution, the fluctuations of convective states around the statistical equilibrium can be represented across the range of model horizontal resolutions.

One of the main components of the shallow cumulus ensemble framework is the cloud mass flux distribution function, while the total mass flux in the cloud ensemble is the main parameter defined by the parameterization closure. Thus, the distribution function of the cloud mass flux is first derived by combining the theory and LES and the distribution parameters are related to the large-scale average properties of the cumulus ensemble. The shape of the cloud mass flux distribution influences the variance of other cloud properties, thus besides the parameterization development, the stochastic cumulus ensemble framework is used as a tool to study what controls the shape of the mass flux

distribution and as well what controls the variability in the convective ensemble. This part of the study is described in Chapter 2 of this thesis.

When developing a parameterization in a full 3D atmospheric model there is a number of choices to be made regarding the complexity of the parametrization schemes. In the second part of this thesis the stochastic model based on the theoretical and LES findings is coupled to the EDMF scheme in a non-hydrostatic numerical weather prediction (NWP) model. In the NWP model on high resolution grids, an additional requirement for parameterization development is the formulation of the cloud layer vertical structure. Thus, we reconsider the formulation of the entrainment rate and the cloud mass flux vertical profile in the EDMF scheme, and discuss the least complex configuration of parameterization sufficient to represent the statistical properties of the RICO case across scales. At the high-resolution scales cloud fields are affected by the convective gray zone and by the grid-scale convective organization, thus a parameterization development addresses these questions as well. The implementation of the stochastic model into the NWP model and the first results and their implications are described in Chapter 3.

The stochastic shallow cumulus parameterization developed in this thesis is intended to cover multiple purposes from extending the knowledge about cloud ensembles to improving the performance of numerical models. In the remainder of this thesis the stochastic scheme is used in an idealized model setup to

- study the properties and structure of a cumulus ensemble and its coupling with the environment,
- maintain the quasi-equilibrium assumption applicable across the range of modelling scales, thus making the parameterization scale-adaptive,
- correctly represent the intrinsic variability of cloud fields,
- search for and develop the least complex mass flux ensemble formulation that is sufficient to represent the average vertical structure of a convective case, its time evolution and its spatial variability,
- improve the model performance in the convective gray zone by dissolving the spurious cloud organization, and
- provide a way to represent uncertainty of the model convective scheme by using a stochastic approach that is physically based (Plant and Craig, 2008).

Concluding remarks about the parameterization development, the main improvements of the parameterization and the new understanding of the cumulus ensemble are given in Chapter 4 of this thesis.

Chapter 2

Fluctuations in a quasi-stationary shallow cumulus cloud ensemble

In this chapter we propose an approach to stochastic parameterization of shallow cumulus clouds to represent the convective variability and its dependence on the model resolution. To collect information about the individual cloud lifecycles and the cloud ensemble as a whole, we employ a large eddy simulation (LES) model and a cloud tracking algorithm, followed by conditional sampling of clouds at the cloud-base level. In the case of a shallow cumulus ensemble, the cloud-base mass flux distribution is bimodal, due to the different shallow cloud subtypes, active and passive clouds. Each distribution mode can be approximated using a Weibull distribution, which is a generalization of exponential distribution by accounting for the change in distribution shape due to the diversity of cloud lifecycles. The exponential distribution of cloud mass flux previously suggested for deep convection parameterization is a special case of the Weibull distribution, which opens a way towards unification of the statistical convective ensemble formalism of shallow and deep cumulus clouds.

Based on the empirical and theoretical findings, a stochastic model has been developed to simulate a shallow convective cloud ensemble. It is formulated as a compound random process, with the number of convective elements drawn from a Poisson distribution, and the cloud mass flux sampled from a mixed Weibull distribution. Convective memory is accounted for through the explicit cloud lifecycles, making the model formulation consistent with the choice of the Weibull cloud mass flux distribution function. The memory of individual shallow clouds is required to capture the correct convective variability. The resulting distribution of the subgrid convective states in the considered shallow cumulus case is scale-adaptive – the smaller the grid size, the broader the distribution.

This study is published as a research paper in **Sakradzija, M.**, Seifert, A., and Heus, T.: Fluctuations in a quasi-stationary shallow cumulus cloud ensemble, Nonlin. Processes Geophys., 22, 65-85, doi:10.5194/npg-22-65-2015, 2015.

2.1 Introduction

To set a path towards the development of a stochastic shallow-cloud parameterization for numerical atmospheric models, we study how the unresolved convective processes relate to the resolved grid-scale variables in an ensemble of shallow cumulus clouds. According to a conventional deterministic approach to cloud parameterization, the outcome of shallow cumulus processes within a grid box of a numerical model is represented as an average over the cloud ensemble or as a bulk effect. However, different microscopic configurations of a convective cloud ensemble can lead to the same average outcome on the macroscopic grid scale (Plant and Craig, 2008). If a one-to-one relation between the subgrid and grid scales is assumed, the spatial and temporal variability of convection that is observed in nature and in the cloud-resolving simulations will not be represented in atmospheric models. At the same time, the improvement in parameterization should address the dependence of the subgrid- to grid-scale relation on the model resolution and physics time step (e.g. Jung and Arakawa, 2004). This is especially important on the meso-γ atmospheric scales, since moist convection and rain formation are recognized as the most uncertain processes acting on these scales and the core reason for the short mesoscale predictability limit (e.g. Tan et al., 2004; Zhang et al., 2003, 2006; Hohenegger et al., 2006).

Commonly used tools to study convective cloud processes at a high temporal and spatial resolution in order to develop parameterizations are the cloud resolving models (CRMs). To represent deep convective clouds explicitly, CRMs are used at the grid scale of 1 km order of magnitude, while shallow convective clouds become explicitly resolved at a grid scale of O(10–100 m), which is the size of the largest energy-producing eddies in the turbulent boundary layer, hence the name large eddy simulation (LES). To formulate the effects of clouds on their environment across the different scales of atmospheric flow, a technique of coarse-graining can be applied to the CRM and LES fields (see, for example, Shutts and Palmer, 2007, Section 3). In this way, a relation between the subgrid convection and the resolved flow can be emulated to reveal the properties and components of the parameterization and to reflect its dependence on the model grid resolution.

From the previous studies of deep convective cloud fields using CRMs and the coarse-graining methods, it is known that the subgrid- to grid-scale relation is neither fully deterministic nor diagnostic, which suggests that stochastic and memory components should be included in a parameterization. These components are sensitive to the spatial and temporal scales of a numerical model. As the horizontal resolution of a model gets higher, the stochastic component of the subgrid- to grid-scale relation becomes more pronounced (Xu et al., 1992; Shutts and Palmer, 2007; Jones and Randall, 2011). At the same time, an increase in horizontal resolution implies a shorter model time step and, as a consequence, a larger impact of the memory component on parameterization. In this case, changes in the resolved flow take place on a timescale close to or less than the convective response timescale, and the convective cloud system exhibits a nondiagnostic behaviour (e.g. Pan and Randall, 1998; Jones and Randall, 2011). Along with the effects of time lag in the convective response, memory of convection also comprises a feedback process by which the past interactions between convective elements and thermodynamic fields on the near-cloud scale modify convection at the current time (Davies et al., 2013). Furthermore, a delay in the convective response becomes longer with the

emergence of mesoscale cloud organization (Xu et al., 1992), and can be interpreted as an additional convective memory effect (Bengtsson et al., 2013). The importance of memory effects on subgrid processes is also assessed in a more general study of Wouters and Lucarini (2012, 2013), where they show that a coupling between two dynamical systems with different characteristic timescales involves a deterministic perturbation, a stochastic perturbation and a memory term with a pronounced scale dependence.

A behaviour of the subgrid- to grid-scale relation similar to the behaviour of deep convection, but on the smaller spatial scales, can be confirmed in LES studies of shallow convection. The stochastic effects in a coarse-grained shallow convective cloud ensemble become dominant on the scales close to 10 km and less (see Fig. 2 in Dorrestijn et al., 2013). We will refer to these spatial scales as the "stochastic" scales for the shallow convective ensemble.

Parameterization schemes developed specifically for shallow convection are in most cases based on the mass flux concept (Bechtold et al., 2001; von Salzen and McFarlane, 2002; Deng et al., 2003; Bretherton et al., 2004; Neggers, 2009). In a mass flux scheme, clouds within a model grid box are parameterized as a single bulk updraft or as a spectrum of cloud updrafts via a simple entraining–detraining plume model, and the vertical transport is determined by the upward mass flux through the cloud base. Estimation of the bulk or ensemble average cloud-base mass flux is a part of the model closure and is based on some form of the quasi-equilibrium assumption (Arakawa and Schubert, 1974). According to the quasi-equilibrium assumption, in a slowly varying large-scale environment, the subgrid convective ensemble is under control of the large-scale forcing with a statistical balance fulfilled between the unresolved and resolved processes. However, at the stochastic scales, the quasi-equilibrium assumption is no longer valid. The model grid box is not large enough to contain a robust statistical sample of shallow clouds and the timescale of parameterized processes can not be separated from the timescale of the resolved processes. This suggests that a stochastic and nondiagnostic approach to parameterization is necessary not only for representing the small-scale variability of convection, but also for representing the cloud field adequately by providing a way to make the parameterization scale-adaptive, and to avoid the scale separation problem.

Increasing horizontal resolution of atmospheric models is also strongly connected to the mesoscale predictability limit, which is reached faster on the smaller scales of the resolved motion (Lorenz, 1969). The reason for a shorter predictability time on the smaller spatial scales comes from the faster error growth on these scales due to moist convection (Zhang et al., 2003, 2006). In the simulations with the grid resolution of the order of 1 km, the small-scale initial errors spread fast throughout the domain and exponentially amplify over the regions with the convective instability (Hohenegger et al., 2006). Due to nonlinear interactions, initial uncertainties propagate upscale in a process known as the "inverse error cascade" and degrade the forecast quality on the larger scales (Lorenz, 1969; Leith, 1971). Here the stochastic term of a parameterization plays a role in representing the subgrid fluctuations that, due to the nonlinearity of the process, lead to the error growth and upscale error propagation. Thus, the stochastic term provides a way to quantify the uncertainties coming from the formulation of the subgrid cloud processes and is necessary to improve the ensemble spread in the ensemble prediction systems – EPS (see the review of Palmer et al., 2005).

Recently, EPS have been developed for the limited area models at the convection-permitting grid resolution to address the sensitive dependence on initial conditions (e.g. Kong et al., 2007; Gebhardt et al., 2008; Clark et al., 2009; Migliorini et al., 2011). The main goal of this new field of research is the improvement of the quantitative precipitation forecasts and the forecasts of convective and storm events. In the convection-permitting models, deep convective clouds are explicitly represented on the grid scale, while the planetary boundary layer (PBL) convection and shallow clouds are still subgrid processes and have to be parameterized. Nevertheless, the introduction of the stochastic physics into the convection-permitting EPS has been limited so far. The stochastically perturbed parameterization tendencies (SPPT) scheme of Buizza et al. (1999) is adapted and applied in a short-range convection-permitting EPS by Bouttier et al. (2012) to improve the ensemble reliability and the ensemble spread–error relationship. Another example is the recent work of Baker et al. (2014), where another similar method of parameter perturbation of the model physics tendencies called the random parameters (RP) scheme (Bowler et al., 2008) is modified and applied to a convection-permitting EPS. Both of these approaches are rather pragmatic and general in perturbing the physical tendencies in a model. The effect of stochastic schemes specifically developed for the shallow clouds and based on the underlying physical processes has not been investigated so far, mainly because stochastic schemes for shallow clouds have not been formulated until recently. One example is the scheme developed for stochastic parameterization of convective transport by shallow cumulus convection (Dorrestijn et al., 2013), based on LES studies of nonprecipitating shallow convection over the ocean. In this scheme, the pairs of turbulent heat and moisture fluxes are randomly selected as corresponding to different states of a data-inferred conditional Markov chain (CMC). In another approach, two stochastic processes are implemented in the eddy-diffusivity mass-flux (EDMF) scheme (Siebesma et al., 2007; Neggers, 2009), the Monte Carlo sampling of the convective plumes and the stochastic lateral entrainment (Sušelj et al., 2013).

The goal of our study is to formulate a shallow convective parameterization that encompasses the stochastic and memory effects of convection, using the theoretical and empirical findings about the cloud ensemble. We study a shallow convective-cloud case (Rain in Cumulus over the Ocean – RICO) using large eddy simulation (LES). RICO is a precipitating quasi-stationary shallow convective case that also shows some mesoscale organization. We coarse-grain the cloud ensemble to study the subgrid- to grid-scale relation and its dependence on the horizontal resolution. The variability of shallow convection and its scaling with the horizontal resolution is then quantified. Individual cloud lifecycles and the role of the diversity of cloud lifetimes are examined employing the cloud tracking routine of Heus and Seifert (2013). This numerical study gives a path to apply the theory of fluctuations in an equilibrium convective ensemble of Craig and Cohen (2006) to a shallow convective case.

In the following, we propose a generalization of the theory of fluctuations in a convective ensemble by including the system memory and by considering the impact of the diversity in cloud lifecycles on the cloud-base mass flux distribution shape. This provides a stochastic and memory term in the subgrid- to grid-scale relation, and a deterministic component is also retained in adequate proportion, depending on the grid scale. This combined empirical–theoretical concept is then structured in a stochastic stand-alone model of a shallow cumulus ensemble, similar to the approach of Plant and Craig (2008)

for deep convection, referred to as PC-2008 in the following text. A spectral representation of the cloud field with the cloud lifecycles modelled explicitly introduces the memory of individual clouds and opens the way to estimating the impact of this memory on the variability of convection. Sensitivity tests of the gradual generalization of the convective-fluctuation theory provide a definition of a consistent and least complex model formulation.

Large eddy simulation and the cloud tracking algorithm necessary for the analysis are described in Section 2.2. Physical and statistical properties of a cloud ensemble are described here and the cloud mass flux distribution is analysed. A stand-alone stochastic model is constructed based on empirical and theoretical findings and the model formulation is derived for the different levels of system generalization (Section 2.3). Different formulations of the stochastic model are discussed, and tested against LES results, to decide on minimal and consistent representation of all relevant features of subgrid convection and its variability (Section 2.4).

2.2 Shallow cumulus ensemble statistics

To develop a stochastic parameterization for shallow cumuli that includes convective memory in its formulation, a detailed description of the cloud ensemble and the processes acting on the scale of an individual cloud is necessary. A large eddy simulation as a cloud-resolving model suffices for the detailed description of the shallow cumuli field in a large horizontal area, while the cloud tracking as a post-processing routine collects the information about every simulated cloud during its lifetime.

2.2.1 Large eddy simulations and cloud tracking

We use the UCLA-LES (University of California, Los Angeles – Large Eddy Simulation) model, a version from Stevens (2010), to simulate shallow convection. The dynamical core of the LES model is based on the Ogura–Phillips anelastic equations, discretised over the doubly periodic uniform Arakawa C-grid (Stevens et al., 1999, 2005). The set of anelastic equations is solved for the prognostic variables: velocity components (u, v, w), total water mixing ratio q_t, liquid water potential temperature θ_l, number ratio of rainwater N_r and mass mixing ratio of rainwater q_r. The time integration is solved using a third-order Runge–Kutta numerical method. A directionally split monotone upwind scheme is used for the advection of scalars, and directionally split fourth-order centered differences are used for the momentum advection. The subgrid fluxes are modelled by the Smagorinsky–Lilly scheme, and the warm-rain scheme of Seifert and Beheng (2001) is used for the cloud microphysics as described in Stevens and Seifert (2008).

In this study, the LES model is set up to simulate the GCSS (GEWEX Cloud Systems Studies) RICO shallow cumulus case, as in van Zanten et al. (2011), see also Appendix A.1. The RICO case is based on the Rain In Cumulus over the Ocean field study (Rauber et al., 2007). It represents the average conditions during an undisturbed period from 16 December 2004 to 8 January 2005 in the trade-wind region over the western Atlantic. The focus of this field study was on the processes related to the

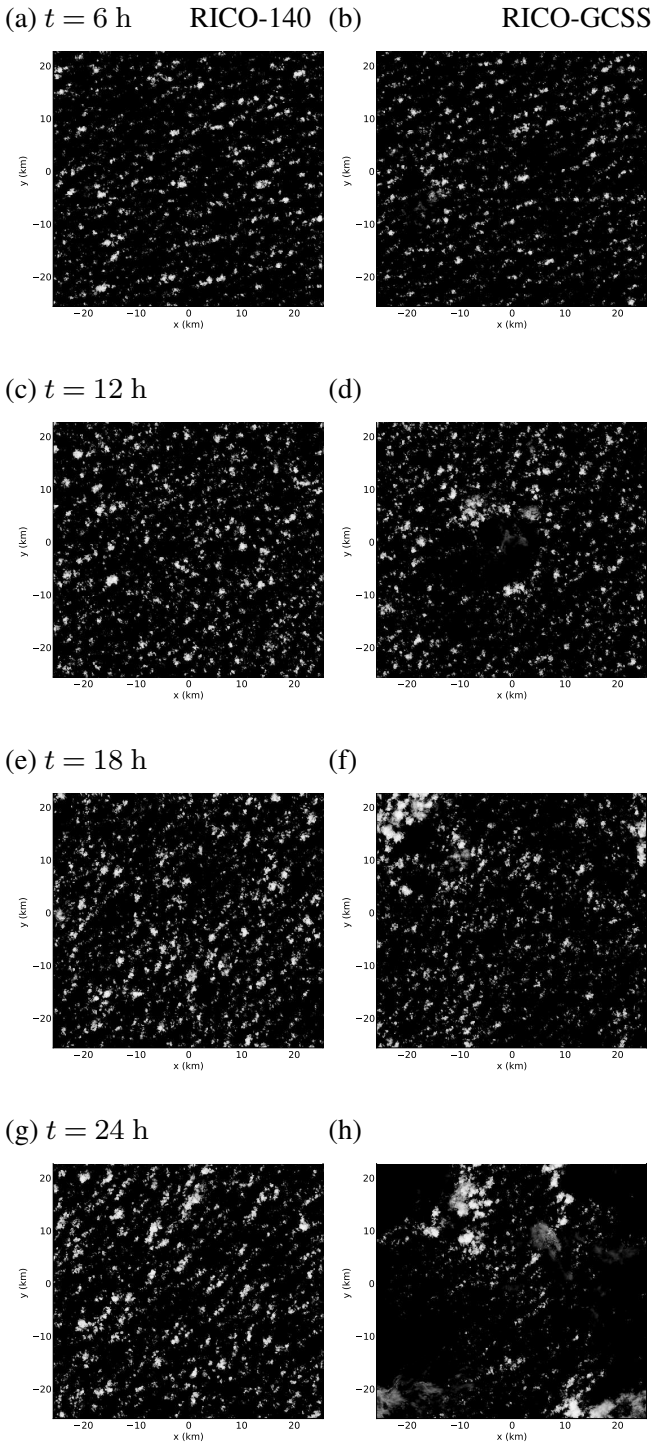

Figure 2.1: Snapshots taken every 6 h during RICO simulations showing the cloud albedo: the higher cloud droplet number density RICO case (RICO-140) vs. the standard RICO case (RICO-GCSS). These horizontal cloud field snapshots are a courtesy of T. Heus. The RICO case simulations are performed by Heus and Seifert (2013)

rain formation in shallow cumuli and on how the rain modifies the individual cloud and the cloud ensemble statistics.

The standard RICO-GCSS case was simulated over a large domain of around 50 km × 50 km, with the horizontal grid spacing of 25 m and vertical resolution of 25 m up to 4 km in height. In such a large domain and on a high-resolution grid, a cloud field can evolve into an organized mesoscale convective system, forming clusters and line-like structures (Seifert and Heus, 2013). This transition to an organized cloud field depends mostly on precipitation rate and, for the RICO-GCSS simulation, the first organized cloud clusters develop around the twelfth hour of the simulation (Fig. 2.1d). In the RICO-140 case, which has a doubled cloud droplet number density, $N_c = 140\,\mathrm{cm}^{-3}$, and is virtually nonprecipitating, the cloud field remains quasi-random, but the individual clouds grow in size throughout the simulation time (Fig. 2.1a, c, e and g). The convective variability in an organized case is, of course, very different from the variability of a quasi-random cloud field. This is discussed in more detail later in Section 2.4.2, where we discuss RICO-GCSS and RICO-140 to quantify the effects of organization, but for most of the analysis we focus on the simple case of the RICO-140 with a quasi-random cloud field.

The cloud tracking algorithm developed by Heus and Seifert (2013) is used as a post-processing tool for the LES simulation results. The tracking is based on the vertically integrated liquid water content, namely the liquid water path. The clouds are projected onto a two-dimensional plane and are identified as consisting of the adjacent points with the liquid water path exceeding a chosen threshold value. Cloud merging and splitting is done in two directions: forward and backward in time. Along with the projected cloud area, cloud buoyant cores, subcloud thermals and rain are tracked during the simulation, with the links among them retained. The choice of the two-dimensional tracking of the projected clouds came from the limitations imposed by the computational expenses and the large memory resources that are required. For more details and validation of the tracking method, see Heus and Seifert (2013).

To develop a cloud parameterization based on the mass flux concept, the cloud mass flux has to be estimated at the cloud-base level. For the RICO case, we choose the level at 700 m, which is the first or second height level above the cloud base during most of the simulation time. Thus, it is necessary to identify the area that every cloud occupies at the 700 m level. Because the liquid water path threshold of $5\,\mathrm{g\,m}^{-2}$ is taken as a definition of a cloudy column in the cloud tracking algorithm and the clouds are projected onto a two-dimensional surface, we check what the error is introduced by the tracking regarding the domain average cloud variables at the 700 m height. We define the cloudy air at the 700 m height level as points holding the liquid water content q_c larger than $0.01\,\mathrm{g\,kg}^{-1}$, which is the same definition as in the LES model analysis. In this way, we are able to test the tracking and the cloud conditional sampling routine, comparing the outcome statistics with the original LES statistics. The relative difference in cloud fraction before and after the tracking is 1.93 %, which is a negligible difference in absolute value, and can be neglected.

2.2.2 Cloud definition and the distribution of cloud-base mass flux

Starting from the sixth hour of RICO simulation to avoid the model spin-up period, we choose several sequential time frames of 6 h duration and apply the tracking method to the cloud field. Each individual cloud in the simulated cloud field is tracked in space and time during its life and cloud properties are recorded each minute of the simulation. Clouds are taken into account only if their existence started during the selected time frame, but if their duration spanned beyond the time frame, they are tracked further on to complete their lifecycles. We study the lifetime average cloud properties, contrary to the instantaneous properties of the cloud field at a single model time step.

How should clouds be defined in a parameterization? A definition of the cloud entity is chosen depending on the processes that will be introduced in a parameterization. We aim for a unified scheme, which will be used to reproduce the cloud fraction, cloud vertical transport of mass and scalars, and possibly also rain formation. Therefore, we test how the distribution of cloud mass flux depends on the choice of the cloud entity as a cloud condensate, cloud buoyant core or a cloud updraft. To identify the points that form the cloud entity on a certain height level, a conditional sampling is performed with the three different criteria (as in Siebesma and Cuijpers, 1995; de Roode et al., 2012):

1. cloud sampling over the points with liquid water content: $q_c > 0\,\mathrm{g\,kg^{-1}}$;

2. buoyant core sampling, by comparing the virtual potential temperature of each cloudy point with the slab average: $\theta_v > \overline{\theta}_v$ and $q_c > 0\,\mathrm{g\,kg^{-1}}$;

3. and cloud updraft sampling over the cloudy points with positive vertical velocity: $w > 0\,\mathrm{m\,s^{-1}}$ and $q_c > 0\,\mathrm{g\,kg^{-1}}$.

Following the work of Cohen and Craig (2006), the mass flux of an individual cloud at a certain height level is defined as

$$m_i = \rho a_i \overline{w_i}, \quad i = 1, 2, \ldots, n, \tag{2.1}$$

where ρ is the domain average density, a_i is the cloud area, $\overline{w_i}$ is the vertical velocity averaged over the cloudy points, and n is the number of clouds (Arakawa and Schubert, 1974).

The cloud-base mass flux of each individual cloud that appeared during the time frame of 6 h (from the sixth to the twelfth hour) is averaged over the cloud lifetime and the distribution of lifetime-averaged mass flux is calculated for all three cloud entity definitions (Fig. 2.2). This distribution is defined as the cloud rate distribution of cloud-base mass flux $g(m,t)\mathrm{d}m\mathrm{d}t$, which gives the number of clouds with the lifetime-average mass flux in the range $[m, m+\mathrm{d}m]$ generated during the time interval $[t, t+\mathrm{d}t]$. The integration of $g(m,t)$ with respect to m results in the cloud generation rate, $G(t)$, which is the number density of clouds generated per unit time:

$$G(t) = \int_0^\infty g(m,t)\mathrm{d}m. \tag{2.2}$$

The total number of clouds in a domain, $N(t)$, can be estimated by integrating the instantaneous distribution $n(m', t)$ with respect to m':

$$N(t) = \int_0^\infty n(m', t)\mathrm{d}m', \tag{2.3}$$

where m' is the instantaneous cloud mass flux. By definition, $n(m', t)\mathrm{d}m'$ gives the number of clouds that exist at the time t with the instantaneous cloud mass flux in the range $[m', m' + \mathrm{d}m']$. The instantaneous distribution describes the cloud field as it exists at a certain moment in time, while the cloud rate distribution carries the information about individual cloud lifecycles. A similar concept is introduced in astrophysics (e.g. Chabrier, 2003), where the time-dependent distribution function called the galactic stellar creation function, corresponding to our $g(m, t)$, is introduced to relate the present-day stellar mass function to the initial stellar mass function. In this study, we are limiting our case to 6 h time frames to stay within a stationary regime. Therefore, the dependence on time in $g(m, t)$ can be left out for notational simplicity, and in the further text we will write $g(m)$. When we are referring to the probability density function, $g(m)$ normalized by G, the notation $p(m)$ will be used.

The shape of $p(m)$ does not depend strongly on the choice of the cloud entity definition (Fig. 2.2). The main factor influencing the shape of $p(m)$ is the liquid water content criterion, which is the reason for the similar look of the three lines in Fig. 2.2. Including buoyancy shifts the distribution slightly towards higher density values. The reason is that only the clouds that are positively buoyant at the 700 m level are taken into account, so the total number of clouds is reduced and some of the smallest clouds are left out. For further analysis we choose to sample the cloud mass flux from a distribution of the cloud ensemble whose elements are defined using the most general cloud definition: connected points holding a cloud condensate, $q_c > 0\,\mathrm{g\,kg^{-1}}$.

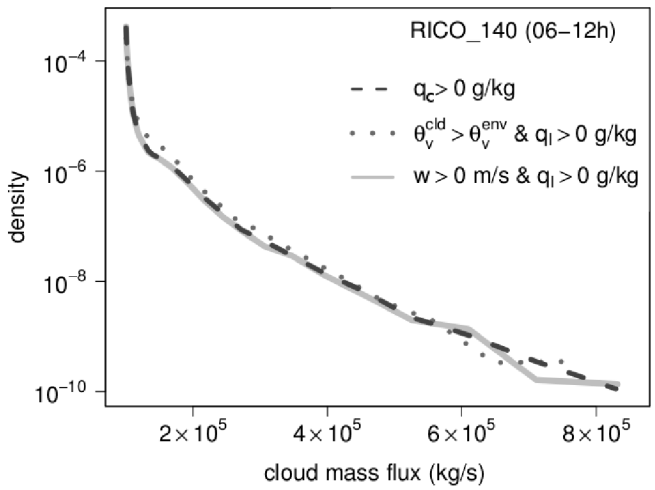

Figure 2.2: Semi-logarithmic plot of the cloud rate probability density function of cloud-base mass flux for the different cloudy point definitions (1–3). This plot corresponds to the RICO-140 simulation time frame of 6–12 h.

2.2.3 Shallow cloud subtypes

The shallow cumulus cloud ensemble is composed of different cloud subtypes (Stull, 1985). Shallow clouds that originate from the convective updrafts overshoot into the inversion layer at the top of the mixed layer. If a cloud has enough inertia to overcome the convective inhibition and reaches the level of free convection (LFC), its growth is fuelled further up. Those are the active buoyant clouds. Clouds that never reach the LFC and remain negatively buoyant above the mixed layer are the forced clouds. Another cloud group is made of passive clouds, which are remnants of the old decaying clouds or are formed due to gravity waves.

Following the definition of an active cloud in the tracking routine as a cloud holding a buoyant core with the maximum in-cloud excess of θ_v exceeding the threshold of 0.5 K (Heus and Seifert, 2013), we divide the cloud ensemble from the RICO-140 simulation (6–12 h time period) into two separate groups: the active-cloud group comprising the clouds with single or multiple buoyant cores, and all the other clouds in the passive-cloud group.

The two different groups of shallow cumuli form the two modes of the cloud rate distribution and the joint distribution of cloud mass flux and other cloud properties (Fig. 2.3). In the RICO cloud ensemble, passive clouds are large in number and can develop a smaller area at the cloud base and transport less mass compared to the active clouds. This can be identified at the cloud rate distribution of cloud-base mass flux, as the passive cloud group takes the lower range of the mass flux and higher probabilities in the distribution, and the active cloud group takes a higher mass flux range and the distribution tail (Fig. 2.3a). In a random shallow cumulus field, small-scale turbulent motion controls the in-cloud processes and the interaction of clouds with their environment. As a result of the quasi-random processes, the cloud fields are highly variable and the cloud properties are vastly diverse. It is obvious that clouds of equal area at the cloud base do not have a unique magnitude of the other cloud properties; they are in fact highly dispersed. However, the joint distribution of cloud mass flux and cloud lifetime shows some correlation, with a Spearman rank correlation coefficient (as defined in Wilks, 2006, p.55) of $r_\rho = 0.79$. This joint distribution can be well approximated with two power-law relations $\tau_i = \alpha_i m_i^\beta$ with $i = 1, 2$ describing a power-law increase in cloud lifetime with the cloud mass flux for each cloud group separately (Fig. 2.3c). Similarly, the two different cloud groups form the two modes of the joint distribution of cloud mass flux and cloud vertical velocity (Fig. 2.3b). In this case the correlation coefficient is $r_\rho = 0.48$ and it is evident that the cloud-base mass flux does not scale with the vertical velocity. Therefore, the lifetime averaged cloud-base mass flux of an individual cloud is mainly controlled by the horizontal area that it occupies at the cloud base.

During the selected 6 h time frame (6–12 h) of the RICO-140 simulation, passive clouds form around 72 % of the total cloud number in the ensemble. Even though a single passive cloud on average contributes less to the upward transport and cloud fractional cover than an active cloud, their collective contribution can not be neglected, because they are large in number and can also live long (see Fig. 2.3c). The contribution of active clouds to the vertical transport of mass and scalars is around 63 %, even though they form only 27 % of the total cloud number in the ensemble, while the contribution of active clouds to the cloud fraction is only slightly higher than the contribution of the passive cloud group, around 54 % (Table 2.1).

(a) cloud rate distribution

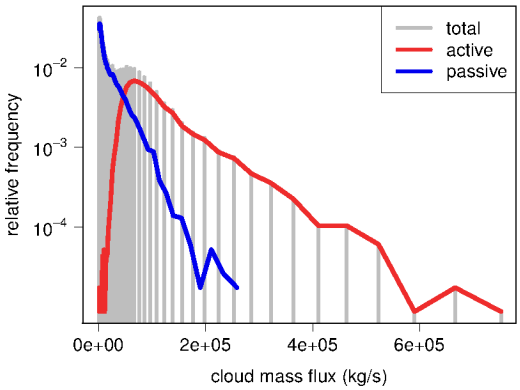

(b) cloud vertical velocity

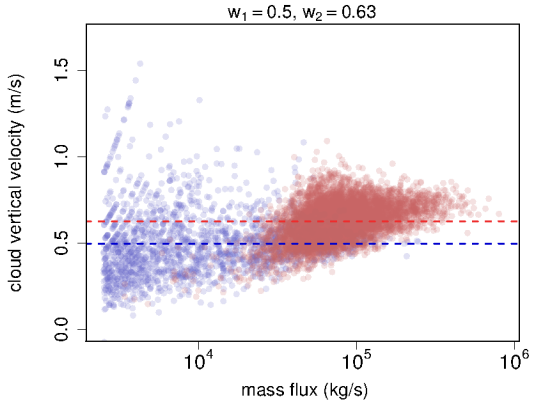

(c) cloud lifetime

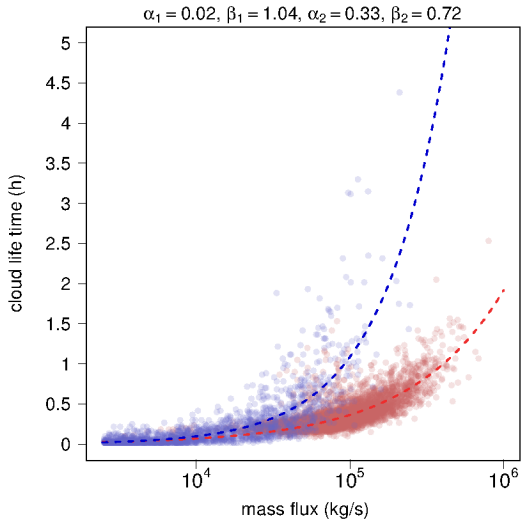

Figure 2.3: a) Cloud rate density distribution of cloud-base mass flux with the split into active and passive distribution modes. b) Scatter plot of the average in-cloud vertical velocity and average cloud mass flux and c) cloud lifetime and average cloud mass flux. Active clouds are shown as red points, while the passive clouds are in blue. The nonlinear least square fit of the relation $\tau_i = \alpha_i m^{\beta_i}$, $i = 1, 2$ is plotted for both cloud groups, with parameters α_i and β_i corresponding to the passive (1) and active (2) cloud groups. Vertical velocity w_i, $i = 1, 2$ is averaged over all clouds in each group and plotted as a horizontal line.

Table 2.1: Contribution of the different cloud subtypes $r_{\langle N\rangle}$, $r_{\langle C\rangle}$ and $r_{\langle M\rangle}$ to the total cloud number $\langle N\rangle$, cloud fraction $\langle C\rangle$ and vertical mass flux $\langle M\rangle$, respectively. Given results are the time averages for the time frame 6–12 h of the LES RICO-140 simulation.

700 m level	Passive (1)	Active (2)	Total
Domain size (km^2)	-	-	51.2^2
$\langle N\rangle$ (no.)	1258.3	476.16	1734.45
$\langle C\rangle$ (–)	0.0206	0.0246	0.0452
$\langle M\rangle$ ($kg\,s^{-1}$)	30.11×10^6	51.82×10^6	81.94×10^6
$r_{\langle N\rangle}$ (%)	72.55	27.45	100
$r_{\langle C\rangle}$ (%)	45.64	54.36	100
$r_{\langle M\rangle}$ (%)	36.75	63.25	100

2.2.4 Canonical cloud ensemble distribution

According to the theory of fluctuations in an ensemble of weakly interacting deep convective clouds that is in statistical equilibrium with the large-scale environment (Craig and Cohen, 2006), the cloud mass flux distribution follows an exponential law

$$p(m) = \frac{1}{\langle m\rangle} e^{-m/\langle m\rangle}, \tag{2.4}$$

where $m > 0$ is the average mass flux of an individual cloud, and $\langle m\rangle$ is the cloud ensemble average mass flux per cloud. This distribution was derived in analogy to the Gibbs canonical distribution of microstates of a physical system.

In the case of shallow convection, the cloud rate distribution of mass flux at the 700 m height level is more complicated than a simple exponential function. This distribution is a superposition of two modes (Fig. 2.4a), due to the existence of different cloud subtypes forming the shallow cumulus ensemble (Stull, 1985): passive clouds in one mode and active buoyant clouds in the second mode (see Section 2.2.3). Forced clouds are not defined separately in the cloud tracking routine, but based on the buoyancy criterion, we can assign them to the passive cloud distribution mode. Furthermore, the cloud rate distribution deviates from the exponential distribution. This is observed from the semi-logarithmic plot in Fig. 2.4a, where the density distribution function does not form a straight line for either of the modes, and the best fit suggests a more general distribution function.

The cloud rate distribution of mass flux is a highly right-skewed distribution with a heavy tail and can be well modelled as a two-component mixture of the generalized exponential distribution (i.e. mixed Weibull distribution, Fig. 2.4a):

$$p(m) = f\frac{k}{\theta_1}\left(\frac{m}{\theta_1}\right)^{k-1} e^{-(m/\theta_1)^k} + (1-f)\frac{k}{\theta_2}\left(\frac{m}{\theta_2}\right)^{k-1} e^{-(m/\theta_2)^k}, \tag{2.5}$$

where f is a fraction of the cloud ensemble belonging to the first passive mode and $1 - f$ is a fraction of the cloud ensemble belonging to the second active mode. The Weibull distribution is a special case of the generalized gamma distribution family and is frequently used in the survival analysis field of statistics to model the physical systems with components that age during the time towards their

failure. The parameters $\theta_1 > 0$ and $\theta_2 > 0$ refer to the scale of the two distribution modes, and parameter $k > 0$ is the distribution shape.

Here we are making a parallel between the cloud mass flux distribution and a lifetime distribution to explain the deviation of the cloud rate distribution of mass flux from the exponential shape through the parameter k. The parameter k introduces the effect of system memory in the cloud rate distribution of mass flux. The two main types of convective memory effects recognized in the CRM studies (Davies et al., 2013) are a memory effect due to the time evolution of a cloud field in a changing environment, and a memory effect due to the finite individual cloud lifetimes. In our case, because of the stationarity assumption, we only include the latter effect, and the distribution shape k is smaller than 1 due to the different and finite lifetimes of individual clouds. This local memory effect is accounted for through the correlation of cloud-base mass flux of individual clouds with their lifetime (see Appendix A.2 for more details).

(a) mixed Weibull distribution fit

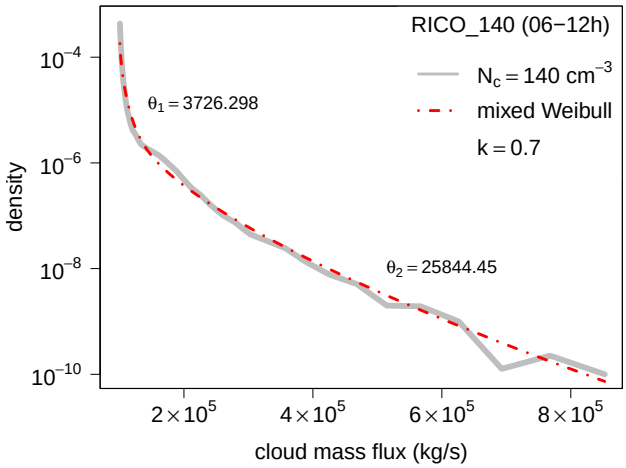

(b) failure rate function h as a count of failures per an interval of mass flux $\Delta m = 10000$ kg/s, conditioned on the lifetime average mass flux

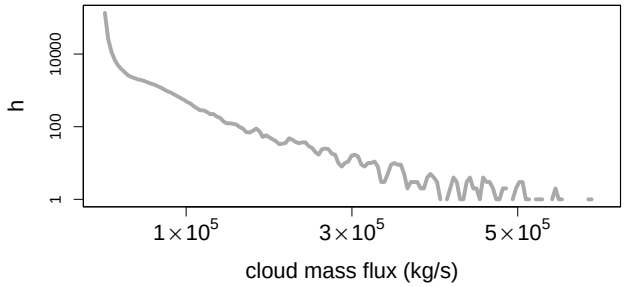

Figure 2.4: Semi-logarithmic plots of the cloud rate density distribution of cloud-base mass flux and the cloud failure rate function. These plots correspond to the RICO-140 simulation time frame of 6–12 h. The cloud rate density distribution is fitted using the *mixdist* R package (R Development Core Team, 2013), and the distribution shape parameter is set as equal for both distribution modes: $k_1 = k_2 = k$.

If the shape parameter lies in the interval $0 < k < 1$, the Weibull distribution describes a cloud population with the failure rate decreasing with the cloud mass flux by following the failure rate function

$$h_i(m) = \frac{k}{\theta_i}\left(\frac{m}{\theta_i}\right)^{k-1}, \quad i = 1, 2, \tag{2.6}$$

where $h(m)$ is the failure rate defined as the frequency of failures per unit mass flux, conditioned on the average mass flux of a cloud. If a cloud has already developed higher mass flux, it is more likely that it will be able to transport an additional portion of the mass through its cloud base compared to a cloud that has developed lower mass flux. The results from LES support the theoretical failure rate function of cloud population, showing a decrease in the failure rate with the cloud-base mass flux (see Fig. 2.4b). In the case of a shallow cumulus population, the Weibull distribution with $0 < k < 1$ provides a good fit to the empirical data, since the cloud ensemble consists of a large number of short-lived clouds in the lower range of the cloud-base mass flux, and with fewer long-lived clouds in the high mass flux range (see Fig. 2.3c).

A special case of the Weibull distribution, when $k = 1$ and the failure rates are constant, i.e. $h(m) = 1/\langle m \rangle$, is the exponential distribution. A population would have an exponential distribution if the system was memoryless and if the system constituents had equal lifetimes. When describing a realistic cloud ensemble, this distribution is likely to be bimodal, with each mode being right skewed and heavy tailed ($0 < k < 1$). This comes from a reasoning that in any cloud ensemble, it is more likely that large clouds will live longer and develop higher mass flux compared to the smaller clouds. In the cloud ensemble of the RICO case, the best fit suggests the shape parameter $k = 0.7$ (Fig. 2.4a). However, the value of parameter k might change with the changes in the large-scale environment and with the emergence of the cloud field organization, since both of these features carry a component of convective memory. We will discuss the sensitivity of the ensemble statistics to this parameter further in Section 2.4.

An important aspect of applying the Weibull distribution to the parameterization of clouds is its potential universality as a cloud mass flux distribution. During the transition of a cloud field from shallow to deep convection, the shape parameter might change from approximately $k = 0.5$ in the case of a shallow cloud field to close to $k = 1$, corresponding to the exponential distribution function which has been suggested for deep convective clouds. With this in mind, it might be possible to unify the parameterization of fluctuations in shallow and deep convective cloud systems within the same scheme. Furthermore, this approach can be considered to be an empirical generalization of the Gibbs formalism to convective cloud systems with memory.

2.2.5 Variability of the small-scale convective states

The domain of the LES RICO-140 simulation is successively divided into areas of different sizes, to mimic the different grid sizes of the stochastic model, and cloud properties are averaged or summed over these areas. In this way, we obtain the distribution of compound subgrid convective states depending on the horizontal resolution of the model.

Figure 2.5 shows the subgrid cloud fraction histograms for the different coarse-graining resolutions: 1.6, 3.2, 6.4, 12.8, and 25.6 km. Small-scale states in each spatial bin vary from the realizations in the surrounding bins, even though the given forcing is spatially uniform and constant in time. The smaller the averaging area, the more possible states exist and histograms become significantly broader, since the averaged values of cloud properties can take wider ranges. The variability arises from a different number of clouds in areas of the same size and from the fact that individual clouds can be stronger or weaker (Plant and Craig, 2008).

The distribution of compound cloud properties changes its shape from exponential-like in the case of high-resolution grids to Gaussian-like for the coarse grids. A grid box in a model with the coarser horizontal resolution will contain a larger number of clouds and the outcomes of the subsampling approach the expected value of distribution (the distribution becomes narrower), which is in agreement with the law of large numbers. This kind of variability results from the small-scale convective processes themselves and does not originate from the changes in large-scale dynamic forcing, though it can be influenced by these changes.

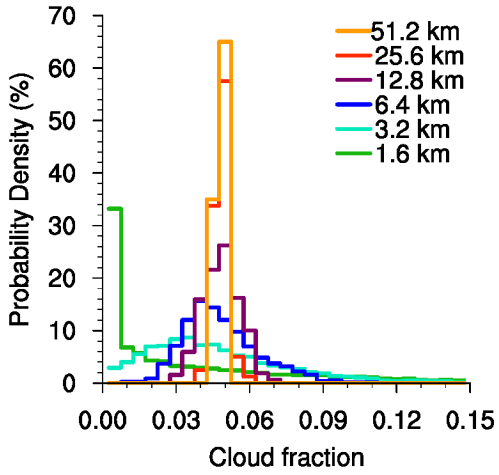

Figure 2.5: Histograms of the fractional cloud cover at the 700 m height level for the different horizontal resolutions of the LES coarse-graining.

2.3 Empirical–theoretical model formulation

According to the parameterization framework of Plant and Craig (2008), a model grid box contains a subset of a cloud ensemble, and represents one possible outcome of the response to the large-scale forcing. Therefore, around each model grid box, we choose a large area A containing the "full" cloud ensemble (Fig. 2.6), assuming that the total mass flux in a cloud ensemble is determined by the large-scale environment. By doing so, we assume that quasi-equilibrium is valid on a large scale. For this assumption to hold, the number of clouds in an ensemble has to be very large so that area A contains the full spectrum of the cloud sizes. For the purpose of this study, we set the large-scale area A to the domain size of the LES RICO simulation.

The initialization of n clouds in the area A is modelled as a random Poisson process and the cloud mass flux m is drawn randomly for each individual cloud from the generalized ensemble distribution (Eq. 2.5) defined for the selected area A around the grid box (see Fig. 2.6). After initialization, the clouds are distributed uniformly over the area A so that in every grid box the distribution of the initialized cloud number also follows the Poisson distribution. A cloud lifetime is assigned to each

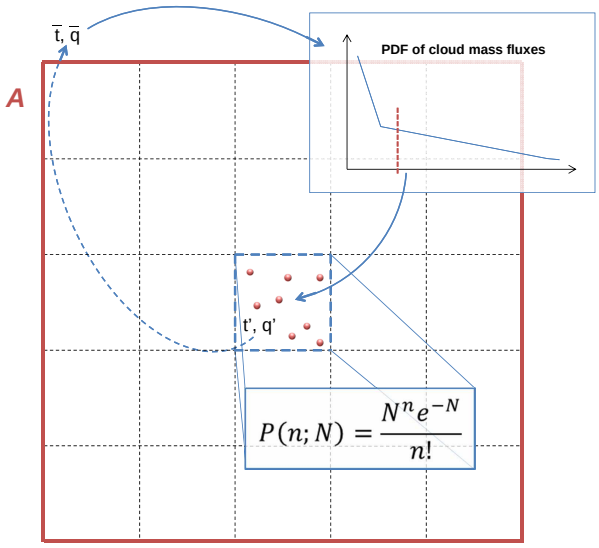

Figure 2.6: Schematic representation of the stochastic PC-2008 approach.

initialized cloud as a function of the cloud mass flux, according to the fit obtained from Fig. 2.3b. During the model run, clouds are treated as individual objects with their own memory and duration. A lifecycle is assigned to each cloud, with the cloud properties changing accordingly, and after the lifetime expires the cloud is removed from the simulation. So, at each model time step, which is set to 1 min, the subgrid convective processes are represented by the effects of all clouds that exist in a grid box, at the different stages of their lifecycles.

The large-scale properties driving the model are the ensemble mean properties: total cloud number $\langle N \rangle$ and total cloud-base mass flux $\langle M \rangle$. In addition, cloud fraction $\langle C \rangle$ is also taken as a third quantity, because we aim for a scheme that unifies the representation of the cloud vertical transport and cloud cover. Thus, as a result of the stochastic modelling, we get the fractional cloud cover C and the total mass flux M in each model grid box, and the correct variability, depending on the choice of the model horizontal resolution (see also Keane and Plant, 2012). With the cloud ensemble statistics formulated in this way, the variability of small-scale states is represented in a physically based manner, resulting from the random and limited sampling (Plant and Craig, 2008).

2.3.1 Counting the clouds

Initialization of new clouds within a model time step is done through a Poisson counting process, after which the clouds are uniformly and randomly distributed over space. In this section we test whether the temporal Poisson distribution holds for the RICO case.

For a process to be described as a random Poisson process, events should be independent of each other and the distribution of events should follow the Poisson distribution. The Poisson distribution is often found in nature, since it results from a process subject to the law of rare events: "where a certain event may occur in any of a large number of possibilities, but where the probability that the event does occur in any given possibility is small, then the total number of events

that do happen should follow, approximately, the Poisson distribution" (Pinsky and Karlin, 2011). This law can be interpreted as a very low probability of occurrence of two exactly identical clouds in a given area, even though this area can contain a large number of clouds. Therefore, according to the law of rare events, the number of generated clouds in the area should approximately follow the Poisson distribution. If we assume that the shallow cumuli are point-like events with a low probability of occurrence and that the events occur randomly but with a constant cloud production rate G, as in Craig and Cohen (2006), the probability that n clouds will be generated in a domain during the time interval $(t, t + \Delta t]$ is given by the Poisson distribution

$$p(n) = \frac{(G\Delta t)^n e^{-G\Delta t}}{n!}, \quad n = 0, 1, 2, \ldots \tag{2.7}$$

Consequently, we assume that the distribution of the total number of clouds in a domain also approximately follows the Poisson distribution. This approximation is necessary for the estimation of variance of the compound cloud mass flux distribution in Section 2.3.3.

To test the validity of an assumption for the Poisson distribution, we show the empirical histogram of the total number of clouds in the LES RICO case domain, and a fit to the theoretical Poisson model for the 6 h period of simulation (Fig. 2.7b). The rate parameter for the distribution fit is estimated from empirical LES-RICO results using the method of moments. Even though the RICO case is not ideally stationary (the number of clouds has a decreasing trend, see Fig. 2.7a), for a limited time period of 6 h, these two distributions are similar. Figure 2.7c shows the quantile–quantile plot (Q–Q plot as defined in Wilks, 2006) with the points representing the pairs of quantiles of the theoretical vs. empirical distributions. The two distributions match closely, with the points lying approximately on the straight $x = y$ line.

(a) total cloud number time series (6-12 h)

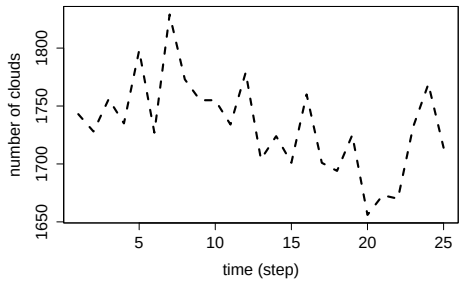

(b) histogram of the total cloud number

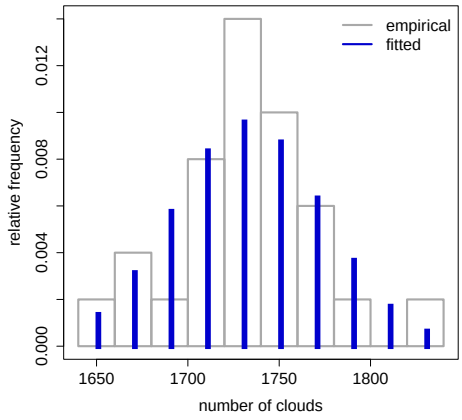

(c) Q-Q plot

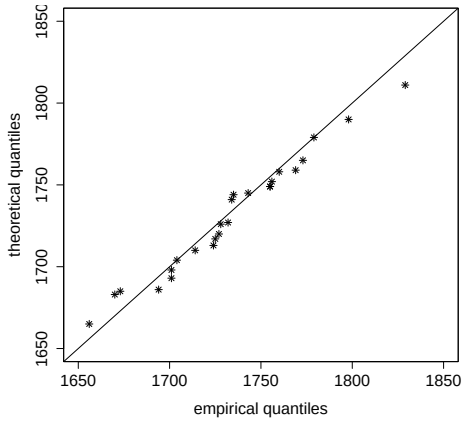

Figure 2.7: The total cloud number time series, and a corresponding histogram plot with a fit to the Poisson model, and a Q–Q plot as a goodness of fit test. The distribution is fitted using the method of moments, while the histograms and Q–Q plots are made using R libraries (R Development Core Team, 2013). The time interval between the snapshots is 10 min.

2.3.2 Closure for the distribution parameters

The cloud rate distribution of cloud mass flux $g(m)$ relates to the instantaneous distribution $n(m')$ through the information about the cloud lifetime $\tau(m)$. So, in the ensemble average limit, we can assume that

$$\langle g(m)\rangle = \frac{\langle n(m)\rangle}{\langle \tau(m)\rangle}. \tag{2.8}$$

Because of the stationarity, the ensemble average equals the time average in our case and will be denoted with $\langle . \rangle$. Note that a similar relation is also used for the galactic stellar creation function as a product of the distribution of stars (mass function) and their formation rate (function of time) (e.g. Chabrier, 2003, Eq. 6). This relation is also implicitly used in the scheme of Plant and Craig (2008).

We approach the formulation of closure by approximating the cloud rate distribution of mass flux with a two-component mixed Weibull function

$$g(m) = \sum_{i=1}^{2} G_i \frac{k}{\lambda_i^k} m^{k-1} e^{-(m/\lambda_i)^k}, \tag{2.9}$$

with scale parameters λ_i and shape parameter k related to the average mass flux per cloud as $\langle m\rangle_i = \lambda_i \Gamma(1+\frac{1}{k})$. The cloud generating rate G, as the number of generated clouds per second in a given area, is the intensity parameter of the Poisson distribution, and the index i refers to the two cloud subtypes (see Section 2.2.3).

The ensemble average number of clouds in a domain can be derived by integrating the instantaneous distribution of cloud mass flux:

$$\langle N\rangle = \int_0^\infty \langle n(m')\rangle \mathrm{d}m' = \int_0^\infty \langle \tau(m)\rangle \langle g(m)\rangle \mathrm{d}m. \tag{2.10}$$

We use a power-law relation for the cloud lifetime dependence on the cloud mass flux:

$$\tau_i = \alpha_i m^{\beta_i}, \quad i = 1, 2. \tag{2.11}$$

The parameters α_i and β_i for the two cloud subtypes are obtained from the nonlinear least square fitting of the joint distribution of cloud mass flux and cloud lifetime (Fig. 2.3c).

After substitution of Eqs. (2.9) and (2.11) into Eq. (2.10) and integration, we get an expression for the ensemble mean number of clouds:

$$\langle N\rangle = \sum_{i=1}^{2} \langle N_i\rangle = \sum_{i=1}^{2} G_i \alpha_i \lambda_i^{\beta_i} \Gamma\left(1 + \frac{\beta_i}{k}\right). \tag{2.12}$$

An expression for the ensemble mean cloud fraction $\langle C\rangle$ can be derived using the Riemann–Stieltjes integration of the instantaneous distribution function

$$\langle C\rangle = \int_0^\infty \langle a(m')\rangle \, \langle n(m')\rangle \mathrm{d}m', \tag{2.13}$$

where $a(m')$ is the instantaneous cloud area just above the cloud base (700 m level). From the definition of the cloud mass flux it follows that the lifetime-averaged cloud area is $a(m) = m/(\rho\overline{w})$, and we assume that the density equals $\rho = 1\,\mathrm{kg\,m^{-3}}$ for notational simplicity. The average vertical velocity is also a closure parameter, and here we simplify it by using an average over all clouds, $\overline{w} = \langle M\rangle/(\langle C\rangle A)$. By applying the relation between the instantaneous and cloud rate mass flux distribution Eq. (2.8), we get

$$\langle C\rangle = \int_0^\infty \langle a(m)\rangle\langle\tau(m)\rangle\langle g(m)\rangle \mathrm{d}m. \tag{2.14}$$

After substitution and integration, and assuming that $\overline{w}$ is constant among individual clouds, we find

$$\langle C\rangle = \sum_{i=1}^{2}\langle C_i\rangle = \sum_{i=1}^{2}\frac{G_i\alpha_i}{\overline{w}\rho}\lambda_i^{1+\beta_i}\Gamma\left(1+\frac{1}{k}+\frac{\beta_i}{k}\right), \tag{2.15}$$

and, similarly, for the total cloud mass flux,

$$\langle M\rangle = \sum_{i=1}^{2}\langle M_i\rangle = \sum_{i=1}^{2}G_i\alpha_i\,\lambda_i^{1+\beta_i}\Gamma\left(1+\frac{1}{k}+\frac{\beta_i}{k}\right). \tag{2.16}$$

When $k = 1$, Eqs. (2.12)–(2.16) describe a system with exponentially distributed cloud-base mass flux. In the case of a constant cloud lifetime among all clouds in the ensemble, Eqs. (2.12)–(2.16) reduce to

$$\langle N\rangle = \sum_{i=1}^{2}G_i\tau_i, \tag{2.17}$$

$$\langle C\rangle = \sum_{i=1}^{2}\frac{G_i}{\overline{w}\rho}\tau_i\frac{\lambda_i}{k}\Gamma\left(\frac{1}{k}\right), \tag{2.18}$$

$$\langle M\rangle = \sum_{i=1}^{2}G_i\tau_i\frac{\lambda_i}{k}\Gamma\left(\frac{1}{k}\right). \tag{2.19}$$

This formulation results in a system of two equations, Eqs. (2.12) and (2.15) or Eq. (2.16), with three unknowns, G, $\langle m\rangle = \lambda\Gamma(1+\frac{1}{k})$ and k, for each cloud subtype. For the purpose of this study, we set the parameter k to 0.7 for both cloud groups, as estimated from the empirical RICO case distribution (Fig. 2.4a). The parameters of the power-law relation for the cloud lifetime Eq. (2.11), α_i and β_i, $i = 1, 2$, are estimated from the empirical results from LES and are of secondary importance for the variability in our model (see Section 2.4.2). This leaves us with a closed system, if the ensemble average number of clouds $\langle N_i\rangle$ and cloud fraction $\langle C_i\rangle$ or cloud-base mass flux $\langle M_i\rangle$ are known, and the stochastic model can be constrained to reproduce the correct ensemble average statistics and the small-scale variability. In this study we focus on the variability of convection when the forcing is constant and the ensemble average properties are taken as known quantities from the results of the cloud tracking.

However, in a large-scale numerical model, it is not likely that the information about the total cloud number in a domain will be available. It would also be useful if the distribution parameters were

constrained by the closure formulation as dependent on the large-scale model quantities, so that the distribution shape could change with the cloud field evolution. To avoid counting the clouds and fitting the cloud number and cloud mass flux distribution empirically, a more robust quantity could be used – the average lifetime per cloud, $\langle\tau\rangle = \langle N\rangle/G$. In a large-scale model, the constraint on $\langle M\rangle$ or $\langle C\rangle$ is given from the resolved scales in an existing mass flux parameterization, and the information necessary to divide the cloud ensemble into passive and active cloud groups is available from the separate treatment of the active and passive cloudiness (for example, see Neggers, 2009). Therefore, the closure of $\langle m\rangle$ and $\langle\tau\rangle$ has to be developed from empirical studies or from theory, so that we are left with the two equations and two unknowns: G and k. In the PC-2008 scheme, as a first approximation, the parameters $\langle m\rangle$ and $\langle\tau\rangle$ are set to a constant value, though they might depend on the changes in the large-scale environment. We assume that this approximation holds for the RICO simulation, since the cloud evolution is quasi-stationary and the forcing is constant. Results from the cloud tracking of RICO clouds support this approximation (Table 2.2). For the three successive time frames from 6 to 24 h of simulation, the average mass flux per cloud is around 1×10^5 kg s^{-1} for the active cloud group and around 1×10^4 kg s^{-1} for the passive cloud group, and the average lifetime is roughly 20 min for active clouds and 5 min for passive clouds.

Table 2.2: Model closure parameters estimated from the cloud tracking results.

Parameter	Unit	6–12 h	12–18 h	18–24 h
$\langle m\rangle$	kg s^{-1}	1.91×10^4	1.82×10^4	1.67×10^4
$\langle m_1\rangle$	kg s^{-1}	1.05×10^4	1.04×10^4	1.12×10^4
$\langle m_2\rangle$	kg s^{-1}	8.87×10^4	8.97×10^4	10.16×10^4
$\langle\tau\rangle$	min	7	5	3
$\langle\tau_1\rangle$	min	5	4	3
$\langle\tau_2\rangle$	min	20	18	18

2.3.3 The variance of compound distribution

The total mass flux M in a model grid box can be interpreted as a random sum of the individual cloud mass fluxes of a random number of clouds n (as in Craig and Cohen, 2006):

$$M = \sum_{i=1}^{n} m_i, \tag{2.20}$$

where the cloud mass flux is constant during the cloud lifetime, so that $m' = m$. We assume that the total number of clouds in some region (or a model grid box) follows the Poisson distribution

$$p(n) = \frac{\hat{N}^n e^{-\hat{N}}}{n!}, \quad n = 0, 1, 2, \ldots \tag{2.21}$$

which can be justified with the good fit to the empirical results (Fig. 2.7). Here $\hat{N}$ is the average number of clouds within a model grid box. In the case of the Weibull-distributed lifetime-average

cloud mass flux, the distribution at a certain instant in time is given by

$$p(m') = \frac{\tau(m)}{\langle\tau\rangle}\frac{k}{\lambda^k}m^{k-1}e^{-(m/\lambda)^k}, \tag{2.22}$$

where $\langle\tau\rangle$ is the average lifetime per cloud.

The probability distribution of the sum of n independent identically distributed random variables m, conditioned on the number n, is the compound distribution or the distribution of the random sum

$$p(M) = \sum_{n=1}^{\infty} p(n)f^n(M), \tag{2.23}$$

where $f^n(M)$ is the n-fold convolution of $p(m')$ as defined in (Pinsky and Karlin, 2011, p.74). Properties of this distribution depend on the random number of clouds n and are analysed empirically for the RICO case in Section 2.2.5. In the case of exponentially distributed individual cloud mass fluxes, this distribution is defined as the compound Poisson distribution of cloud population, and can be analytically expressed (Eq. 14 in Craig and Cohen, 2006).

By definition, the expected value of a compound distribution can be expressed as

$$E[M] = E[n]E[m] \tag{2.24}$$

and the variance as

$$\mathrm{Var}[M] = E[n]\mathrm{Var}[m] + (E[m])^2\mathrm{Var}[n] \tag{2.25}$$

(Pinsky and Karlin, 2011).

In a cloud field with variable cloud lifetime and Weibull distributed cloud mass flux, the expected value of the compound distribution is

$$E[M] = \hat{N}\frac{\alpha}{\langle\tau\rangle}\lambda^{\beta+1}\Gamma\left(\frac{\beta+k+1}{k}\right), \tag{2.26}$$

and the variance is

$$\mathrm{Var}[M] = \hat{N}\frac{\alpha}{\langle\tau\rangle}\lambda^{\beta+2}\Gamma\left(\frac{\beta+k+2}{k}\right). \tag{2.27}$$

The variance of the compound distribution that encompasses the diversity of cloud lifetimes depends on the average number of clouds in a region $\hat{N}$, average cloud mass flux $\langle m\rangle$ functioning through λ and k, the β exponent from the lifetime relation, and the average lifetime per cloud $\langle\tau\rangle$. The average cloud lifetime is defined as

$$\langle\tau\rangle = \langle N\rangle/G = \alpha\lambda^{\beta}\Gamma\left(\frac{\beta+k}{k}\right). \tag{2.28}$$

Please note that in Eq. (2.28) $\langle N\rangle$ corresponds to the full convective ensemble in a large equilibrium area, while $\hat{N}$ introduced in this section corresponds to the model grid box of an arbitrary size.

To test the scale adaptivity of the compound distribution variance, we derive the relation to describe how the normalized variance of total mass flux changes with the average number of clouds:

$$\frac{\mathrm{Var}[M]}{(E[M])^2} = \frac{\Gamma\left(\frac{\beta+k}{k}\right)\Gamma\left(\frac{\beta+k+2}{k}\right)}{\Gamma^2\left(\frac{\beta+k+1}{k}\right)}\frac{1}{\hat{N}}. \tag{2.29}$$

When $k = 1$, this reduces to the expression valid for the exponential function case with the cloud lifetimes defined as Eq. (2.11) for a single exponential mode:

$$\frac{\mathrm{Var}[M]}{(E[M])^2} = \frac{(\beta+2)}{(\beta+1)}\frac{1}{\hat{N}}, \tag{2.30}$$

and furthermore, if it is assumed that the lifetimes of all clouds are equal, this reduces to

$$\frac{\mathrm{Var}[M]}{(E[M])^2} = \frac{2}{\hat{N}}, \tag{2.31}$$

as in Craig and Cohen (2006, their Eq. 18).

2.3.4 Cloud lifecycle

In the case of shallow convection, large variability in the cloud size and cloud lifetime can be found. Individual shallow clouds can have a lifetime ranging from a couple of minutes to several hours. Therefore, in contrast to the PC-2008 where the cloud lifetime is constant among different clouds, we introduce the varying cloud lifetime depending on the cloud mass flux and we model the cloud lifecycles explicitly.

On the convection-permitting scales of resolved motion, the subgrid shallow convection is in a nonequilibrium regime, i.e. there is no timescale separation between the subgrid and resolved processes. To adjust to the changes in forcing, convection requires a finite time that can span longer than the model time step. This timescale is referred to as the convective adjustment or the closure timescale in the literature. Using cloud-resolving simulations of deep convection, Davies et al. (2013) identified another memory timescale that is not carried by the large-scale mean thermodynamic fields, but by the structures on the near-cloud scale. These structures are the result of individual clouds modifying their environment throughout their lifecycles. This type of convective memory expresses itself through the effects of past convection modifying the convection at the present time. A first step to introducing the aspects of these two timescales of convective memory into the parameterization is to represent the cloud lifecycles explicitly.

The cloud lifetime of individual clouds $\tau(m)$ can be evaluated empirically from LES (Fig. 2.3c) by approximating the joint distribution of cloud mass flux and cloud lifetime with a simple power-law relation Eq. (2.11). This distribution is highly dispersed and the power-law fit is biased by the smallest clouds that are large in number. The implications of this crude simplification of a highly dispersed joint distribution are not significant, and will be explained further in Section 2.4.

(a) short lifetime, $\tau < 30$ min

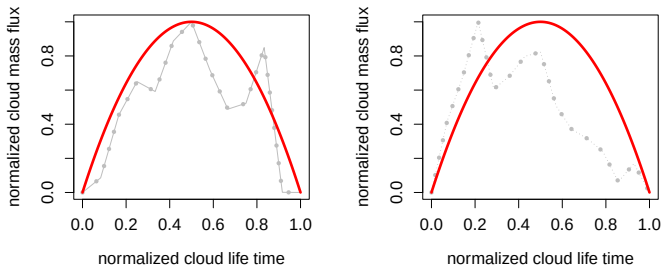

(b) medium lifetime, $30 < \tau < 60$ min

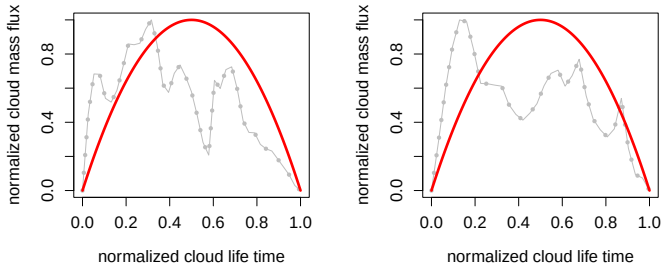

(c) long lifetime, $\tau > 60$ min

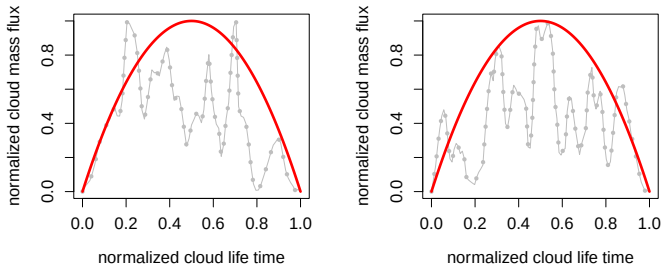

Figure 2.8: Idealized function for the cloud lifecycle (red line) and the examples of individual cloud lifecycles (gray dots) from the LES RICO-140 case, after the cloud tracking. The purpose of this plot is to describe the actual lifecycles of LES clouds and their vast variability. The red curves are not intended to actually fit the LES cloud lifecycles.

Having the average mass flux of each cloud in a model grid box, an idealized cloud lifecycle can be assigned to each cloud following a simple lifecycle function

$$\frac{m'}{m} = \frac{3}{2}\left|4 \cdot \frac{t}{\tau}\left(\frac{t}{\tau} - 1\right)\right| \tag{2.32}$$

(similar to Herbort and Etling, 2011, where a sine function was used for the temporal development of deep convective shower cells). The cloud mass flux of each cloud at each time step m' is normalized by the lifetime average cloud mass flux m and changes according to Eq. (2.32) as a function of the normalized cloud time t/τ. The empirical cloud lifecycles from LES and cloud tracking results are much more complicated than the idealized cloud lifecycle function (Fig. 2.8). Smaller, short-lived clouds follow the idealized cloud lifecycle function more closely (Fig. 2.8a), compared to the longer-lived clouds (Fig. 2.8b). The discrepancy from Eq. (2.32) is especially pronounced if the cloud is a long-lived multi-pulse entity (Fig. 2.8c). We approach the modelling of the cloud lifecycle

function without statistically fitting the actual LES cloud lifecycles, but instead the idealized function Eq. (2.32) is used to prove that the details in the exact lifecycle function shape are not a necessary requirement to model the variance of subgrid cloud properties correctly (see Section 2.4.3). In the previous section, derivation of the total mass flux variance (Eq. 2.29) did not incorporate the cloud lifecycle function (Eq. 2.32), and only the variability in the cloud lifetimes in a convective ensemble was taken into account.

2.4 Tests with different levels of model complexity

The goal of every parameterization is to represent the subgrid processes using a simplified conceptual approach and as few parameters as possible, but on the other hand the simplification of process formulation should not degrade the quality and level of produced information. The consistency of the parameterization assumptions can provide a valuable guidance to choose a certain set of assumptions over another. In the following, we compare different formulations of the stochastic model, to test what the level of complexity necessary to model the shallow convective cloud ensemble is, and discuss possible inconsistencies, especially in simplified models. The stochastic model should reproduce the ensemble average quantities and the variability of subgrid convective states.

The stochastic model is run as an ensemble with 50 members on the horizontal domain of 51.2 km × 51.2 km. The ensemble model runs are performed multiple times with the different model formulation and each of these runs is repeated five times using the different horizontal grid resolutions of the stochastic model: 1.6, 3.2, 6.4, 12.8, and 25.6 km. The empirical coarse-grained LES quantities (Section 2.2.5) are used for the validation of results from the stochastic model ensemble runs. To stay within the quasi-stationary regime of the RICO case, we limit the time frame to 6 h, focusing on the time period from the sixth to the twelfth hour of the simulation.

Table 2.3: Parameters for the model formulation with the two-component mixed Weibull distribution.

Parameter	Value	Unit
Domain size	51.2^2	km^2
k	0.7	–
λ_1	7269.08	$\mathrm{kg\,s^{-1}}$
λ_2	29 868.46	$\mathrm{kg\,s^{-1}}$
f_1	0.81	–
f_2	0.19	–
G	4.55	$\#\,\mathrm{s^{-1}}$
G_1	3.69	$\#\,\mathrm{s^{-1}}$
G_2	0.86	$\#\,\mathrm{s^{-1}}$
α_1	0.02	$\mathrm{kg^{-1}}$
β_1	1.04	–
α_2	0.33	$\mathrm{kg^{-1}}$
β_2	0.72	–
$\overline{w}$	0.69	$\mathrm{m\,s^{-1}}$

Distribution parameters are estimated as a function of the large-scale quantities: ensemble average cloud cover $\langle C_i \rangle$, total mass flux $\langle M_i \rangle$ and total number of clouds in a domain $\langle N_i \rangle$, which are taken from the LES tracking results (Table 2.1). The distribution parameters, λ_i, $i = 1, 2$ for the cloud rate mass flux distribution and G_i, $i = 1, 2$ for the Poisson cloud number distribution, are calculated using Eqs. (2.12)–(2.16), and their values are given in Table 2.3. Estimation of the parameters in this way ensures that the model reproduces the correct ensemble average quantities.

The fraction of the active cloud mode is calculated as $f_2 = G_2/(G_1 + G_2)$ and the fraction of the passive cloud mode as $f_1 = 1 - f_2$ (Table 2.3). The cloud-base mass flux is sampled for each cloud individually, depending on the group it belongs to, following the procedure for generating the random variates from the mixed exponential function described in Wilks (2006, p. 127). The choice for the splitting into two groups is given by generating a random number $f = [0, 1]$. The initialized cloud becomes active if the fraction f is less than f_2; otherwise, it is assigned to the passive cloud group.

2.4.1 Generalization of the exponential distribution

In this section, we compare the performance of the stochastic model depending on the choice for the cloud rate distribution, starting from a single-parameter single-mode exponential function and then gradually increasing the distribution complexity by adding a second mode and one more parameter – the distribution shape.

Compared to the LES domain average statistics, the cloud ensemble average properties are reproduced well using the different formulations of the stochastic model, with the relative error below 0.6 % (Table 2.4 showing the mixed Weibull case). Low errors in the ensemble average quantities prove that the model equations and the numerical methods are consistent with the theoretical model formulation.

Table 2.4: Ensemble average cloud properties resulting from the stochastic model ensemble runs with the different horizontal resolutions.

Mixed Weibull distribution function with the explicit cloud lifecycles						
Resolution (km)	$\langle N \rangle$ (no.)	Error (%)	$\langle C \rangle$ (–)	Error (%)	$\langle M \rangle$ (kg s^{-1})	Error (%)
1.6	1724.95	0.55	0.04515	0.15	81 810 364	0.15
3.2	1725.10	0.54	0.04517	0.11	81 847 963	0.11
6.4	1725.81	0.50	0.04511	0.25	81 730 366	0.25
12.8	1726.21	0.47	0.04510	0.27	81 716 417	0.27
25.6	1724.41	0.58	0.04511	0.25	81 730 047	0.25

From the snapshots taken over six hours of simulation (6–12 h), the frequency distributions of the compound cloud mass flux at the 700 m height level are constructed for the different horizontal resolutions of the stochastic model and compared with the coarse-grained LES results (Fig. 2.9). It can be concluded, already by visual inspection, that the LES and the stochastic model frequency distributions are highly similar. Limited sampling of the cloud ensemble produces a correct frequency distribution of the subgrid convective states for the different choices of the model grid size. This signifies that the stochastic model is scale-adaptive and that the variability of small-scale convective states depends on

the model grid resolution. There is a lack of variability when the cloud mass flux is sampled from an exponential function with constant cloud lifetime (exp. $\tau = 20$ min, Fig. 2.9). This model set-up would correspond to the prescribed exponential function for deep convection in PC-2008, with the constant cloud lifetime $\tau = 45$ min. Thus, in a shallow convective case, a more complicated distribution function that encompasses the effect of cloud lifecycles should be used. This statement is supported by the improvement in performance of the stochastic model in the case of a mixed Weibull distribution including the explicit cloud lifecycles (mix wei. $\tau = \alpha m^{\beta}$, Fig. 2.9). The reason for this improvement could be the generalization of the cloud rate distribution, the introduction of the second distribution mode, the introduction of the cloud lifecycles, or a combination of all three. We examine all three reasons in the rest of this chapter.

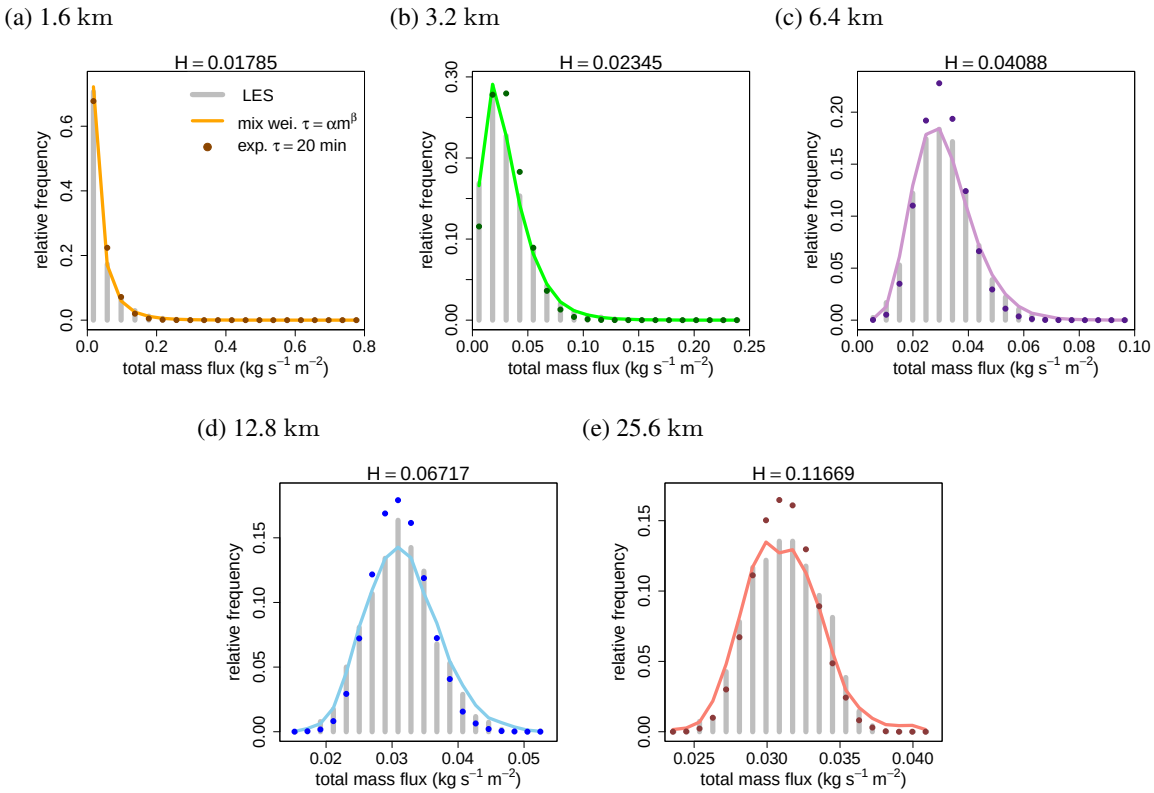

Figure 2.9: Histograms of the compound cloud mass flux at the 700 m height level normalized by the grid box area of the different horizontal resolution: coarse-grained LES tracking results vs. stochastic model results. Plots show the two stochastic model cases: a two-component mixed Weibull case with explicit cloud lifecycles ($k = 0.7$; coloured lines) and a single-mode exponential case without cloud lifecycles ($k = 1$; coloured dots). Colours also correspond to Fig. 2.5. Hellinger distance H stands for the mixed Weibull case.

As a tool for quantitative comparison between the frequency distribution resulting from different runs of the stochastic model and the reference distribution obtained from the LES coarse-graining, we use the Hellinger distance as a measure of distribution similarity. The Hellinger distance H between the two discrete probability distributions P and Q is defined as

$$H(P,Q) = \frac{1}{\sqrt{2}} \sqrt{\sum_{i=1}^{k} (\sqrt{p_i} - \sqrt{q_i})^2}, \tag{2.33}$$

where p_i and q_i are the corresponding probability measures. A useful property of the Hellinger distance is its skew independence, which enables us to compare the scores between the distribution pairs of different skewness resulting from the different choice of horizontal grid resolution (Fig. 2.9).

The Hellinger distance H confirms a high level of similarity between the distributions of different resolution pairs, with the H values in a very low range, from 0.018 to 0.12 (Fig. 2.9a–e). Comparison of the results from the stochastic model set-up using a single exponential function vs. a mixed exponential or a mixed Weibull function via Hellinger distance shows the importance of modelling the two distribution modes for each cloud group separately (Fig. 2.10). For the distribution similarity, the introduction of the second mode in the cloud rate distribution (mix exp. vs. exp., Fig. 2.10) has a larger impact than the explicit modelling of the cloud lifecycles (exp. $\tau = \alpha m^{\beta}$ vs. exp. $\tau = 20$ min, Fig. 2.10). The difference in performance of a mixed exponential case vs. a mixed Weibull case (i.e. $k = 1$ vs. $k = 0.7$) is not so evident from the point of view of frequency distribution match, but it becomes distinct for evaluation of the variability measure (see Section 2.4.2).

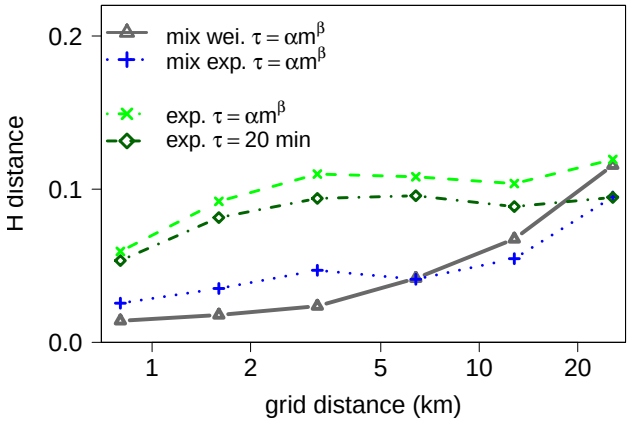

Figure 2.10: Comparison of the Hellinger distance between the distribution pairs from simulations using different model configurations: a single exponential (exp.) configuration with and without cloud lifecycles, and a mixed exponential (mix exp.) and mixed Weibull (mix wei.) configuration with explicit cloud lifecycles.

2.4.2 Quantifying the variability

According to the theory of fluctuations in a convective ensemble (Section 2.3.3), the normalized variance of the compound distribution scales inversely with the cloud number following Eqs. (2.29)–(2.31). With the increasing complexity of the cloud rate distribution, from a single mode exponential

to a mixed Weibull distribution, the variance of subgrid convective states becomes more accurately represented (Fig. 2.11a), taking the LES coarse-grained variance scaling (RICO_140 6–12 h) as a reference case.

The magnitude of normalized variance is controlled by the number of clouds in the subgrid regions. The smaller the grid box, the smaller the number of clouds it can contain, and the variance gets higher. Here, the cloud lifecycles play a role as well, since the cloud number will be influenced by the individual cloud lifetimes (see Section 2.4.3). The effect of introducing a second distribution mode (exp. to mix exp.) on the variance scaling is approximately equal to the effect of a generalization of the cloud rate distribution from exponential to Weibull (mix exp. to mix wei., Fig. 2.11a). The latter points to the fact that the shape parameter k has a significant impact on the variance (Fig. 2.11b and Eq. 2.29), since the change from a mixed exponential to a mixed Weibull distribution happens through the change in k from 1 to 0.7. The effect of excluding the explicit cloud lifecycles from the model formulation using a single exponential distribution mode (exp. $\tau = 20$ min, Fig. 2.11a) is a minor and negligible improvement, but it still reveals a more correct formulation of the model.

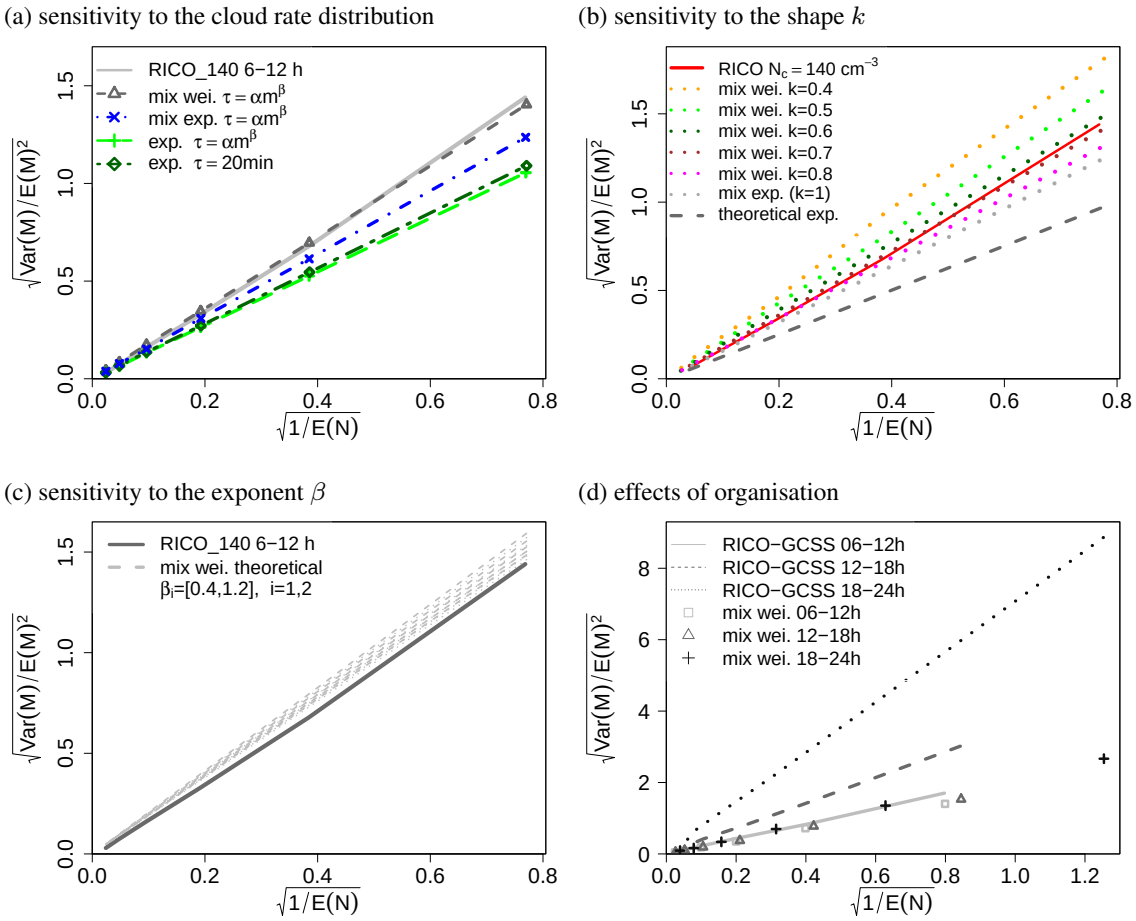

Figure 2.11: The variance of compound mass flux as a function of the inverse cloud number. Cloud lifecycles are explicit in all simulations and the time frame is 6–12 h, if not stated otherwise. The grid size is decreasing from the left (50 km) to the right (1 km) side of the graph.

The parameter k controls the range of the cloud mass flux that can be sampled from the probability density function in the model. Setting the value of the shape parameter to $0.6 \leq k \leq 0.7$, the stochastic model generates a cloud ensemble with a large number of short-lived small clouds and fewer large clouds, which fits the cloud ensemble of the RICO case (Fig. 2.11b). When increased to $k = 1$ (mix exp. Fig. 2.11b), this parameter describes a cloud ensemble of equal lifetimes not depending on the cloud size. Constrained by the model formulation, the exponential probability distribution function, from which the cloud mass fluxes are sampled, does not span across a large enough range of the cloud mass flux values to match the results from the LES. With the decrease in k, the sensitivity of the variance scaling becomes higher, which means that in a cloud ensemble with more diversity in the cloud lifecycles, the shape of the distribution changes faster with the further increase in diversity.

The sensitivity of the stochastic model is also tested with regard to the exponent of the cloud lifetime relation, β. A relatively large range for β_i, $i = 1, 2$ is explored (Fig. 2.11c), and Eq. (2.29) is used as a theoretical model for this test. The variability of convection does not depend highly on the exponent β of the cloud lifetime relation Eq. (2.11), as long as the lifetime increases with the cloud mass flux following a power law within the dispersion range of Fig. 2.3c.

The stochastic model was constructed using the assumption of a random cloud field with noninteracting cloud elements (clouds could interact only through the large-scale flow). From the results presented in Figs. 2.9 and 2.11, we conclude that this assumption is valid for a quasi-random cloud field (Fig. 2.1a–c, e, and g) before the emergence of cloud clusters or arcs. With the ageing of the cloud field, the variability does not change unless the cloud field starts to show a pronounced spatial organization. Therefore, we test the effects of organization on the variability of small-scale convective states (Fig. 2.11d). The variance produced by clustering of the clouds in the time frame from 12 to 18 h (Fig. 2.1d, f) and organization into the mesoscale structures during the time frame from 18 to 24 h (Fig. 2.1f, h) have approximately the same magnitudes as the effects of the convective intensity in the domain in terms of the range of cloud mass flux of individual clouds in a domain. The emerging organization of clouds will cause a decrease in the shape parameter of the mass flux distribution, though this decrease will be small and visible as a change in a distribution tail (not shown here). This indicates that the effects of organization are important for the convective variability, but they are clearly not introduced solely through the mass flux distribution and the individual cloud lifecycles. We speculate here that the additional source of memory and spatial correlations related to the mesoscale organization are a mechanism responsible for the increase in variance. Convective organization and the correct convective variability are not represented in commonly used deterministic convective parameterizations in numerical weather and climate models. Stochastic approaches are a promising tool for addressing this problem; a good example of a mechanism for parameterization of convective organization is the cellular automaton (e.g. Palmer, 2001; Bengtsson et al., 2013). How a stochastic model, assuming a locally random cloud field, will be able to model convective organization when coupled to a three-dimensional atmospheric model, poses an interesting question for future studies.

2.4.3 Different choices for the cloud lifecycles

In this section, we test how the explicit representation of the cloud lifecycle influences the resulting frequency distribution and scale-adaptivity of the stochastic model. The focus is on the definition of the cloud lifetime in the stochastic model, which can be set to a constant value as in the scheme of Plant and Craig (2008) or can be set as a variable, depending on the cloud-base mass flux. Even though the lifetime of a cloud is not a deterministic function of the cloud-base mass flux, it can be approximated with a power-law function relating it to the cloud mass flux (Fig. 2.3c). In the case of a constant cloud lifetime, the cloud lifecycles are not modelled explicitly, and the lifetime average cloud-base mass flux is used instead of the simplified lifecycle function (Eq. 2.32).

The stochastic model is run using the different model configurations:

1. mixed Weibull, $\tau = 10\,\text{min}$, no lifecycles;
2. mixed Weibull, $\tau = 20\,\text{min}$, no lifecycles;
3. mixed Weibull, $\tau = 30\,\text{min}$, no lifecycles;
4. mixed exponential, $\tau = 20\,\text{min}$, no lifecycles;
5. and mixed Weibull, $\tau_i = \alpha_i m^{\beta_i}$, $i = 1, 2$, with lifecycles.

The best match of the frequency distribution across the high-resolution scale of the model is achieved in case (5), where the cloud lifetime depends on the magnitude of the cloud-base mass flux, with the two cloud groups treated separately, and with an explicit lifecycle (Fig. 2.12a). The Hellinger distance degrades for the coarser grid resolution, where the mixed exponential case with a constant cloud lifetime (4) performs better. Cases (1)–(3) evidently all perform worse than (4)–(5), with the further degradation of the scale-adaptivity.

The reason for the degradation of the distance measure in case (5) comes from the larger error in the ensemble average (Table 2.4) for the coarser model grid resolution compared to the fine resolution. However, this error is less than 0.3 %, which is negligible, and therefore the increase in the Hellinger distance is not significant. In case (4) there is no such degradation with coarsening of the resolution, except for the scales larger than 20 km. In case (4) the error in the ensemble mean is between 0.42 and 0.74 %, which is larger than the error in case (5), but is not increasing with the coarsening of the resolution. However, due to the compensation of the error in the ensemble mean with the error of under-sampling of the mass flux distribution function and the error introduced by excluding the cloud lifecycles, the Hellinger distance in case (4) is lower than in case (5) for the coarse-grid resolutions.

As a result of equal lifetimes in a cloud population (cases 1–3), convective compound variance is overestimated by the same amount for the different choices of the cloud lifetime (Fig. 2.12b). This independence from the specific value of the constant lifetime (from 10 to 30 min) means that, on the grid-scale level, the system has no memory and the effects of the individual clouds average out. The same would apply for case (4) if we test for a different constant τ, with the difference that the underestimation of the variance in this case comes from the distribution shape choice ($k = 1$ vs.

(a) Hellinger distance, H

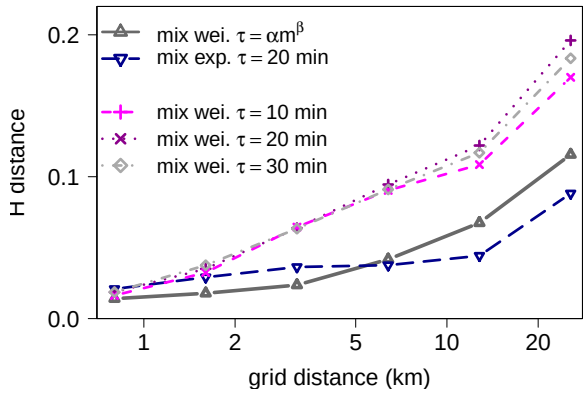

(b) Normalized variance of the compound cloud-base mass flux

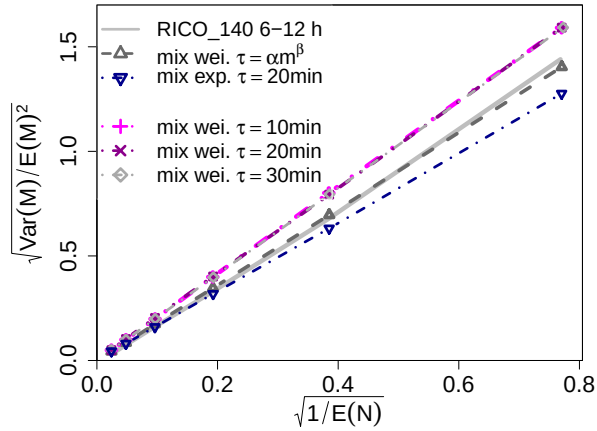

Figure 2.12: Comparison of the distribution pairs from the simulations using a constant and the mass-flux-dependent cloud lifetime.

$k = 0.7$). In case (5), the effects of convective memory will be carried on by the clouds that are small in number but that live longer. On the other hand, a large number of small short-lived clouds will have less effect on the future state of convection, which depicts a more realistic situation.

The question of consistency in the model formulation enters here. The error compensation in case (4) can be justified by the consistency in combining the different effects in the model formulation, which is more important than the accuracy and complexity in the representation of the separate processes. There are two options for the model formulation, consistent with our understanding of the cloud ensemble statistics:

1. a memoryless system, bearing in mind the stationarity of our case, which should be described using a mixed exponential distribution and a constant lifetime among clouds (similar to PC-2008), and

2. a system with memory, with diverse cloud lifecycles modelled explicitly and with the corresponding Weibull distribution for the cloud-base mass flux.

This raises the question of the importance of the system memory, introduced by the diversity of cloud lifecycles, for the parameterization of convection. From the results shown in Fig. 2.12b we conclude that the convective memory, and hence the model set-up (2), is necessary to reproduce the convective variability accurately, with a higher importance of the system memory for the more diverse cloud field (smaller k) and for the higher model resolution.

In the reference case of the stochastic model test runs, which corresponds to model set-up (2), the cloud vertical velocity is set to a constant value applied to all clouds, and the cloud lifetime is sampled from a deterministic power-law relation to the cloud-base mass flux. This is in disagreement with the empirical results from LES, which show a highly scattered joint distribution for both quantities (Fig. 2.3). Is a deterministic relation between the mass flux and other cloud properties a valid approximation? The variance of compound Poisson distribution depends on the number of convective elements in a model grid box, and scales as $\mathrm{Var}[M]/(E[M])^2 = 2/\langle N \rangle$ (Craig and Cohen, 2006). With the introduction of the cloud-base mass-flux-dependent cloud lifetime Eq. (2.30), this relation incorporates a weak dependence of variance on the cloud lifetime relation through the exponent β, while in the case of the more general Weibull distribution Eq. (2.29), also on parameter k. Having in mind such weak dependence of variance on the cloud lifetime relation (Fig. 2.11c), it is not likely that the variability could be enhanced by the conditional random sampling of the joint probability distribution of the cloud-base mass flux and cloud lifetime. Therefore, there is no need for the further sophistication of the stochastic model; i.e. a deterministic relation between the cloud mass flux and other cloud properties is sufficient.

2.5 Summary and conclusions

Subgrid-scale convective processes can be related to the mean large-scale field through a parameterization that comprises a deterministic component, a stochastic component and the convective memory carried by the finite lifecycles of clouds. These three components change in their contribution to the overall subgrid effects, depending on the resolution of the model. Thus, a cloud parameterization should be developed in such a way as to adapt to the different resolutions of model grid and model time step.

We have studied the fluctuations in a shallow convective ensemble of the Rain in Cumulus over the Ocean (RICO) case, which is a precipitating shallow convective case in the trade-wind region. Shallow cumulus ensemble statistics are analysed using LES, and cloud tracking is applied to study the cloud lifecycles. The theory of fluctuations in an equilibrium convective ensemble of Craig and Cohen (2006) is extended and applied to shallow convection, combining it with the empirical findings. As a first step towards a stochastic shallow convective parameterization, the stochastic stand-alone model has been developed. The model is based on an approach similar to the PC-2008 stochastic scheme, in which the subgrid convective state is represented as a subsample of the full convective ensemble.

The diversity of shallow cloud lifecycles causes the deviation of the cloud-base mass flux distribution from the exponential memoryless distribution. Therefore, we introduce the dependence of the cloud

mass flux on the cloud lifetime by generalizing the cloud mass flux distribution to a Weibull probability density function. In this way, the variability of cloud lifecycles is introduced in the stochastic representation of shallow convection. We also account for the different shallow cloud subtypes by defining two modes of the cloud-base mass flux distribution.

The convective ensemble average statistics and convective variability are constrained by the model closure by setting implicitly the value of two parameters, the average mass flux per cloud $\langle m \rangle$ and the average ensemble cloud lifetime $\langle \tau \rangle$. The model formulation is such that, depending on how these two parameters might change due to the forcing, the underlying distribution and its relation to the cloud lifecycles would dynamically adapt to these changes.

Clouds are initiated in a model grid box assuming that their number follows the Poisson distribution and the cloud-base mass flux is drawn randomly for each cloud from the mixed Weibull probability density function. The model is forced with the domain ensemble average cloud properties from LES and the probability density function parameters are fitted theoretically using a formulation for the system closure. Limited sampling of clouds in a model grid box results in the compound Poisson distribution of small-scale convective states, which possesses an inherent property of scale-adaptivity. In this way the model is constrained to give the correct ensemble average values, and the variability of subgrid convective states is reproduced in a physically based manner.

As a measure of convective variability, the variance of the subgrid compound distribution is dependent on the number of clouds in a grid box and the range of their cloud-base properties. We show that the correct variability can be reproduced by the model by accounting for the system memory through the cloud-base mass flux distribution and by modelling the cloud lifecycles explicitly. The resulting histograms of subgrid convective states are simulated with a high level of agreement with LES across the different scales. Even though the individual cloud properties are highly dispersed, the compound distribution of subgrid convective states is robust and insensitive to the randomness of local cloud properties. This implies that the simplicity of the stochastic model can be retained and that the assumption about deterministic relations between the cloud mass flux and other cloud properties is valid.

This study provides a generalization of the convective ensemble theory of Craig and Cohen (2006), using a formulation that attempts to unify the stochastic parameterization of shallow and deep convective clouds depending on two parameters: $\langle \tau \rangle$ and $\langle m \rangle$. These parameters are related to the large-scale information that is controlled by the convective regime, and are possibly also dependent on the changes in the large-scale forcing. Therefore, it is necessary to develop a closure for these two parameters, based on the large-scale processes controlling the atmospheric boundary layer and transition to deep convection. In this chapter, we establish the applicability of the convective fluctuation theory to shallow convection, generalizing it by the introduction of system memory.

In the next chapter, the stochastic model is developed further by coupling it to an existing mass flux-based shallow convective parameterization in a numerical model.

Chapter 3

An approach to parameterize shallow cumuli across scales

The parameterization of shallow cumuli across a range of spatial resolutions in atmospheric models faces at least three major difficulties: 1. the closure assumptions of existing parameterization schemes are not valid on the scales below approximately 10 km, 2. there is a substantial amount of convective variability that increases with coarse-grained resolution in LES studies and that is not captured using a common deterministic approach, and 3. on model grids with a resolution that falls into the convective gray zone, grid-scale dependent secondary circulations can develop and introduce artificial variability modes in the cloud fields. In this chapter, we present a detailed description of the developed parameterization of shallow cumuli using a stochastic and scale-aware approach in a nonhydrostatic model on kilometer-scale grids. The new scheme represents the stochastic and scale-dependent fluctuations around the equilibrium state of a shallow cumulus ensemble, and provides a way to maintain the validity of closure assumptions across scales. In addition, we discuss the influence of the convective gray zone on variability in parameterized convective cloud fields.

3.1 Introduction

Behavior and characteristics of numerically modelled convection and clouds are highly dependent on the horizontal resolution of atmospheric models. The convergence of a modelled state to the real state of a physical system is not entirely a numerical problem caused by the finite-difference methods used to solve the dynamical equations (e.g. Jung and Arakawa, 2004; Arakawa, 2004). It is the parameterization of subgrid physical processes, especially convection and clouds, that does not converge to the real physics as the model resolution is increased (Kiehl and Williamson, 1991; Giorgi and Marinucci, 1996; Williamson, 1999; Pope and Stratton, 2002; Bryan et al., 2003; Jung and Arakawa, 2004).

This study is in preparation for publication as **Sakradzija M.**, and A. Seifert: An approach to parameterize shallow convection across scales, in preparation, 2015.

Besides the nonconverging model physics, in a convective boundary layer modelled on the gray zone grids, convectively induced secondary circulations can develop and support the emergence of grid-dependent organized cellular or roll structures (Jung and Arakawa, 2004; Piotrowski et al., 2009; LeMone et al., 2010; Honnert et al., 2011; Zhou et al., 2014; Ching et al., 2014). Thus, the model dynamics also exhibit a grid-scale dependent behavior in form of the spurious convective organization. This type of organization does not reflect the state of a natural system, but instead it reflects a state resulting from a combination of numerical artifacts and model dynamics (Bryan, 2005; Piotrowski et al., 2009). The fact that model physics does not converge with increasing resolution suggests that there is a need for a scale-aware parameterization of clouds and convection in high-resolution models. Moreover, the tendency of model dynamics to develop convective transport and organized convection on the grid scale also points out the need for a unified parameterization of turbulence, convection and clouds, because these processes are tightly linked and causally connected. This connection is mostly visible through variability in the cloud field that is highly influenced by the grid-scale dependent convective circulation and organization.

One of the main reasons for nonconverging behavior of model physical parameterizations are the assumptions made in order to close the model equations and to provide the basic parameterizability criterion. These assumptions are mostly defined on the coarse model grids, for which the parameterization is originally intended. One of the main assumptions in a conventional cloud parameterization is the validity of the statistical quasi-equilibrium between a subgrid cloud ensemble and the grid-scale flow. On coarse grids with horizontal resolutions in the range of 20 to 50 km, convection and shallow cumuli ensembles are considered as subgrid phenomena and the statistical quasi-equilibrium is widely applied. In this case the convective ensemble average is used as the representative of subgrid convective processes. On the other side of the spatial scale range, on very high resolutions of O(10-100 m), the dynamics of convection and clouds is taken as effectively resolved. On the intermediate spatial scales between these two asymptotic cases, in the range of O(100 m-10 km), the dominant convective scale is comparable to the scale of the model grid, and convection is no longer effectively resolved, but at the same time it is not effectively parameterized. This refers to the convective gray zone, also called “terra incognita“ by Wyngaard (2004) who recognized and defined the problem of numerical modelling of turbulent flows on the intermediate scales. In the gray zone, the inherent variability of convection becomes larger with the increase of grid resolution, and a model grid cell can hold only a subsample of the convective cloud ensemble, which invalidates the statistical quasi-equilibrium assumption (see Plant and Craig, 2008; Dorrestijn et al., 2013, and also Chapter 2). The stochastic method developed in Chapter 2 provides a way to include the variability of convection around the statistical equilibrium and its dependence on the model grid resolution into a parameterization of shallow cumuli.

Parameterization of shallow convection across scales inevitably involves the question of the interaction of model physics and model dynamics in the convective gray zone. On the gray zone range of spatial scales, the multi-scale convective and cloud processes are not fully subgrid phenomena, but nevertheless they are artificially truncated at the model resolution scale into the subgrid- and grid-scale processes. The energy spectrum of the atmospheric flow is continuous and there is no evident reason for such separation of the scales of motion (Nastrom and Gage, 1985). Thus, the artificial

truncation of convective processes and cloud ensembles at the model grid-resolution scale causes an artificial interaction between the model dynamics and subgrid physical parameterizations. In an undisturbed, slowly changing convective situation, the solution of the model dynamical equations leads to emergence of organized convective motion on the model grid in form of convective cells or rolls. This type of organized motion is similar in mechanism to the Rayleigh-Bernard convection, and emerges when the buoyancy forces overcome the viscous momentum transfer in the flow. In the zone between effectively resolved convection, which is considered at the grid scale of 10-100 m, to the effectively subgrid convection, which is considered on the spatial scales of 20-50 km, organized convective circulations are highly grid-dependent, overenergetic compared to the natural convection and in that sense artificial (e.g. Piotrowski et al., 2009; Zhou et al., 2014; Ching et al., 2014). This brings additional uncertainty into the parameterization of clouds in numerical atmospheric models on the gray zone grids, because this kind of organization inflates the variance and reverses the skewness of subgrid cloud properties.

To address these two major model properties that degrade the convergence, i.e. the validity of statistical equilibrium and the gray zone convective variability, in this chapter we extend the eddy-diffusivity mass-flux (EDMF) scheme in the nonhydrostatic ICON model by introducing the stochastic shallow cumulus ensemble model (Chapter 2) into the EDMF framework. The main purpose of the new shallow cumulus cloud scheme is to introduce the variability of subgrid convective states around the statistical equilibrium in a scale-aware and physically sound manner, similar to the Plant and Craig (2008) scheme developed for deep convection. As in Chapter 2, the developed scheme is used to simulate the Rain In Cumulus over the Ocean (RICO) case. The condition for the statistical quasi-equilibrium is fulfilled by applying a deterministic model closure across a large area around each model grid cell, while the subgrid convective states are subsampled from a quasi-equilibrium distribution defined in a compound stochastic process. In this way, the macroscopic state of the cloud ensemble is constrained based on the physical principles of model closure, and the uncertain microscopic states of the cloud subensembles within model grid cells are governed by a probabilistic law. This approach draws further benefits by applying other parameterization assumptions on the scale at which they are valid, such as the assumption of a very small fractional area covered by clouds $a_c \ll 1$, which is an inevitable component of common mass flux cloud parameterizations (e.g. Arakawa and Schubert, 1974; Arakawa and Jung, 2011).

Relaxation of the quasi-equilibrium assumption by accounting for the subgrid stochastic variability of convection is beneficial on the coarse grids as well, and the application of stochastic cloud physics is far more broad than the application to the gray zone convection. The stochastic parameterization of convection represents the uncertainty of the model physics in the ensemble prediction systems by inflating the ensemble spread (e.g. Palmer, 2001; Teixeira and Reynolds, 2008). The stochastic convective perturbations can grow and propagate to the synoptic scales and thereby represent the upscale growth and propagation of the model error (Teixeira and Reynolds, 2008; Selz and Craig, 2015). The unresolved convective variability has a substantial impact on the ability of numerical models to represent the low-frequency variability modes of the atmosphere in the tropics on intraseasonal and longer timescales (Lin and Neelin, 2000, 2002). There are as well indications that convectively generated spatial variability in atmospheric thermodynamic fields can influence the timing of the diurnal

cycle of convection over land (Stirling and Petch, 2004), thus a stochastic parameterization of convection could be beneficial in improving the modelling of the short-timescale atmospheric variability. A stochastic multicloud convective parameterization (Khouider et al., 2010) improves the variability of tropical convection by simulating the intermittent structure of synoptic and mesoscale convective systems and convectively coupled waves better compared to a deterministic scheme (Frenkel et al., 2012). The subgrid stochastic celular automata (CA) scheme that parameterizes the lateral organization of convection and convective memory can mimic the organization by gravity waves originating from deep convection (Bengtsson et al., 2011). There are also indications that a stochastic convection parameterization can increase the forecasting skill of the model (Bright and Mullen, 2002; Berner et al., 2015) and reduce the systematic model biases (Berner et al., 2012). Thus, the aim of a stochastic convection parameterization is not merely to induce a statistical impact in the ensembles and improve the measure of uncertainty, but also to improve the physical aspects of a modelled system.

In this chapter, we describe the development of the stochastic EDMF parameterization in ICON, and we present the first results of the multi-resolution tests of the new stochastic EDMF moist convection scheme. We also quantify the effects of the spurious convective organization on the convective variability in the RICO simulations using the deterministic and stochastic shallow convection schemes and we discuss the implications of these convective circulations on the further development of PBL parameterizations. Description of the ICON model and the convective case study is provided in Section 3.2. The unified EDMF parameterization of turbulence, convection and clouds is described in Section 3.3, where the main closure assumptions of the scheme are documented as well. Section 3.4 contains the description of the stochastic EDMF scheme in ICON, while the results of numerical simulations using both the deterministic and the stochastic model are given in Section 3.5.

3.2 Description of the model and case study

A multi-scale approach to parameterization of shallow convective clouds is partly motivated by the new-generation sophisticated models that offer the possibility of local grid refinement and on-line nesting (e.g. Tomita and Satoh, 2004; Skamarock et al., 2012; Zängl et al., 2015). In such a model configuration, parameterization schemes have to adapt to the model resolution automatically without the possibility of additional tuning of the scheme parameters and activity depending on the model resolution. The ICON model, developed jointly by the German Weather Service (Deutscher Wetterdienst - DWD) and the Max Planck Institute for Meteorology (MPI-M), is one example of such a model, built on the icosahedral horizontal mesh of points with local grid refinement (Zängl et al., 2015).

In this study we use the fully compressible nonhydrostatic version of ICON. Model equations are discretized over a numerical grid of triangular cells with Arakawa C staggering. The description of the model equations and numerical methods are described in Zängl et al. (2015) and are not provided here because the full model description would be out of the scope of this thesis. The model configuration used in this study is a limited-area version of ICON, with cyclic boundary conditions on a pseudo 2D torus triangular grid similar to the one used in Dipankar et al. (2015), who developed this configuration of ICON for the large eddy simulation (LES) purposes. In this configuration

the horizontal resolution is uniform and the vertical coordinate is height-based. Instead of the LES physical parametrization package developed by Dipankar et al. (2015), for the purpose of this study we apply the numerical weather prediction package (NWP) developed at DWD. For the parameterization of turbulence, convection and shallow clouds we employ the EDMF scheme, and beside the numerical diffusion scheme, EDMF is the only parameterization included. The parameterization of radiation, grid-scale condensation and precipitation, and deep convection is excluded from the model configuration. Radiative, large-scale advection and subsidence tendencies are applied through the prescribed large-scale forcing as defined in the UCLA-LES RICO case (Appendix A.1). The LES RICO-140 case, which is the case with suppressed precipitation, is used as a reference simulation like in Chapter 2. The surface boundary conditions of the RICO case are as well adopted from the UCLA-LES boundary conditions specification (Appendix A.1) and are prescribed locally within the EDMF scheme. These surface conditions are the constant sea surface temperature, the constant surface pressure, and a simple surface layer parameterization for the surface turbulent fluxes (Appendix A.1).

3.3 Unified treatment of convective boundary layers in ICON

Turbulence, convection and shallow planetary boundary layer clouds are parameterized within a unified framework of the eddy-diffusivity mass-flux scheme (EDMF) in ICON. In this scheme the turbulent flux of a conserved quantity $\phi = \{\theta_l, q_t\}$ is decomposed into the diffusive and convective transport terms (Siebesma et al., 2007) scaled by the diffusive area fraction $\mathcal{A}^K$ and convective area fraction $\mathcal{A}^{up}$ respectively:

$$\overline{w'\phi'} = \mathcal{A}^K \overline{w'\phi'}^K + \mathcal{A}^{up} \overline{w'\phi'}^{up} \tag{3.1}$$

The first term on the right hand side represents local turbulent mixing and is parameterized by the eddy-diffusivity approach, and the second term represents nonlocal transport by strong organized updrafts via the mass flux approach:

$$\overline{w'\phi'} = -K\frac{\partial \overline{\phi}}{\partial z} + M_u(\phi_{up} - \overline{\phi}), \tag{3.2}$$

where K denotes the eddy-diffusivity, $\partial\overline{\phi}/\partial z$ is a local vertical gradient of a conserved quantity, M_u is the convective updraft kinematic mass flux, and $\phi_{up} - \overline{\phi}$ is the excess of the updraft property ϕ in respect to the environment. The eddy-diffusivity approach used within the EDMF framework is the K-profile scheme of Troen and Mahrt (1986) and Holtslag and Boville (1993). The kinematic mass flux is defined as a product of updraft area fraction a_{ui} and updraft vertical velocity w_{ui}:

$$M_{ui} \equiv a_{ui} w_{ui}. \tag{3.3}$$

Neggers et al. (2009) extended the EDMF framework into the dual-updraft mass flux formulation (EDMF-DualM) by splitting the mass flux term into the dry ($i = 1$) and moist ($i = 2$) updraft terms to

represent the shallow convective clouds that form on top of the boundary layer moist updrafts:

$$\mathcal{A}^{up}\overline{w'\phi'}^{up} = \sum_{i=1}^{2} M_{ui}(\phi_{ui} - \overline{\phi}). \tag{3.4}$$

In this way, the dry boundary layer formulation is extended to represent moist boundary layer convection. This is still a bulk approach to shallow convection parameterization, though the two plumes can be considered as the simplest multi-plume model possible, and is considered the least complex mass flux scheme that consistently couples the subcloud layer updrafts and shallow cumulus clouds in the study of Neggers et al. (2009). The dry bulk updraft ($i = 1$) represents all subcloud layer updrafts that do not condense their water and that terminate at the top of the mixed layer. The moist bulk updraft ($i = 2$) represents all updrafts that condense water and give rise to the positively buoyant cumulus clouds. The mass flux approach for the moist convective updrafts in the subcloud layer extends to the cloud layer in a consistent way and the vertical transport below and within the cloud layer is modelled using the same entraining plume model.

The focus of our study is on the updraft mass flux term, and the shallow cumulus cloud scheme that is coupled to the convective transport parameterization within the EDMF-DualM framework (Neggers et al., 2009). In the following, we will call this parameterization simply EDMF, but we will always refer to the dual-mass-flux framework.

3.3.1 The entraining plume model

Vertical profiles of thermodynamic and momentum tendencies are estimated in EDMF by applying an updraft plume model to both dry and moist updrafts in the scheme. The updraft budget equations for a conserved variable ϕ used in EDMF are formulated as in Siebesma et al. (2007) and citations therein:

$$\frac{1}{M_{ui}}\frac{\partial M_{ui}}{\partial z} = \epsilon - \delta \tag{3.5}$$

$$\frac{\partial M_{ui}\phi_{ui}}{\partial z} = \epsilon M_{ui}\overline{\phi} - \delta M_{ui}\phi_{ui} + a_{ui}F_{\phi_{ui}} \tag{3.6}$$

ϵ and δ are the lateral entrainment an detrainment rates, and $F_{\phi u}$ contains all external sources and sinks of the conserved quantity ϕ.

When all the external sources and sinks for ϕ are excluded, and Eq. (3.5) is substituted into Eq. (3.6), the outcome is an entraining updraft equation (see also Betts, 1975)

$$\frac{\partial \phi_{ui}}{\partial z} = -\epsilon_{ui}(\phi_{ui} - \overline{\phi}), \tag{3.7}$$

where ϵ_{ui} is the fractional entrainment rate.

Substitution of the mass flux definition into Eq. (3.6) results in the vertical velocity budget equation (Siebesma et al., 2007):

$$-\frac{1}{2}\frac{\partial w_{ui}^2}{\partial z} - \epsilon_{wi}w_{ui}^2 + P_{ui} + B_{ui} = 0 \tag{3.8}$$

where ϵ_{wi} is the fractional entrainment rate for vertical velocity, which is assumed to be proportional to the fractional entrainment rate for ϕ with the factor of proportionality $b = 0.5$, i.e. $\epsilon_{wi} = b\ \epsilon_{ui}$ (Siebesma et al., 2007). In the updraft velocity equation, the main source terms are the pressure P and buoyancy B terms. The pressure term P is expressed as proportional to the vertical velocity variance (Schumann and Moeng, 1991; Siebesma et al., 2007):

$$P = -\frac{1}{\rho}\frac{\partial \overline{p}}{\partial z} = \frac{\partial \overline{w^2}}{\partial z} \approx \frac{\partial \mu w^2}{\partial z}, \tag{3.9}$$

where $\mu \approx 0.15$.

Substituting $\epsilon_{wi} = b\ \epsilon_{ui}$ and Eq. (3.9) into Eq. (3.8) results in vertical velocity budget equation as used in Neggers et al. (2009):

$$\frac{1}{2}(1-2\mu)\frac{\partial w_{ui}^2}{\partial z} = -b\epsilon_{ui}w_{ui}^2 + B_{ui}, \tag{3.10}$$

where

$$B_{ui} = \frac{g}{\overline{\theta}_v}(\theta_{v,ui} - \overline{\theta}_v). \tag{3.11}$$

Eqs. (3.7) and (3.10) are solved for the initial conditions given by the updraft initialization at the lowest model level. The integration terminates at the height where $w_{ui}^2 = 0$. The mass flux equation (3.5) is not explicitly solved in the EDMF formulation, because it becomes obsolete with the formulation of closure for the vertical structure of the moist updraft mass flux based on the buoyancy sorting of environmental and updraft air mixtures (see the following section). Furthermore, the entrainment rate formulation is not employed in the estimation of the mass flux profile, and is used only in the updraft budget equations for the conserved quantities. So, dilution of the plumes by entrainment and shape of the mass flux profiles are parameterized separately in EDMF (Neggers et al., 2009).

3.3.2 Main closure assumptions in the EDMF scheme

The three main closure assumptions in the EDMF formulation are the moist updraft area fraction a_{u2} closure based on the boundary layer equilibration mechanism described in (Neggers et al., 2006; van Stratum et al., 2014), the closure for lateral entrainment rate for dry and moist updrafts ϵ_{ui}, and estimation of the vertical structure of the moist updraft mass flux (Neggers et al., 2009). In the remainder of this section, we describe these three EDMF closure assumptions in detail, because some aspects of these assumptions will have to be reconsidered for the development of the stochastic scale-aware parameterization.

Moist updraft area fraction

The feedback mechanism between the mixed layer humidity, convective mass flux and mixed layer depth is responsible for a steady-state shallow cumulus boundary layer over the ocean with a robust cloud cover and mass flux over the time (Neggers et al., 2006). This mechanism serves as the main

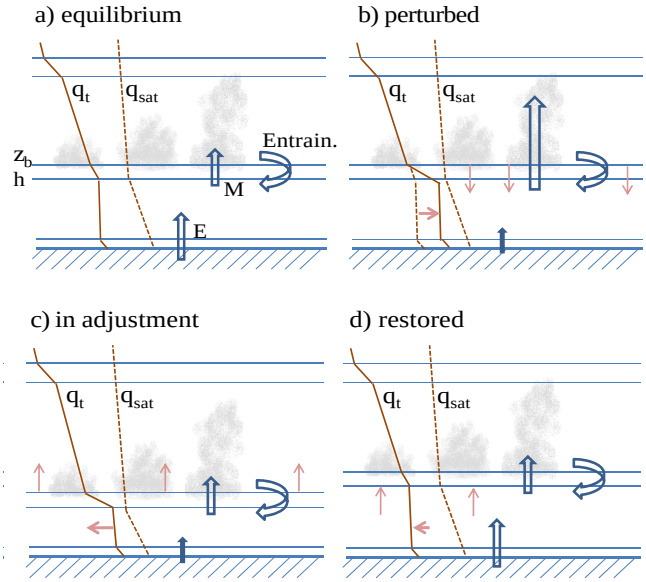

Figure 3.1: The mechanism of the CBL adjustment to equilibrium after a moisture perturbation. This equilibration mechanism has four phases: a) the typical equilibrium phase that is observed very often in the trade wind regions over the ocean, b) the perturbed phase by subcloud layer moistening which increases a_{u2} and M, c) the adjustment phase in which a_{u2} and M are restored to the equilibrium values, and d) the final restored phase. This sketch is reproduced from Neggers et al. (2006).

physically based closure assumption in the cloud scheme of EDMF, so in the following we include the description of this mechanism as explained in (Neggers et al., 2006).

In an equilibrium state (Fig. 3.1a), a typical cumulus cloud fraction over the trade wind region is only a few percent, and the mixed layer top is always held close to the cloud-base height (Betts, 1976; Neggers et al., 2006). If the system is destabilized by moistening in the subcloud layer, more rising updrafts will start to condense water at the top of the mixed layer, which will result in the increase of the moist updraft area fraction a_{u2} (Fig. 3.1b). The mass flux M is controlled by the moist updraft area fraction a_{u2} (see also Chapter 2), thus the increase of moist updraft area fraction is followed by an increase in the mass flux (Fig. 3.1b). As more mass gets transported out of the subcloud layer, the subcloud layer shrinks and h becomes lower. At the lower height h temperature is higher and the saturation deficit increases, which restores a_{u2} and M accordingly back to lower values (Fig. 3.1c). In the adjustment phase, the subcloud layer slowly grows again, entraining dry air at the height h, which restores the humidity profile by continuous drying near the subcloud layer top, while near the surface humidity is slowly restored by the reduced surface evaporation (Fig. 3.1d). The distance between h and the cloud-base height is the depth of the transition layer δ_{tr}, a weak inversion layer just below the cloud base, which changes during the equilibration of the system and regulates the convective transport (see also Bretherton et al., 2004). This feedback mechanism was already recognized in early coupled subcloud layer model and mass flux scheme for the shallow-cloud layer of Betts (1976). As one of the main parameters in the coupled scheme of Betts (1976), the transition layer depth plays an important role in cumulus formation by controlling the detrainment of convective

plumes near the cloud base, and thus controlling the fraction of the subcloud updrafts that can rise through the transition layer and form clouds.

Based on the above described equilibration mechanism, the fraction of the updraft area that rises out of the mixed layer and forms buoyant clouds is determined in EDMF by the ratio of transition layer depth δ_{tr} and the subcloud mixed layer depth h. This ratio is multiplied by the proportionality term which depends on the beta distribution function shape, to take into account the distribution of conserved quantities at the cloud base:

$$a_{u2} = \left(\frac{\delta_{tr}}{h}\right) \frac{1}{2p+1} \tag{3.12}$$

where the constant $p = 2.2$ that characterizes the distribution shape is estimated from LES (Neggers et al., 2007b).

Entrainment

The rising plume budget equations, Eqs. (3.7) and (3.10), are applied to both bulk updrafts in the EDMF scheme. Neggers et al. (2009) argue that such an approach is feasible only if the updraft lateral entrainment rate is dependent on the state of the updraft. As in Neggers et al. (2002) the dependence on the state of the updraft is achieved by parameterizing the updraft lateral entrainment rate as inversely dependent on updraft velocity:

$$\epsilon_{ui} = \frac{1}{\tau_\epsilon w_{ui}} \tag{3.13}$$

The entrainment turnover timescale τ_ϵ is constant and is estimated from LES as $\tau_\epsilon = 400$ s. By this entrainment formulation, an updraft that is rising faster through the model grid layer will have less time to mix with the environment and thus will be less diluted, and vice versa. The same updraft entrainment rate is applied to the moist updraft in the subcloud and cloud layers. In the current EDMF configuration in ICON, the dry updraft entrainment rate is further modified by including a term that takes into account the proximity of the surface as in Köhler et al. (2011):

$$\epsilon_{u1} = \frac{1}{\tau_\epsilon w_{u1}} + c_\epsilon \frac{1}{z} \tag{3.14}$$

The entrainment rate of the dry updrafts scales with $1/z$ near the surface, with a factor $c_\epsilon = 0.4$.

Vertical mass flux structure

Detrainment is the dominant mechanism that regulates the vertical structure of mass flux in the cloud layer (Esbensen, 1978; de Rooy and Siebesma, 2008), however, it is a challenging task to derive an explicit formulation of the detrainment rate for the purpose of parameterization. A benefit of the separate treatment of the vertical mass flux structure and plume dilution by turbulent mixing with the

environment is that there is no need for an explicit formulation of the detrainment rate δ (de Rooy and Siebesma, 2008).

The closure for the mass flux vertical structure in EDMF is an implicit version of a buoyancy sorting scheme (see for example Kain and Fritsch, 1990). In such schemes, the turbulent mixing between clouds and their environment takes place at the cloud periphery, and this is represented by the mixtures of cloudy and environmental air that can entrain or detraine the air mass from the cloud. These mixtures differ by their buoyancy, which depends on the fraction of the environmental air χ contained in the mixture. A mixture of cloudy and environmental air will be less buoyant if the fraction of environmental air χ is higher, and more buoyant if χ is lower. A critical mixing fraction of environmental air χ_c is defined as the fraction of environmental air at which the mixture is neutrally buoyant. If $\chi > \chi_c$ the mixture is negatively buoyant, and therefore its role is in detraining of the cloud air. The mixture entrains the fraction of environmental air and dilutes the cloud if it is positively buoyant, that is when $\chi < \chi_c$. By defining such mixtures, the dependence of the mass flux profiles on both the updraft properties and on the environmental conditions is introduced.

In EDMF, instead of explicitly formulating the buoyancy sorting and χ_c, a moist zero buoyancy deficit $q_t^x - \overline{q_t}$ is used instead, where the critical total water mixing ratio q_t^x corresponds to the critical fraction χ_c at which the mixture would be neutrally buoyant. Thus, the critical total water mixing ratio q_t^x is defined as the point on a lateral mixing line between the mean state and the cloud core state, where buoyancy is equal to zero (Fig. 3.2). In terms of this formulation, if the mean total water mixing ratio of a model grid column $\overline{q_t}$ is far from the critical total water mixing ratio q_t^x only a small fraction of the cumulus updraft will be positively buoyant and able to form clouds. And the other way around, if the distance between $\overline{q_t}$ and q_t^x is small, a large fraction of the updraft will become cloudy.

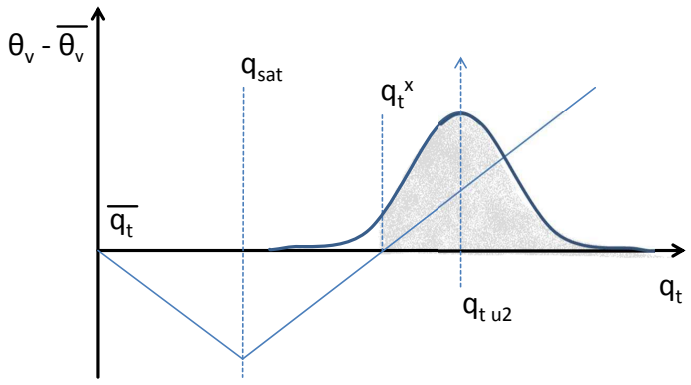

Figure 3.2: A mixing diagram representing the lateral mixing line (blue line) between the cloud and its environment on the total water mixing ratio q_t versus the virtual potential temperature excess $\theta_v - \overline{\theta_v}$ plot. The moist updraft q_t is defined by the normal probability density function with the mean q_{tu2} and standard deviation σ_{qt}^{up}. The point where the mixing line intersects with the zero buoyancy line defines the critical total water mixing ratio q_t^x where the cloudy and environmental air mixtures are exactly neutrally buoyant. Positively buoyant points within the moist updraft that satisfy the condition $q_t > q_t^x$ form the cloud. This diagram is reproduced from Neggers et al. (2009).

The normalized moist zero buoyancy deficit Q_c is defined as:

$$Q_c = \frac{q_t^x - \overline{q_t}}{\sigma_{q_t}} \tag{3.15}$$

where σ_{q_t} is the standard deviation of the total water mixing ratio. The normalized moist zero buoyancy deficit Q_c is correlated to the cloud fraction a_c, which is expressed as a correlation function of the vertical gradients of a_c and Q_c (Neggers et al., 2009):

$$\frac{1}{a_c}\frac{\partial a_c}{\partial z'} = C_a \frac{1}{Q_c}\frac{\partial Q_c}{\partial z'} \tag{3.16}$$

The correlation coefficient C_a is found to be equal to -1.8 based on the LES studies of several different cases, over the ocean and over the land (Neggers et al., 2009). z' is the height above the cloud base normalized by the cloud layer depth.

Using this formulation of buoyancy sorting, the updraft mass flux profile is made dependent on the updraft properties and the excess in total water mixing ratio in respect to the environment. The formulation of gradient scaling scaling relation Eq. 3.16 in EDMF is based on the vertical gradients of normalized moist zero buoyancy deficit Q_c at the cloud base and at the cloud top, after which the moist updraft area fraction is interpolated linearly between the cloud base and the cloud top. This approach is suitable for representing the typical peaks in the cloudiness near the cloud base, as well as near the top of the cloud layer in the convective cases with relatively strong capping inversion, such as RICO (Neggers et al., 2009). Finally, the vertical profiles of the cloud mass flux are calculated using Eq. 3.3.

3.4 Stochastic EDMF scheme

The stochastic model is a nonlocal probabilistic cloud ensemble framework that operates on the full modelling domain and keeps the memory of individual cloud lifecycles. Coupling of the stochastic model to EDMF introduces a spectral cloud ensemble and a local memory component to the otherwise fully diagnostic and bulk EDMF cloud scheme. In this study a spectral cloud ensemble is used for the purpose of parameterizing the subgrid convective variability, while the bulk aspects of EDMF are still retained on the large scales where the quasi-equilibrium assumption is valid. In the future phases of the parameterization development, some aspects of the spectral cloud ensemble such as the individual cloud lifecycles will have more implications, especially in the updraft microphysics parameterization. On a very high resolution, below 6 km approximately, where a single cloud scale approaches the model grid scale, the cloud area and the individual cloud mass flux are allowed to spread across the neighboring grid cells in the stochastic model. This latter feature is a step towards a parameterization in the gray zone for an individual cloud, where the communication between the neighboring grid cells has to be implemented instead of a classic localized grid-column approach.

In this section we describe the coupling between the stochastic model based on the convective ensemble statistics (Chapter 2) and the EDMF scheme in ICON. The variability of subgrid convective

mass flux is parameterized by subsampling the convective cloud ensemble in a scale-aware approach, so that the statistical quasi-equilibrium is applied on the large scale where the convective cloud area fraction is very small $a_{u2} << 1$. The stochastic model developed in Chapter 2 is operating on a two-dimensional horizontal plane, and when it is implemented in the 3D ICON model, the vertical structure of cloud layer also has to be reassessed. So, in this section we also propose two feasible options to develop the parameterization of the cloud layer vertical structure in the stochastic EDMF framework.

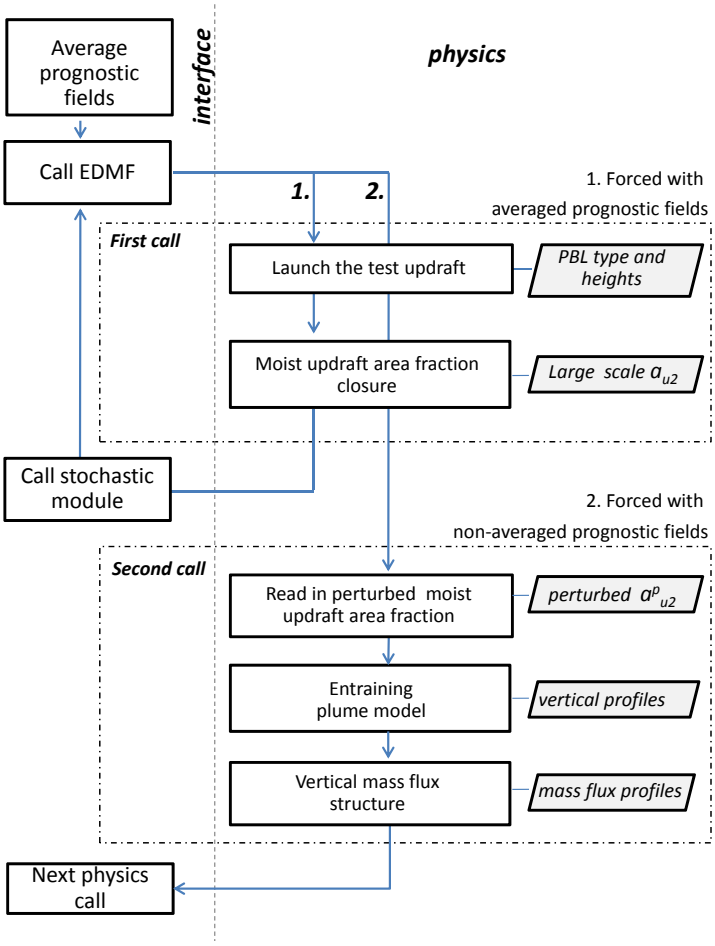

Figure 3.3: The flow chart of the stochastic EDMF scheme in ICON during a single model physics time step. The ICON model consists of the model dynamics level where the prognostic equations are discretized and solved (left side) and the model physics level where the subgrid processes contributions are calculated by using different parameterization schemes, which are mainly diagnostic (right side). The two model components are merged by an interface level at which the exchange of model variables between the model dynamics and physics takes place.

3.4.1 Perturbed moist updraft area fraction

The main variable that represents individual clouds in the stochastic EDMF scheme is the moist updraft area fraction a_{u2}, based on which the convective mass flux M is calculated following Eq. (3.3). The main EDMF quasi-equilibrium closure assumption is applied on a_{u2}, and that is why the definition

of the a_{u2} closure is the point where the stochastic model from Chapter 2 is introduced into the EDMF framework.

The stochastic model generates a compound distribution of the subgrid moist updraft area fraction a_{u2}. This compound distribution is a convolution of the Poisson distribution that counts the clouds and the mixed Weibull distribution that defines the individual cloud mass fluxes (Fig. 3.4). The mixed Weibull distribution consists of two distribution modes, one representing the active clouds and the other one representing the passive and forced clouds. In the EDMF scheme turbulent-diffusive and convective transports are as well described by a bi-modal distribution, thus the passive cloud distribution mode is not implemented into the EDMF scheme, but its estimation is transferred to the diffusive transport and passive cloud parameterization of EDMF. The Weibull mass flux distribution for active clouds is retained in the stochastic ensemble model and is used to define the fluctuations of the moist updraft mass flux M_{u2} and area fraction a_{u2}. The resulting distribution of the perturbed a_{u2}^{p} is scale-adaptive, and its variance and skewness change with the model resolution because the number of initiated cloud elements in the Poisson process depends on the grid cell area. Using this approach, a_{u2} is perturbed in a physically based manner, having the large-scale ensemble average of cloud properties as a physical constraint on the system as formulated in Chapter 2.

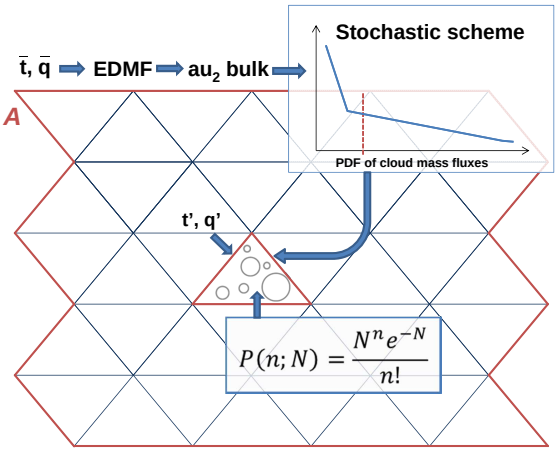

Figure 3.4: A schematic diagram of the stochastic shallow cumulus ensemble on the ICON model grid. The subgrid updraft area fraction is estimated as a random sum of the individual updraft area fractions within each model grid cell. The closure is applied on the large scale around the grid cell (red border), while the EDMF scheme updates the local grid cell thermodynamic properties based on the random subsample of the cloud ensemble.

The time step of the stochastic EDMF parameterization starts with averaging of the prognostic variables that are input to EDMF as shown on the flow chart, Fig. 3.3. The averaging is performed over the large area around each grid cell in ICON (Fig. 3.4), which is currently the full simulation domain. This is justified by the randomness and uniformity of the LES RICO-140 cloud field. The stochastic model is coupled to the EDMF physics scheme in ICON and is implemented at the model dynamics-physics interface level. At the model interface level all physical parameterization schemes are called and the grid-scale prognostic fields are updated by the contribution of the subgrid physical processes. These classic deterministic parameterization schemes are grid point based, with no communication

between the model columns in horizontal direction, while the stochastic model requires a nonlocal spatial averaging. That is why the EDMF scheme is called twice at the model interface level. The first call of EDMF calculates the large-scale closure for the moist updraft area fraction a_{u2} and the updraft vertical velocity w_u averaged over the large-scale area A. The bulk moist updraft area fraction a_{u2} and updraft vertical velocity w_u are then fed into the stochastic model after the first EDMF call at the model interface level. The stochastic model is run for the current time step to perturb a_{u2} in a scale-aware manner, by producing a distribution of subgrid convective area fractions that is dependent on the model resolution. The perturbed area fraction a_{u2}^p is then provided as an input to the second EDMF call, which is now fed with the nonaveraged prognostic fields in the case of the stochastic treatment of cloud layer vertical structure or with the averaged fields in the case of the bulk treatment of the cloud layer vertical structure (see Sections 3.4.2 and 3.5.2). In the second call the EDMF scheme continues further from the a_{u2} closure point to compute the moisture and heat budgets and estimate the vertical structure of the cloud layer (Fig. 3.3).

A requirement of the conventional mass flux schemes is that the cloud area fraction remains much smaller than the total grid cell area fraction, which is not fulfilled on the gray zone grids where the model grid scale approaches the scale of individual clouds. However, in the stochastic EDMF scheme, the closure assumption for the moist updraft area fraction, Eq. (3.12), is assumed to be valid for the large area A around a model grid cell (Fig. 3.4), as in the stochastic model formulation in Chapter 2. Thus, we avoid the gray zone dependence of the closure assumption and Eq. (3.12) is used in the same form as in the deterministic EDMF scheme, but now applied on the scale where the statistical quasi-equilibrium is valid. However, the separation of the grid cell area into the strong updrafts and environment requires an additional definition for the total updraft area fraction, which is originally composed of the sum of dry and moist updraft area fractions

$$\mathcal{A}^{up} = 1 - \mathcal{A}^K = \sum_{i=1}^{2} a_{ui} \tag{3.17}$$

and is a model constant set to $\mathcal{A}^{up} = 0.1$. In the stochastic EDMF scheme, the total updraft area fraction $\mathcal{A}^{up*}$ is grid-dependent, because the moist updraft area fraction a_{u2} is allowed to vary between zero and one. So, if a grid column is likely to hold a cloud, the total convective area fraction in the stochastic formulation $\mathcal{A}^{up*}$ is allowed to grow according to the area fraction occupied by clouds

$$\mathcal{A}^{up*} = MAX(\mathcal{A}^{up},\ a_{u2}^p). \tag{3.18}$$

The dry updraft area fraction a_{u1} is still not parameterized as scale-adaptive in the current model formulation, because we focus on the cloud parameterization component of EDMF in this study.

3.4.2 Scale-dependence of the cloud layer vertical structure

The updraft budget equations, Eqs. (3.7) and (3.10), can in general be applied to a bulk convective updraft within a bulk convection scheme or to a single updraft in a multi-mass-flux approach. The EDMF scheme is a bulk scheme with two separate updrafts, i.e. dry and moist updrafts, and plume

equations are valid for each of these bulk updrafts (previous section). On the gray zone scales, where the convective ensemble is subsampled, the bulk updraft budget equations are not well defined. There are several closure parameters that are defined specifically for the case of a robust statistical sample of an updraft ensemble: the entrainment rate for the conserved quantities ϵ, the entrainment rate for the updraft vertical velocity ϵ_w, and the proportionality parameter μ in the pressure term of the updraft velocity equation (Eq. 3.10). Furthermore, the formulation of the updraft mass flux vertical structure in the cloud layer is not defined at the gray zone scales either. The cumulus ensemble is under-sampled at these scales, and the spread of the employed scaling relation (Eq. 3.16) becomes wider with the increase of resolution (see the next section). There is no unique vertical gradient of the cloud area fraction a_c for each gradient of the normalized moist zero buoyancy deficit Q_c (Eq. 3.16). In this section, we discuss the limitations of closure assumptions for the entrainment and for the vertical mass flux structure on the gray zone grids. We also suggest possible solutions to an adequate parameterization of the cloud layer vertical structure, which we will test later in Section 3.5.2.

Limits of the entrainment formulation

The formulation of the lateral entrainment rate is important to represent the interaction between the updrafts and their environment. The entrainment rate formulation for moist and dry updrafts (Eq. 3.13) is valid in case of a robust cloud ensemble within a grid column, and can be applied to both updrafts because it is formulated as dependent on the updraft vertical velocity (Neggers et al., 2002, 2009). However, the outcome of the EDMF parameterization is sensitive to the value of the timescale τ_ϵ (see Section 3.5.2), which is estimated based on the LES studies. Moreover, it is difficult to define what this parameter exactly represents and it is used mostly as a tuning parameter in models, taking the value in the range from 300 s to 600 s (de Rooy and Siebesma, 2010; Sušelj et al., 2013). A picture on the scale of an individual cloud is somewhat different - the small-scale diffusive turbulent lateral mixing maintains the constant cloud profile with height, where the massive dynamical entrainment takes place at the cloud base, and the massive dynamical detrainment takes place at the cloud top (de Rooy and Siebesma, 2010). Between these two asymptotic configurations of the parameterization, fully bulk or fully spectral, the entrainment rate is not well defined.

Besides the entrainment rate, the parameters μ and b from Eqs. (3.7) and (3.10) also have to be redefined as dependent on the grid cell size, the number of clouds within the grid cell, and the range of the cloud properties within that cell. Due to the cloud ensemble subsampling, these parameters are uncertain, which suggests a stochastic approach to parameterize them. This aligns with the studies in which it is suggested that cloud dilution with height should be parameterized as a stochastic process in order to represent well the thermodynamic structure of the cloudy boundary layer in diverse cases (Raymond and Blyth, 1986; Romps and Kuang, 2010; Sušelj et al., 2013; Dawe and Austin, 2013).

There are indications that the correlation rate of the moist convecting parcel state with the cloud base state is completely lost a few hundred meters above the cloud base and the responsible process for changing the convective parcel state above the cloud base is the stochastic entrainment (Romps and Kuang, 2010). However, Dawe and Austin (2013) suggest that the formulation of the entrainment rate as dependent on the updraft properties should be retained, because both ϵ and δ show a strong

dependence on cloud properties, but at the same time they also exhibit a substantial randomness. They also quantify the variability in entrainment rate, which is in the range $\epsilon \in [0.005, 0.2]$ m^{-1}. Given the uncertainty in τ_ϵ and documented dependence of ϵ on w_u and at the same time documented random characterictics of ϵ, the entrainment rate ϵ still could be parameterized using Eq. (3.13), but instead of a constant τ_ϵ this parameter should be stochasticaly perturbed. As in Sušelj et al. (2013) it would require two stochastic processes to parameterize shallow convection across scales, one to represent the stochastic plume dilution with the height, and the other to represent variability in the moist updraft fraction contained within a model grid column.

Scale-dependence of the vertical mass flux profile

Parameterization of the vertical mass flux profile in terms of the gradient scaling relation (Eq. 3.16) is tested in a coarse-graining study of the RICO-140 LES case. We repeat the gradient scaling relation here for the convenience of the reader:

$$\frac{1}{a_c}\frac{\partial a_c}{\partial z'} = -1.8\frac{1}{Q_c}\frac{\partial Q_c}{\partial z'} \tag{3.19}$$

(Neggers et al., 2009). The gradients of the normalized moist zero buoyancy deficit Q_c and cloud area fraction a_c are estimated from LES, and are plotted on the scatter plots for the different coarse-graining resolutions (Fig. 3.5). The scaling relation Eq. (3.19) is plotted in its original form without fitting it to the LES scatter points (red line on Fig. 3.5). Based on these results, we conclude that on the model grids with a horizontal resolution larger than 20 km the scaling relation Eq. (3.19) is valid because the estimated gradients corresponding to the RICO-140 case fall close to the parameterization line. Therefore, Eq. (3.19) can be applied on the coarse grids in the original deterministic form. On the grids with a horizontal resolution finer than 20 km, the scatter of points that represent the pairs of vertical gradients of Q_c and a_c is wide and the scaling relation is no longer valid.

The lateral mixing line (Fig. 3.2) is reproduced from the LES RICO-140 simulation (Fig. 3.6), by coarse-graining the thermodynamic properties over different-resolution grids, and by following the EDMF buoyancy sorting and mixing line formulation explained in Section 3.3.2. The scatter on the gradient scaling plots on high resolutions (Fig. 3.5c-f) originates mainly from the variability of the grid cell mean states $\overline{q}_t$ along the zero buoyancy line (blue markers on Fig. 3.6). This also partly explains the increase in the scatter of points with resolution because the variability of $\overline{q}_t$ increases with the decreasing grid cell area. There is also some variability in the critical moist zero buoyancy deficit q_t^x point on the lateral mixing line, however, this scatter is much smaller. Thus, the closure scaling Eq. (3.19) is impaired on the high resolution grids because of the uncertainty in the moist zero buoyancy deficit Q_c on the high resolutions, and of course, also because of the high variability in the subgrid cloud fraction a_c on the high resolution grids.

Suggestions for the new vertical structure parameterization

There are at least three possibilities for an adequate application of the updraft budget equations and buoyancy sorting scheme on the gray zone scales:

1. The plume equations and the buoyancy sorting closure in the stochastic EDMF configuration can be applied to the bulk updraft resulting from a summation of all updrafts within a large-scale area A (see figure 3.4). This means that the shape of the ensemble average vertical profile of mass flux and other updraft properties is retained on all resolutions, but on the scale of a single model grid column the profile is scaled with the perturbed area fraction a_u^p within that column. In this way, the variability in the mass flux vertical profiles depending on the cloud subensemble size within a model grid column is not represented, but on the other side, the formulation of the model closure is consistent with the scale at which it is applied. This option for the cloud vertical structure parameterization is tested in Section 3.5.2 as a reference stochastic case.

2. A stochastic parameterization of the mass flux profile based on the cloud subsample properties could be developed in addition to the stochastic parameterization of the moist updraft area fraction. The stochastic model that is coupled to the EDMF scheme provides enough details of the cloud subsample in the gray zone, such as the number of clouds within a model grid column, and individual cloud heights and horizontal area fractions. This information could be included into a parameterization of the vertical mass flux profile and its variability across resolutions. Furthermore, a stochastic parameterization of the lateral entrainment rate used in the plume equations (3.7) and (3.10) is needed, because, as it was explained in previous sections, this parameter is likely to be stochastic and resolution dependent. This option is tested in Section 3.5.2, Test 1 and Test 2.

3. The third option would be to apply the plume equations to each individual updraft corresponding to each individual cloud initiated in the stochastic model. This, however, is not attractive for most applications of NWP or climate models, due to required computational and memory costs.

In this study we consider the first option as our base model setup and show that it might be sufficient for representing the average thermodynamic fields, cloud properties and their time evolution, as well as the variance and skewness of subgrid cloud properties in a shallow cumulus case over the ocean. The second option is tested as well in Section 3.5.2, and compared with the base setup of the stochastic model.

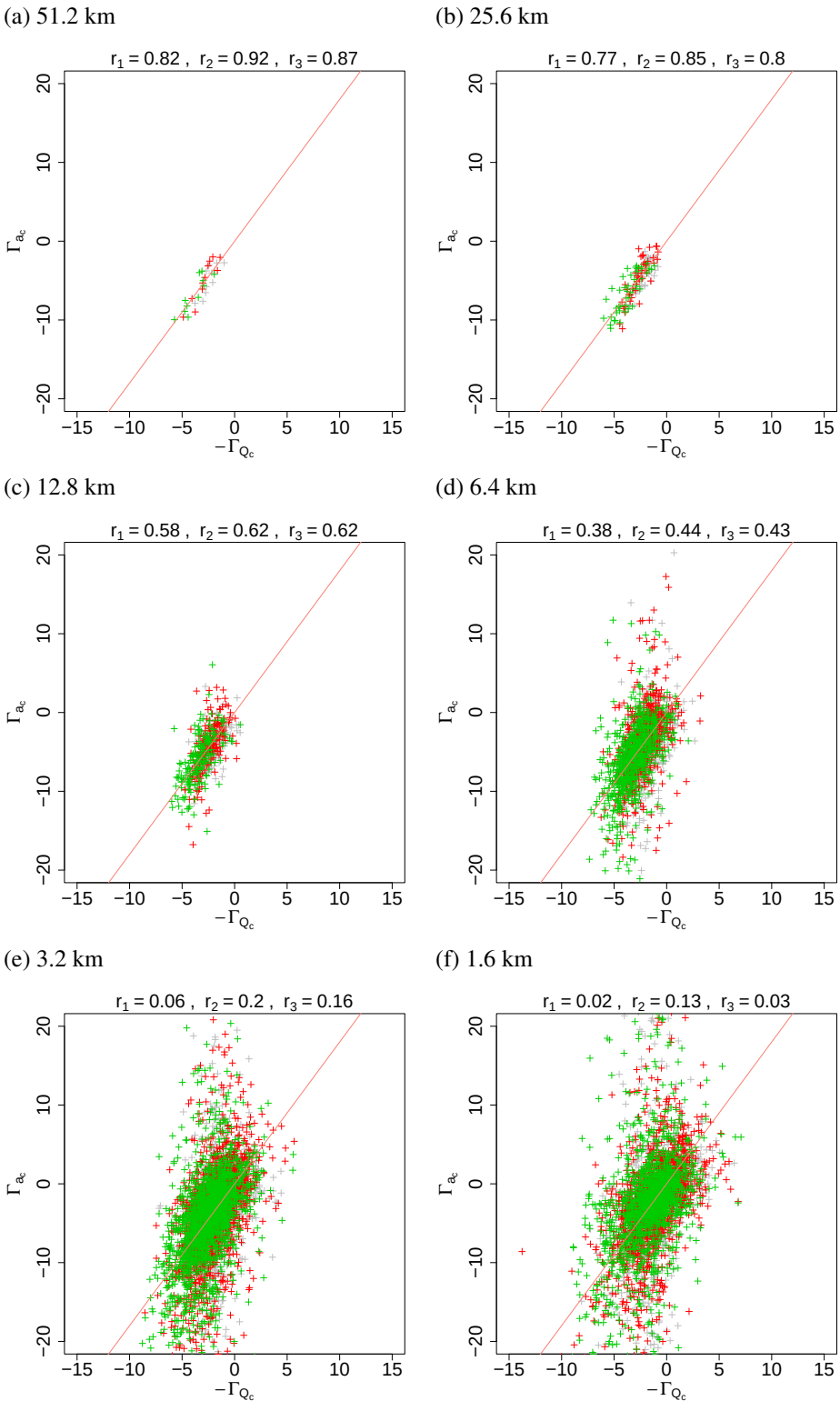

Figure 3.5: A test of the original EDMF closure assumption given by Eq. 3.19 (red line) for the RICO case. Plots are showing the pairs of the vertical gradients of the moist updraft area fraction and zero-buoyancy deficit of q_t above the cloud base, within the time frames starting at 6 (gray), 12 (red) and 18 h (green). Results are coarse-grained across the resolutions, from 51.2 km (top-left) to 1.6 km (bottom-right). Correlation coefficients r_1, r_2, and r_3, are calculated for all three time frames (above the plot).

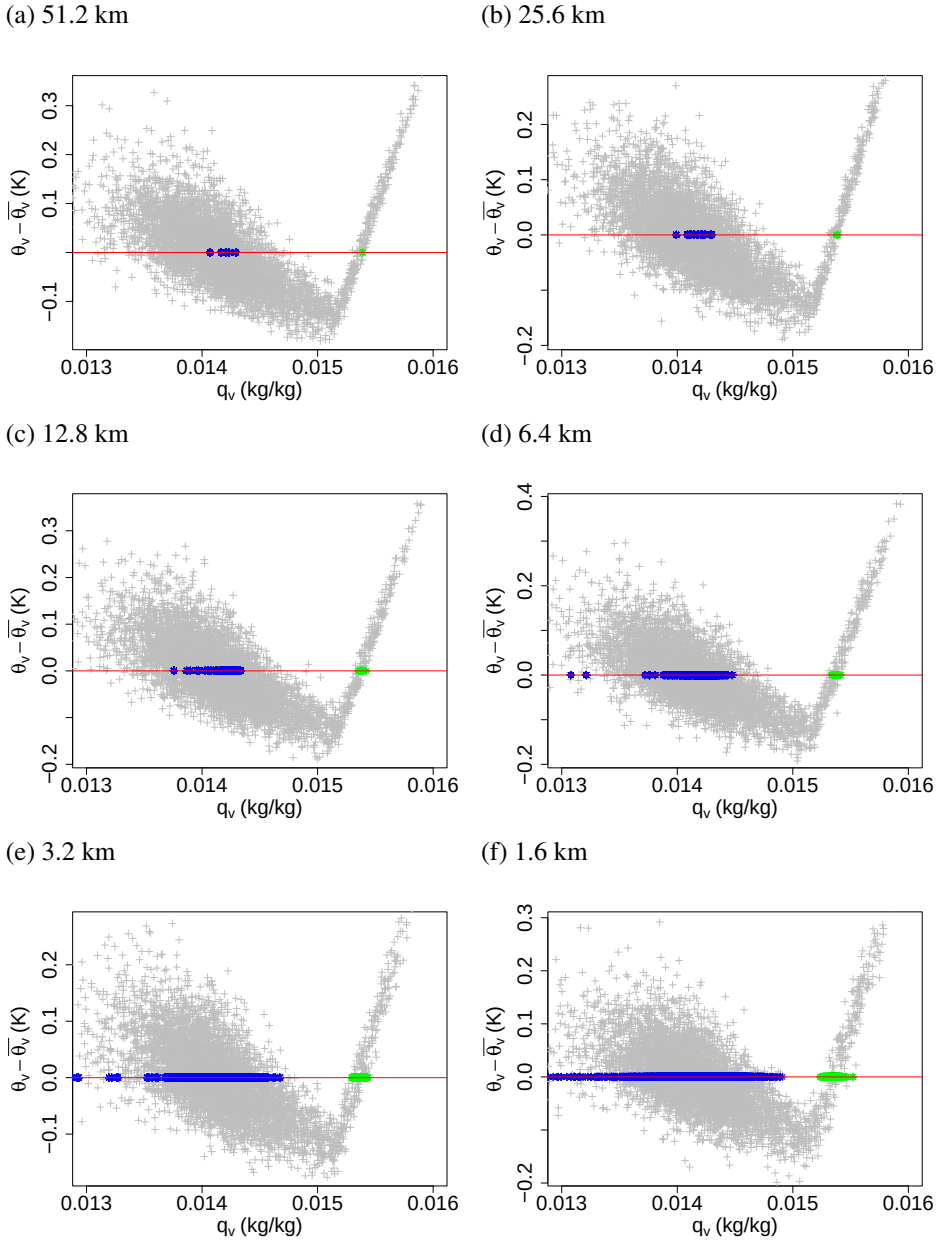

Figure 3.6: The RICO case lateral mixing line at a level above the cloud base on a scatter plot of the virtual potential temperature excess $\theta_v - \overline{\theta}_v$ and total water mixing ratio q_t (gray). The coarse-grained values of the mean total water mixing ratio $\overline{q}_t$ (blue) and the critical value q_t^x (green) at the zero buoyancy line are shown for the range of resolutions, from 51.2 km (top-left) to 1.6 km (bottom-right). The coarsest resolution case shows only five points, representing the five time frames of six hours duration (6-12 h, 12-18 h, 18-24 h, 24-30 h, and 30-36 h), and the number of points increases by the number of grid cells towards the fine resolution cases.

3.5 Numerical simulations

We approach the evaluation and testing of the stochastic parameterization by using an idealized model simulation of the RICO case. A single column model configuration is commonly used to test the newly developed parameterizations, however this approach is appropriate in the case where the sub-grid cloud processes are parameterized assuming no direct communication or correlation between the neighboring model columns, but the interaction takes place only through the mean flow. In the case of the new stochastic EDMF scheme, the entire limited area model domain can be considered equivalent to a single-column setup for testing the parameterization capability to predict the macroscopic state of the system, while the stochastic model is applied across this domain for the probabilistic modelling of the microstates of the system.

In this section we perform deterministic and stochastic model simulations using the ICON model on the double-periodic limited area domain of around 410^2 km^2. Experiments are conducted multiple times using a range of horizontal resolutions from around 1 to 50 km (Table 3.1). In all experiments the vertical grid spacing is stretched with the minimum layer depth of 100 m near the surface and with a total of 50 levels up to 10 km height. Near the top boundary of the modelling domain, the sponge layer is set for wave damping starting at the height of 7 km.

Table 3.1: Model horizontal resolution and time step

triangle edge (km)	rectangular edge (km)	number of points	time step (s)
2.43	1.6	168×196	3
4.86	3.2	84×98	5
9.72	6.4	42×48	10
19.45	12.8	20×24	20
38.90	25.6	10×12	40
77.81	51.2	8×8	80

Turbulence, convection and shallow clouds are parameterized using the unified EDMF parameterization scheme, which is called every fourth dynamics time step, and no other physics schemes are employed to simulate the RICO case. As described in Section 3.2 and in Appendix A.1, the constant large-scale forcing tendencies are applied following the ICON LES framework of Dipankar et al. (2015). A land/ocean surface scheme is as well included in the model configuration, but it is used only for technical reasons because of its hard-coded coupling with EDMF. The constant sea surface properties are prescribed explicitly within the EDMF scheme. This study focuses on the nonprecipitating behavior of the convective case over the ocean, thus the parameterization of precipitation formulated within the moist updraft budget equations is not included in the model configuration.

3.5.1 Deterministic simulations

The deterministic EDMF scheme is tested in ICON by comparing its performance to the LES simulation of RICO-140. The typical RICO domain-averaged quantities, vertical structure of the RICO case and its time evolution are reproduced in ICON model on the meso-γ-scale model grids.

Vertical structure of the convective boundary layer

The vertical structure of the RICO boundary layer is reproduced well in the deterministic EDMF simulations across the model resolutions (Fig. 3.8). Given the homogeneous and constant forcing of the RICO case, it is not surprising that EDMF shows only slight dependence on the model resolution, noticeable mostly in the cloud layer. Cloud fraction and liquid water content are overestimated by the EDMF scheme. However, this is a well known limitation of a bulk approach in EDMF, including the dual-mass-flux EDMF version, and it is evident in other models as well (see Fig. 14 in Neggers, 2009, which results from the case without updraft precipitation.). A bulk approach is not sufficient for parameterizing the more complex, transient cases such as RICO. This indication is supported by the correct profiles of cloud liquid water content and cloud fraction of the RICO case reproduced by the EDMF scheme when a multi-mass-flux approach is employed instead of a bulk plume model (Neggers, 2015; for description of some other multi-mass-flux approaches see also Arakawa and Schubert, 1974; Neggers et al., 2002; Cheinet, 2004; Sušelj et al., 2012).

The high resolution experiments with the grid resolution finer than 10 km show a reduction in cloudiness after 20 hours of simulation, especially near the cloud top, while the cloud layer deepens with the increase in model resolution (Fig. 3.8, top row). The vertical structure of the cloud layer is highly influenced by the vertical structure of the updraft mass flux $M_{ui}, i = 1, 2$, so the reduction of cloudiness results from the reduced mass flux in the high resolution simulations (Fig. 3.8, bottom-rightmost). The behavior of the coarse resolution simulations with the grid resolution coarser than 20 km is the opposite, the cloud mass flux increases with the resolution and that reflects on the cloud fraction vertical profile.

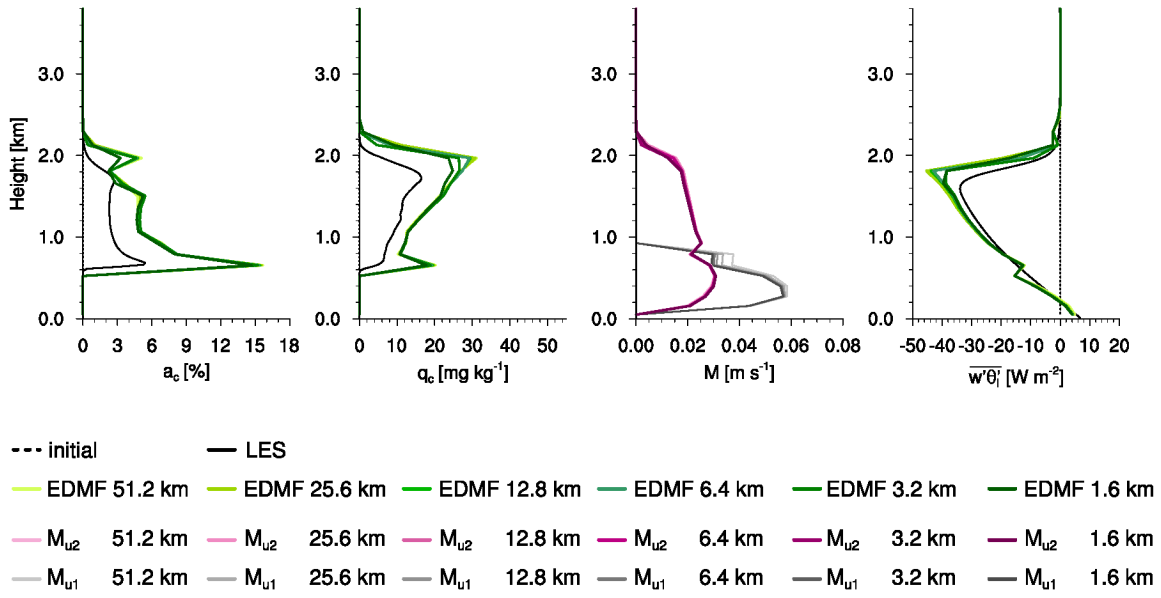

Figure 3.7: Boundary layer vertical profiles in the nonprecipitating deterministic RICO case after 10 hours of simulation, before the simulation dynamics start to diverge at different grid resolutions.

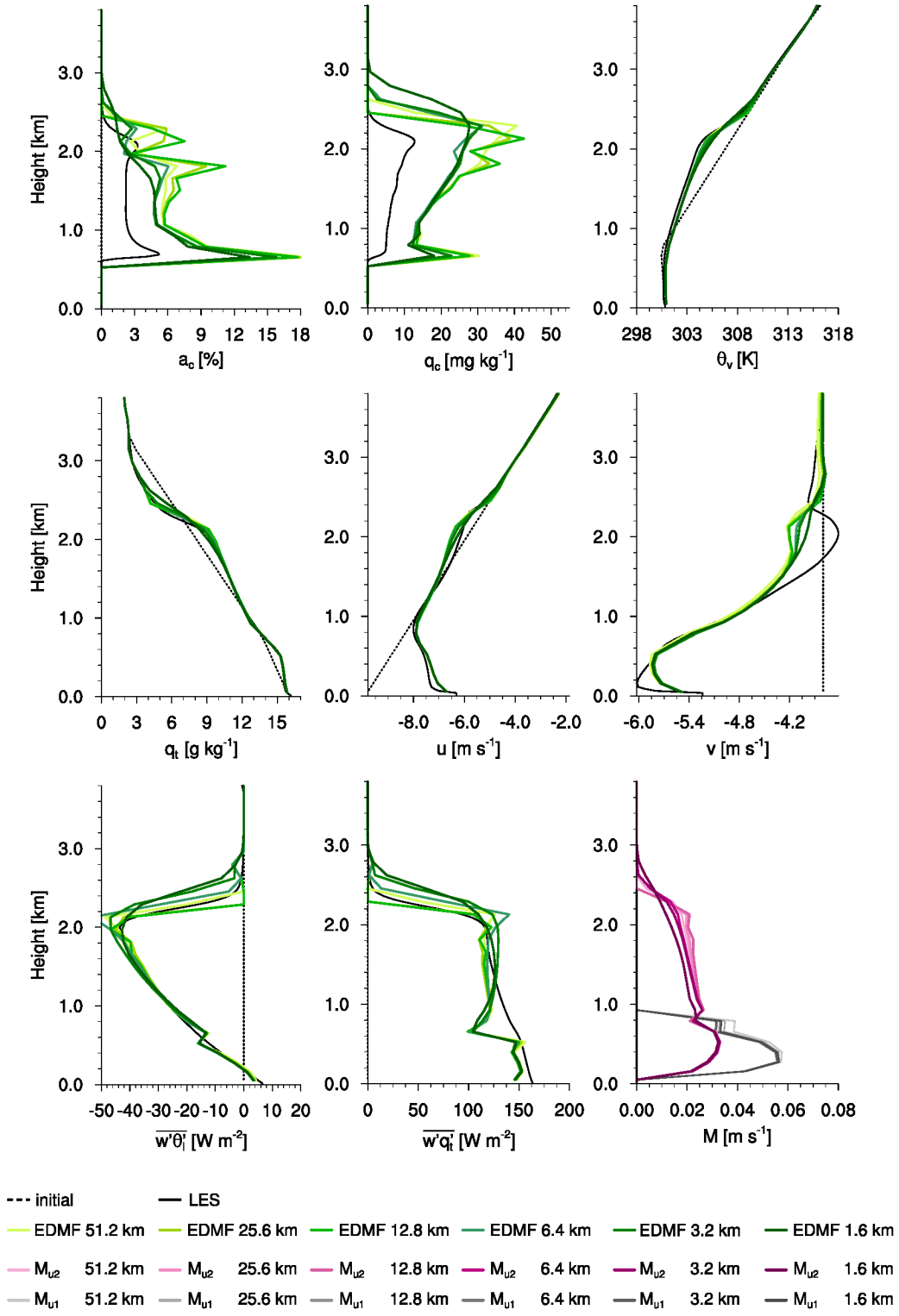

Figure 3.8: Boundary layer vertical profiles of the nonprecipitating deterministic RICO case averaged over the time period from 20-24 h showing: cloud fraction a_c, cloud liquid water mixing ratio q_c, virtual potential temperature θ_v, total water mixing ratio q_t, zonal wind component u, meridional wind component v, sensible heat flux $\overline{w'\theta_l'}$, latent heat flux $\overline{w'q_t'}$, and updraft mass flux M_{ui}, $i = 1, 2$. Please note that we do not compare the updraft mass flux to the LES results.

The opposite behavior between high and coarse resolution simulations is caused by the divergence of grid-scale flows on different model grids that takes place already after 12 hours of the simulation (see section 3.5.4). Before the divergence of grid-scale flows takes effect, the EDMF scheme itself has no resolution dependence, and this is demonstrated by the almost identical vertical profiles of the convective boundary layer properties after only 10 hours of simulation (Fig. 3.7). As it will be described later in Section 3.5.4, on high resolution grids, convective circulations develop and organize into regular roll structures that bring in inhomogeneities into the cloud field and change the convective regime of RICO into an organized case. The inhomogeneities brought in by the convective organization influence the parameterization of the cloud layer vertical structure, and activate the effects of the impaired scaling relation (Eq. 3.19, Fig. 3.5) in the formulation of the vertical mass flux structure. This degrades the vertical profiles of cloud mass flux with the increase in model resolution to the grids with a length finer than 10 km. In the homogeneous cloud field, before the emergence of convective circulations, the scaling relation Eq. 3.19 has the same behavior on different resolutions and does not affect the model convergence.

The apparent divergence of simulations on the coarse model grids, visible mostly in the mass flux M and cloud fraction a_c vertical structure (Fig. 3.8), results from small differences in the evolution of the cloud fields among the simulations. As we will show later, precipitation is not included in the model configuration, so the cloud liquid water piles up and the convective system shows small jumps in cloud liquid water path and higher jumps in cloud cover (see Fig. 3.16). The small jumps and the gradual increase of cloud liquid water path is very similar across the resolutions, thus we see no differences in the absolute value of q_c on the vertical profile plots. On the other hand, the higher jumps in the cloud cover evolution cause small differences across the resolutions, which reflect in the vertical profiles of the cloud fraction. However, it is uncertain if these differences in a_c across the coarse resolutions can be interpreted as a regular divergence pattern of simulations.

Stability of the RICO case in ICON EDMF

RICO is a precipitating shallow cumulus case over the ocean, and in principle, it is a transient case but for the pupose of parameterization it can be considered quasi-stationary on hour timescales (in Chapter 2 we used six-hour time frames). In the EDMF simulations without precipitation, the RICO case becomes unstable approximately after a day and a half. This is expressed as the gradual increase of cloud cover over time to 100 % until the third day of simulation, and very unstable times series of both cloud cover and cloud liquid water path (Fig. 3.9, green). When precipitation is permitted during the five day long simulation, cloud cover and liquid water path time series are stable and the system maintains the balance (Fig. 3.9, purple). Simulations longer than five days were not performed here, but the expectation is that they are feasible using the deterministic EDMF scheme if precipitation is allowed on the subgrid scale.

During the first day of the simulation, the EDMF closure mechanism based on the boundary layer equilibrium described in Section 3.3.2, Fig. 3.1, maintains the low cloud fraction and brings the system close to equilibrium state after every small perturbation. However, after approximately 32 hours of simulation, the EDMF closure assumptions completely break down as too much liquid water is

(a) cloud cover (b) cloud liquid water path

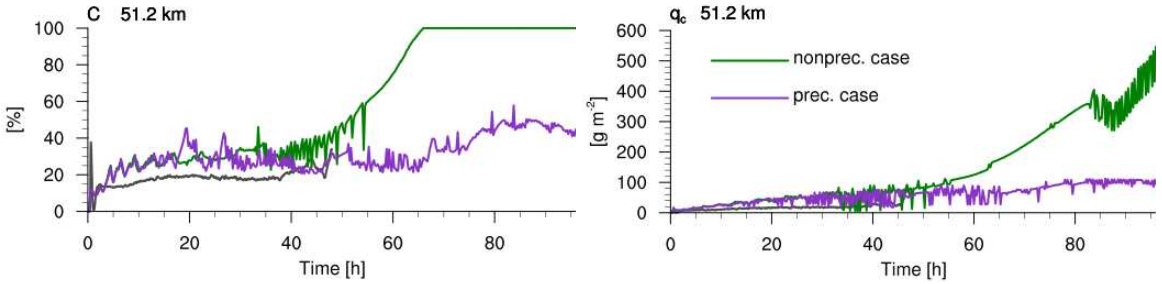

Figure 3.9: Comparison of the time series of cloud cover and cloud liquid water path between the LES RICO case (gray), deterministic EDMF without precipitation (green) and deterministic EDMF with precipitation (purple).

accumulated over the time because its release by precipitation is disabled by the model configuration. After the liquid water path exceeds around 100 g m^{-2} and after the cloud fraction exceeds 30-40 %, the behavior of the scheme is no longer physical and the whole mechanism of equilibration breaks down after which the simulations fails. The main reason for this kind of instability of simulated convection is the assumption of the total convective area fraction of 10 % allowed in the deterministic scheme (Section 3.4.1, $\mathcal{A}^{up} = 10\%$).

In the following, we exclude the subgrid precipitation that originates from convective clouds in the EDMF configuration to isolate the effects of the stochastic EDMF parameterization on the nonprecipitating convective case. Therefore, the RICO case is studied here during a day and a half in all simulations before the instability affects the simulated cloud system.

3.5.2 Stochastic simulations

In this section we present the results of the stochastic EDMF scheme described in Section 3.4 employed to simulate the RICO case in ICON. The stochastic scheme is tested across the range of model horizontal resolutions (Table 3.1). The reference case for the stochastic simulations is resulting from the bulk updraft configuration of the budget equations and the buoyancy sorting scheme applied to the bulk updraft (the first option for the vertical structure formulation in Section 3.4.2). Thus, in the reference configuration, the stochastic approach is affecting the simulations solely through the perturbed updraft area fraction a^p_{u2}.

The vertical profiles of cloud fraction a_c and cloud liquid water mixing ratio q_c demonstrate a decrease in cloudiness with increasing resolution (Fig. 3.10). In a similar way as in the deterministic simulations, this reduction in a_c and q_c results from the changes in the mass flux profile with resolution (Fig. 3.10, bottom right). In general, the stochastic model successfully reproduces the mean thermodynamic vertical structure of the RICO case, and furthermore, the cloud layer profiles of a_c and q_c show an improvement towards the shape of the LES RICO profile. The structure of the cloud layer vertical profiles is very similar but evidently smoother than the structure of the profiles in the deterministic experiments (Fig. 3.10, top row). The turbulent fluxes of heat and moisture are mod-

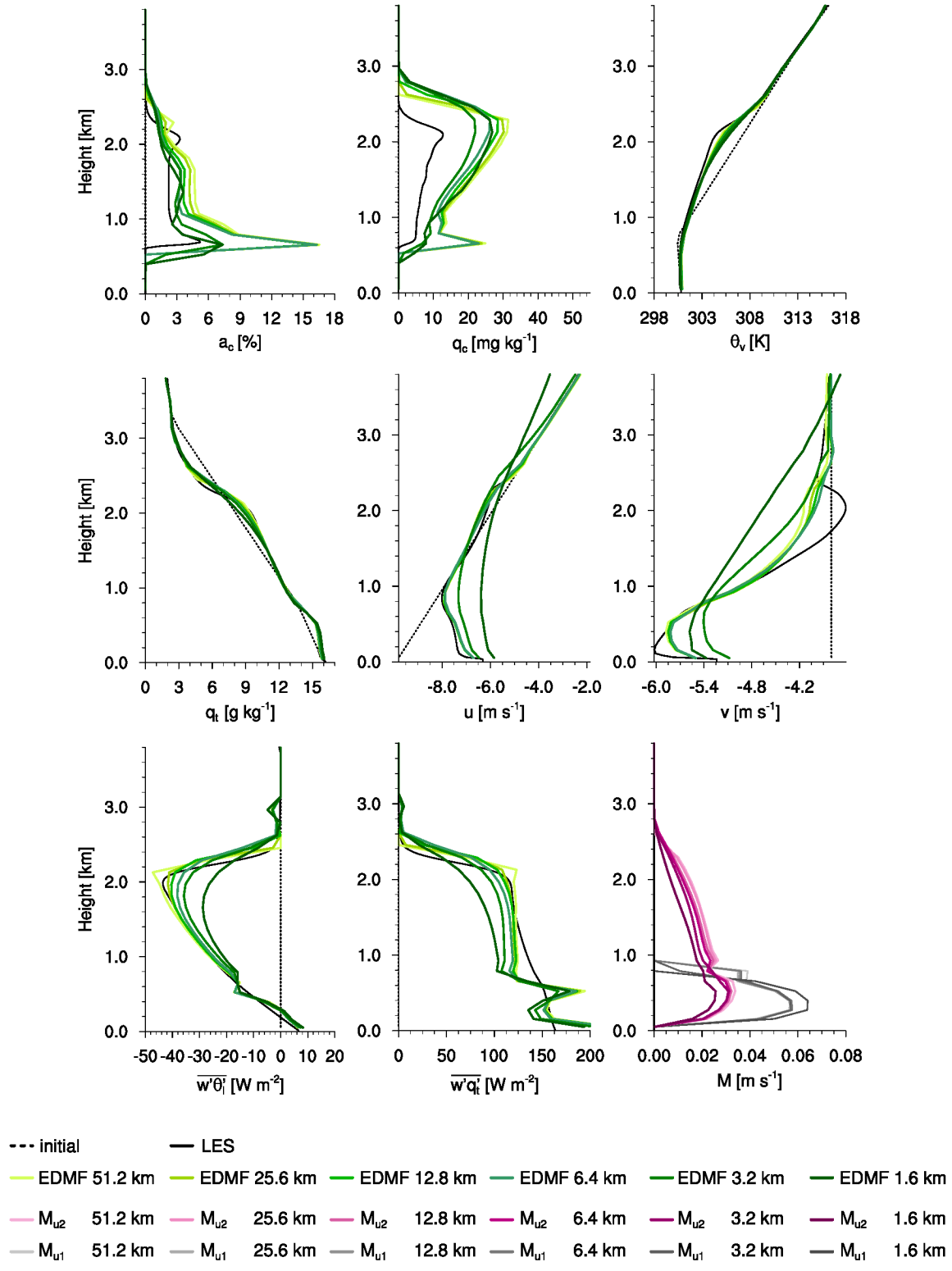

Figure 3.10: Boundary layer vertical profiles in the nonprecipitating stochastic RICO case averaged over 20-24 hour time period, showing: cloud fraction a_c, cloud liquid water mixing ratio q_c, virtual potential temperature θ_v, total water mixing ratio q_t, zonal wind component u, meridional wind component v, sensible heat flux $\overline{w'\theta_v'}$, latent heat flux $\overline{w'q_t'}$, and updraft mass flux $M_{ui}, i = 1, 2$.

elled well, and they show a small dependence on resolution, which also reflects the dependence of the mass flux profile on the model resolution (Fig. 3.10, bottom row).

This resolution dependence is partly caused by the convective circulations that develop on the model grid as a solution of the model dynamics. In difference to the deterministic simulations, this effect acts on all grid resolutions tested in this experiment. Because the convective circulations are grid-scale dependent, the influence they have on the vertical profiles as well depends on the model resolution (see Section 3.5.4). The vertical structure parameterization across the model resolutions is simplified in this model configuration where the shape of the bulk vertical structure is retained on all resolutions (option 1 in Section 3.4.2), which is another factor that causes a reduction in the mass flux, turbulent fluxes and wind profiles with resolution. This suggests that a simplified formulation of the vertical cloud structure in this base stochastic model formulation is not sufficient to reach the complete scale convergence of the CBL parameterization.

The vertical profiles of the wind components are affected by the stochastic model more than the other RICO properties, and are degraded on a very high resolution below $\sim$ 6 km (Fig. 3.10, middle row). The momentum fluxes might require a different treatment of plume dilution with height by lateral mixing, which should is separately defined from the parameterization of thermodynamic fluxes. This difference, however, becomes important on the high model resolutions within the convective gray zone, while the coarse-resolution simulations are not affected.

In the remainder of this section, we will test different formulations of the lateral mixing mechanism and the mass flux vertical structure formulation and try to reproduce the correct thermodynamics and wind profiles on high resolution model grids. However, we do not provide the final or a complete solution for a scale-aware lateral mixing parameterization in the convective gray zone.

Sensitivity of the cloud layer to the entrainment timescale

Given the fact that the entrainment timescale τ_ϵ is uncertain, it is possible that the timescale τ_ϵ has a high influence on the RICO case average vertical profiles in the stochastic model configuration. This is why we test the sensitivity of the RICO case vertical structure to this parameter, by performing two experiments across the range of model resolutions, first with a shorter entrainment timescale $\tau_\epsilon = 300$ s and second with a longer timescale $\tau_\epsilon = 600$ s. A shorter entrainment timescale produces a stronger entrainment rate with height, while a longer entrainment timescale sets a weaker entrainment rate. Here we apply the change in τ_ϵ to both dry and moist updrafts, following Eqs. (3.13) and (3.14).

The cloud layer is highly sensitive to the parameterization of the entrainment timescale as expected (Fig. 3.11). A less vigorous and shallower cloud layer results from the stronger entrainment by setting a short timescale (Fig. 3.11a), and the difference among the simulations on different grid resolutions is more pronounced than in the reference case. On the coarse resolutions, the vertical profiles are unstable, with two or more strong peaks near the cloud base and cloud top levels. Doubling of the entrainment timescale changes the cloud profiles substantially, and the cloud layer becomes significantly deeper (Fig. 3.11b). The cloud water mixing ratio shows a strong dependence on the model resolution in the latter case - as the model resolution increases the cloud liquid water decreases. Cloud fraction

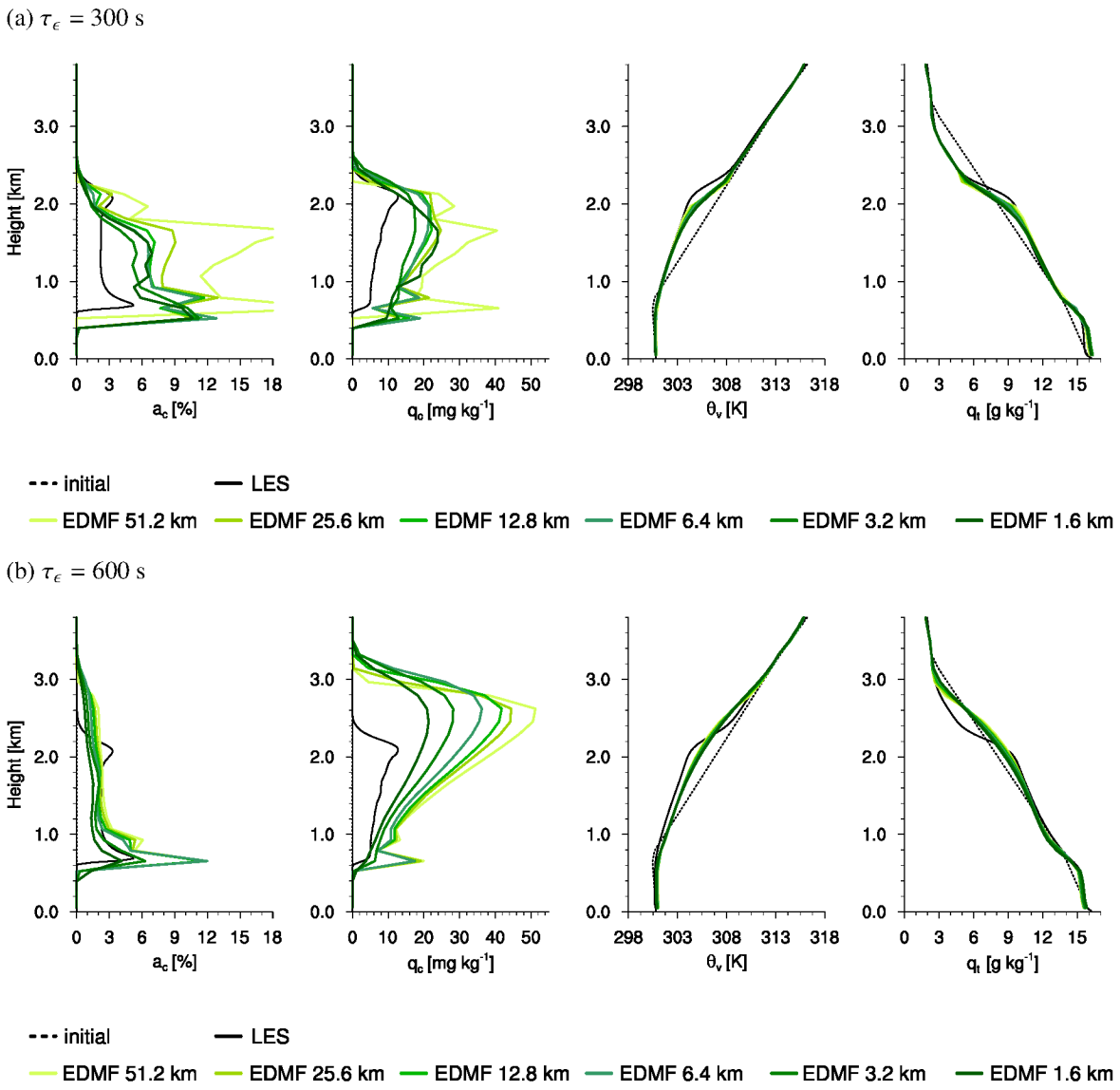

Figure 3.11: Testing the sensitivity of the boundary layer vertical profiles in the nonprecipitating stochastic RICO case on the entrainment timescale τ_ϵ.

is much lower above the cloud base compared to the case with the low entrainment timescale. The evident high sensitivity of the cloud layer to the entrainment timescale τ_ϵ across the range of model resolutions points to the significance of the entrainment formulation for the resolution dependence of simulations.

A stochastic parameterization of the cloud layer vertical structure

In the previous subsection we have learned that the entrainment timescale τ_ϵ has a great impact on the cloud layer vertical structure, and that τ_ϵ also influences the scale-dependence of the cloud layer vertical structure. Besides that, the vertical gradient of cloud area fraction Γ_{a_c} is not an unique function of the vertical gradient of moist buoyancy deficit Γ_{Q_c}, and the spread around the deterministic

scaling relation (Eq. 3.16) becomes wider with the increase of resolution (see Fig. 3.5). These are the two main reasons to parameterize the vertical structure of the cloud layer more adequately. In this section, we test several possible approaches to the cloud layer vertical structure parameterization on the gray zone grids, and we discuss the requirements for a complete scale-aware vertical structure parameterization. The model configurations suggested here correspond to the suggestion for the new vertical structure parameterization, option 2 defined in the section 3.4.2.

Test 1:

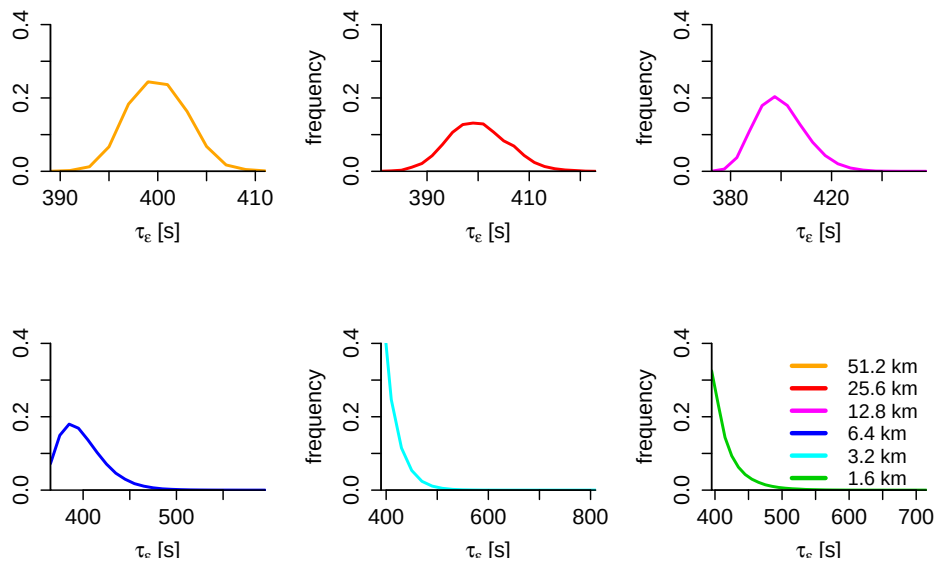

Figure 3.12: Distribution of τ_ϵ across the resolution, as parameterized in a stochastic treatment of the cloud layer vertical structure by Eq. 3.20.

First, we test a semi-stochastic parameterization of τ_ϵ and Γ_{a_c}, with arbitrarily selected and tuned variance of the sampling distribution. The tuning of the sampling distribution variance is performed towards the RICO-140 cloud layer vertical structure. In the case of τ_ϵ, we adopt the scale-dependence of the moist updraft area fraction compound distribution, which is defined in Chapter 2 (see Fig. 2.9), by adding a perturbation term to τ_ϵ as

$$\tau_\epsilon^p = \tau_\epsilon + a_* \frac{a_{u2}^p - a_{u2}}{a_{u2}} \tau_\epsilon, \tag{3.20}$$

where a_{u2}^p is a perturbed moist updraft area fraction, a_{u2} is a nonperturbed bulk moist updraft area fraction, and a_* is a factor that controls the spread of the perturbed entrainment timescale τ_ϵ^p. The factor a_* is a tuning parameter valid for the RICO-140 case at this stage of model development, and it ranges from 0.03 in high resolution simulations to 0.1 in coarse resolution simulations. In this way the distribution of τ_ϵ is scale-aware, with a variance and skewness that increase with model resolution (Fig. 3.12). As the resolution of the model increases, the spread around the nonperturbed deterministic timescale τ_ϵ becomes higher, and the distribution of all possible values of τ_ϵ^p becomes right skewed. Thus the entrainment rate ϵ is still parameterized as a function of the updraft vertical velocity w_{ui}, but it also comprises a quasi-random component introduced through the modified entrainment

timescale τ_ϵ^p. As another stochastic process in this test, the vertical gradient of cloud area fraction Γ_{a_c}

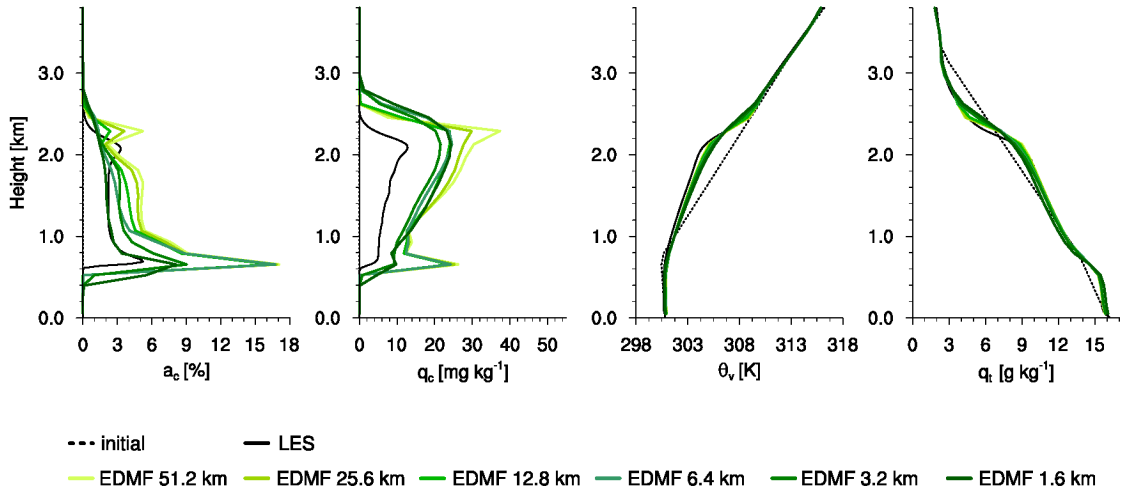

Figure 3.13: Multi-resolution test of the nonprecipitating stochastic RICO case. Figures are showing the boundary layer vertical structure similar as on previous plots (Fig. 3.10). In these simulations, the entrainment timescale is perturbed following the equation Eq. 3.20, while the gradients of the cloud fraction Γ_{a_c} are perturbed by sampling from the normal distribution.

is perturbed by sampling the gradients randomly from a normal distribution with the mean value Γ_{a_c}, and standard deviation that varies from 5 in the case of the coarsest grid resolution to 1 in the case of the highest resolution simulation.

The difference in the simulated cloud field between the stochastic model configuration with the bulk and with the semi-stochastic cloud layer vertical structure is not pronounced (see Fig. 3.13). This simple semi-stochastic parameterization of the cloud layer vertical structure affects the upper part of the cloud layer by recovering the cloud layer top peaks, but only partly and not in the case of the two highest resolution simulations. Perhaps a more sophisticated method is required here to further improve the cloud profiles, especially in order to reduce the cloud liquid water content (see Fig. 3.13, q_c plot).

Test 2:

Second, we test how the parameterization of mass flux vertical structure affects the high resolution simulation with the grid distance of 3.2 km (translated to a rectangular spacing), in which the wind profiles start to degrade. Instead of using the buoyancy sorting mechanism in the EDMF scheme to estimate the mass flux vertical profiles, we collect the individual cloud mass fluxes from the stochastic cumulus ensemble and construct the vertical structure of a random sum of cloud mass fluxes within each model grid column. Individual clouds have a constant mass flux with height but their random sums show the height changing vertical profiles (Fig. 3.15). This approach can be graded as the most appropriate parameterization of the vertical mass flux structure that is consistent with the stochastic cumulus ensemble framework. However, the difficulty of defining the corresponding lateral entrainment formulation remains in this model configuration and the outcome of the simulation is very sensitive to the small changes in the definition of the lateral entrainment timescale τ_ϵ.

(a) τ_ϵ distribution results from equation similar to Eq. 3.20, but instead of using a bulk a_{u2} the median of the a_{u2} distribution is used and the tuning parameter is set to $a_* = 0.08$:

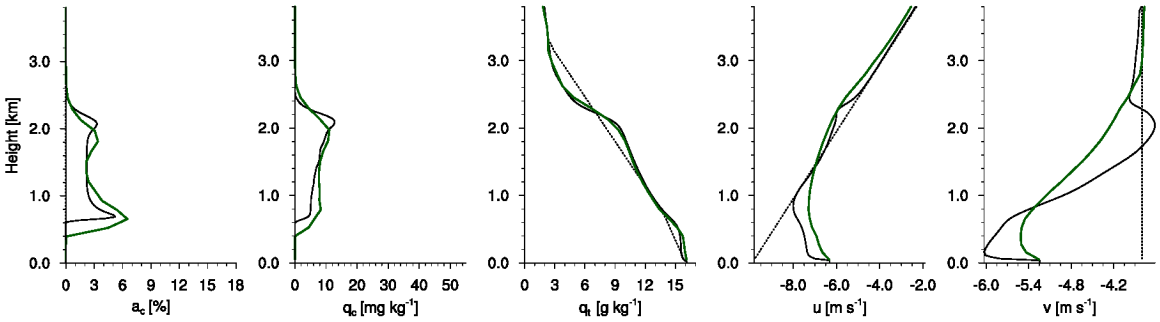

(b) τ_ϵ is normally distributed around the mean $E[\tau_\epsilon] = 400$ s and with the standard deviation of $\sigma_\tau = 60$ s:

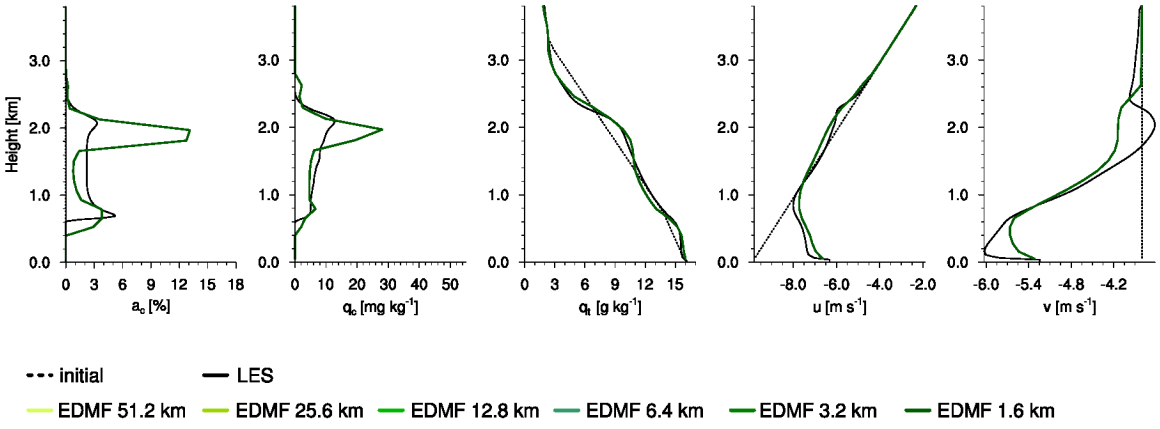

Figure 3.14: Boundary layer vertical profiles in the nonprecipitating stochastic RICO case. Stochastic vertical structure parameterization is tested for the sensitivity of the vertical thermodynamic and vertical wind structures on the lateral entrainment rate parameterization.

We perform two simulations, first by tuning the τ_ϵ sampling distribution (Fig. 3.12) to reproduce the correct thermodynamic structure of the RICO boundary layer, and second by tuning the τ_ϵ distribution to reproduce the correct momentum transport and wind profiles of the RICO case. The results of these two simulations presented on Fig. 3.14 show that when the model is tuned by changing the τ_ϵ distribution to represent correctly the thermodynamic structure, the vertical wind profiles are degraded (as in the previous experiments using the stochastic EDMF scheme, Fig. 3.10). On the other hand, when the τ_ϵ distribution is tuned to represent the vertical wind profiles correctly, the thermodynamic structure and cloud fraction profiles are degraded (Fig. 3.14). This suggests that parameterized momentum transport and thermodynamic transport should use separately defined lateral entrainment mixing mechanisms in the gray zone models.

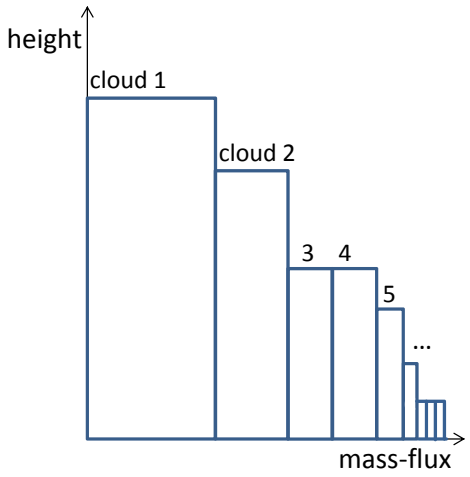

Figure 3.15: A sketch of the subgrid mass flux vertical profile construction. Individual clouds have different heights and intensities and a constant vertical mass flux profile. Depending on the random number of clouds within a grid column, the total cloud mass flux profile will have various shapes.

We conclude here that the stochastic parameterization of a shallow convective ensemble, by subsampling the individual realizations of subgrid convection to represent the fluctuations around the equilibrium, combined with an appropriate vertical structure stochastic parameterization, improves the cloud layer vertical structure in a transient convective case such as RICO. The cloud fraction and cloud liquid water content (Fig. 3.14a) now match the LES RICO profiles closely. Thus, the least complex parameterization that is able to reproduce the RICO case vertical structure properly across scales includes the stochastic cloud ensemble framework and a semi-stochastic cloud layer vertical structure parameterization.

Time series

Now we continue the analysis of the basic stochastic EDMF RICO case (option 1 from Section 3.4.2). The time series of cloud cover and cloud liquid water path are plotted on the panel on Fig. 3.16. It is evident that the deterministic EDMF scheme overestimates cloudiness on all model grids. We know from the previous section that EDMF is unstable if precipitation that originates from moist updrafts is not included into the model configuration (Fig. 3.9). Here we show that the stochastic EDMF captures the RICO time series better than the deterministic scheme and clearly smooths the abrupt peaks in the time series of cloud cover and liquid water content on all model resolutions (Fig. 3.16). So, the most prominent effect of the stochastic model on the time evolution of the RICO convective case is stabilization of the time series of cloud cover and cloud liquid water content (Fig. 3.16).

Resolution dependence is evident in the time series as well, where the high resolution cases develop cloudiness that is reduced throughout the simulation compared to the coarse resolution cases. We

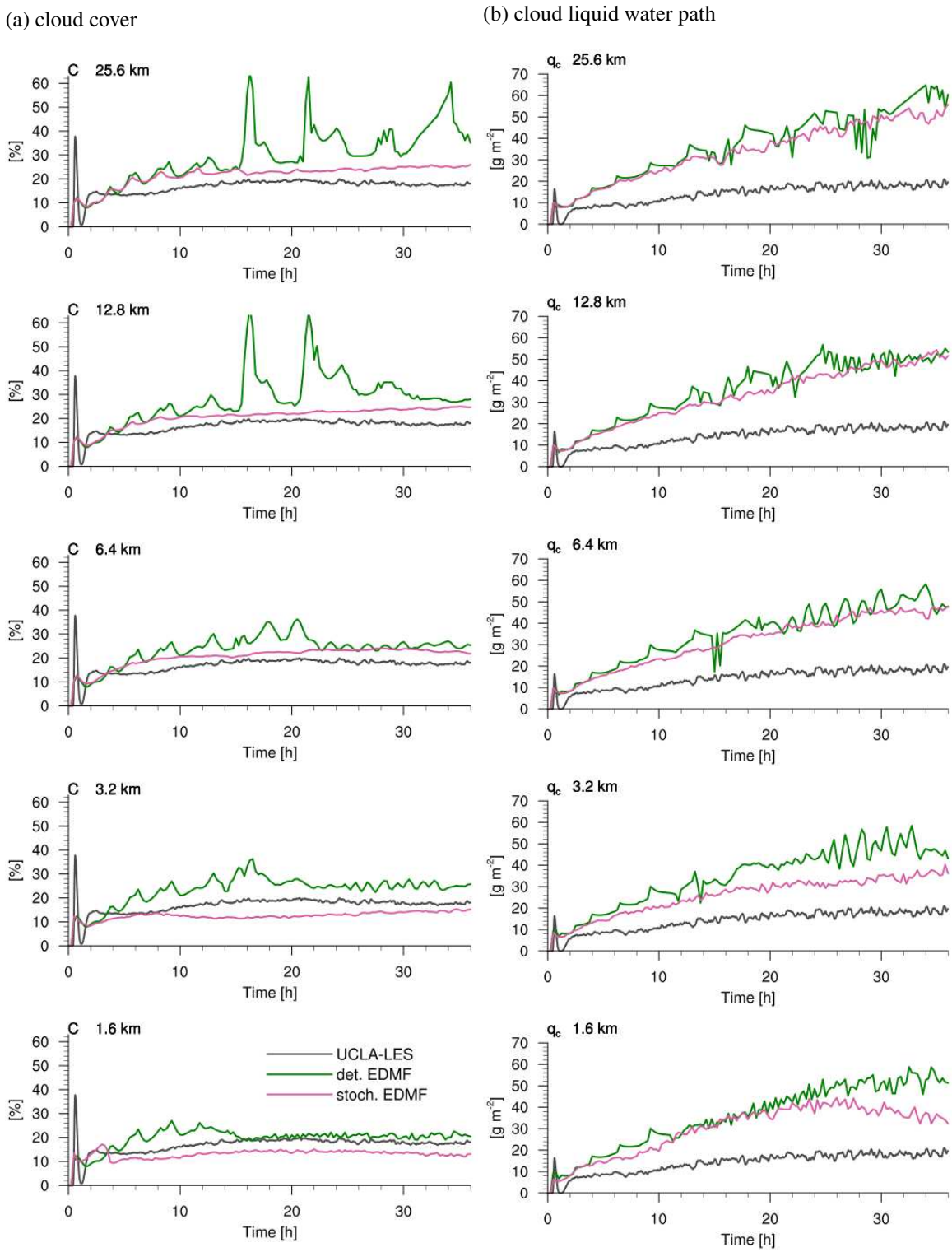

Figure 3.16: The RICO time series of the cloud cover and cloud liquid water path showing the deterministic EDMF (green), stochastic EDMF simulation (pink), and LES RICO-140 time series (gray).

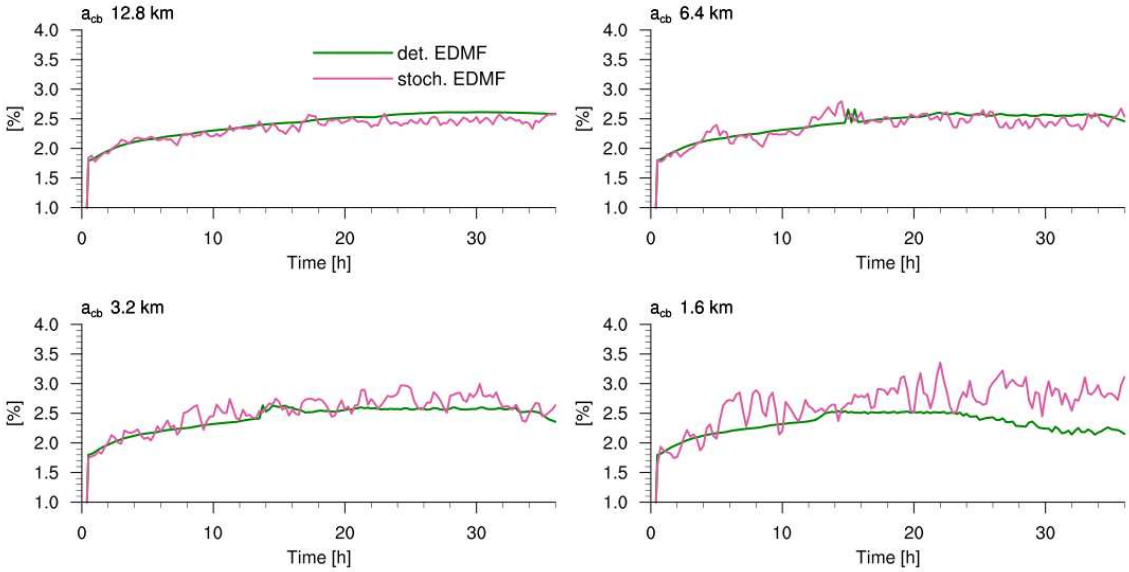

Figure 3.17: RICO time series of the moist updraft area fraction at the cloud-base level showing the deterministic EDMF without precipitation (green) and stochastic EDMF without precipitation (pink).

attribute this reduction partly to the resolution sensitivity of the cloud layer vertical structure parameterization, the entrainment rate formulation and the vertical mass flux structure, and partly to the interaction of EDMF with the convective circulations permitted on the grid scale (see the next two sections). The stochastic model introduced to EDMF perturbs the updraft area fraction and is not directly responsible for the scale-dependence of the time series. To prove the latter statement, we show that there is no scale-dependence of the average updraft fraction at the cloud-base level on Figure 3.17, though the stochastic variability introduced at the cloud base slightly increases with the resolution. The increase of variability in the updraft area fraction at a level above the cloud base reflects the increase of variability in the cloud field caused by the circulations permitted on the grid scale, and is not introduced by the stochastic model. By the applied stochastic approach itself, the fluctuations of the domain average updraft area fraction in time should not be resolution dependent (not shown here).

3.5.3 Convective variability across scales

From the coarse-graining study of the LES RICO case (Chapter 2), we draw the conclusion that the statistical quasi-equilibrium can be considered valid on grid resolutions coarser than approximately 20 km (see Fig. 3.18a). We have to emphasize that this conclusion holds in the case of a quasi-stationary convective cloud field in a slowly changing environment. In this section we show how the fluctuations around the equilibrium develop in ICON, in the deterministic and in the stochastic RICO simulations, forced by the constant large-scale forcing tendencies (see Appendix A.1).

Variability of the subgrid convective states in ICON increases with the model resolution, which is illustrated on the histogram plots (Fig. 3.18b-d).

The histograms resulting from simulations using the deterministic EDMF scheme are very similar and very narrow across the coarse grid resolutions, with the grid scale approximately above 10 km. Samples of cloud fraction are collected from snapshots taken every 15 min during six hours of the deterministic simulations, and the small spread in the coarse-resolution cases is resulting from the time variations of the mean cloud fraction without any spatial variability. On the model grids with resolution below 10 km, the variance and skewness of the subgrid cloud fraction increase. However, the shape of the developed distribution of subgrid cloud fraction is irregular and the distribution can have more than one peak. This kind of variability of the subgrid cloud fractions has different properties and is not comparable to the variability of the subgrid LES cloud fraction. This variability results from the under-resolved convectively induced circulations that develop on the model grid, and its trend is to increase with model resolution.

The cloud fraction histograms resulting from the stochastic simulations (Fig. 3.18c,d) resemble the LES histograms well and show an increase in variance and skewness with resolution. Compared to deterministic simulations, the stochastic scheme improves the histograms especially on the high resolution grids (Fig. 3.18c,d). However, the variance is still overestimated and the skewness of cloud

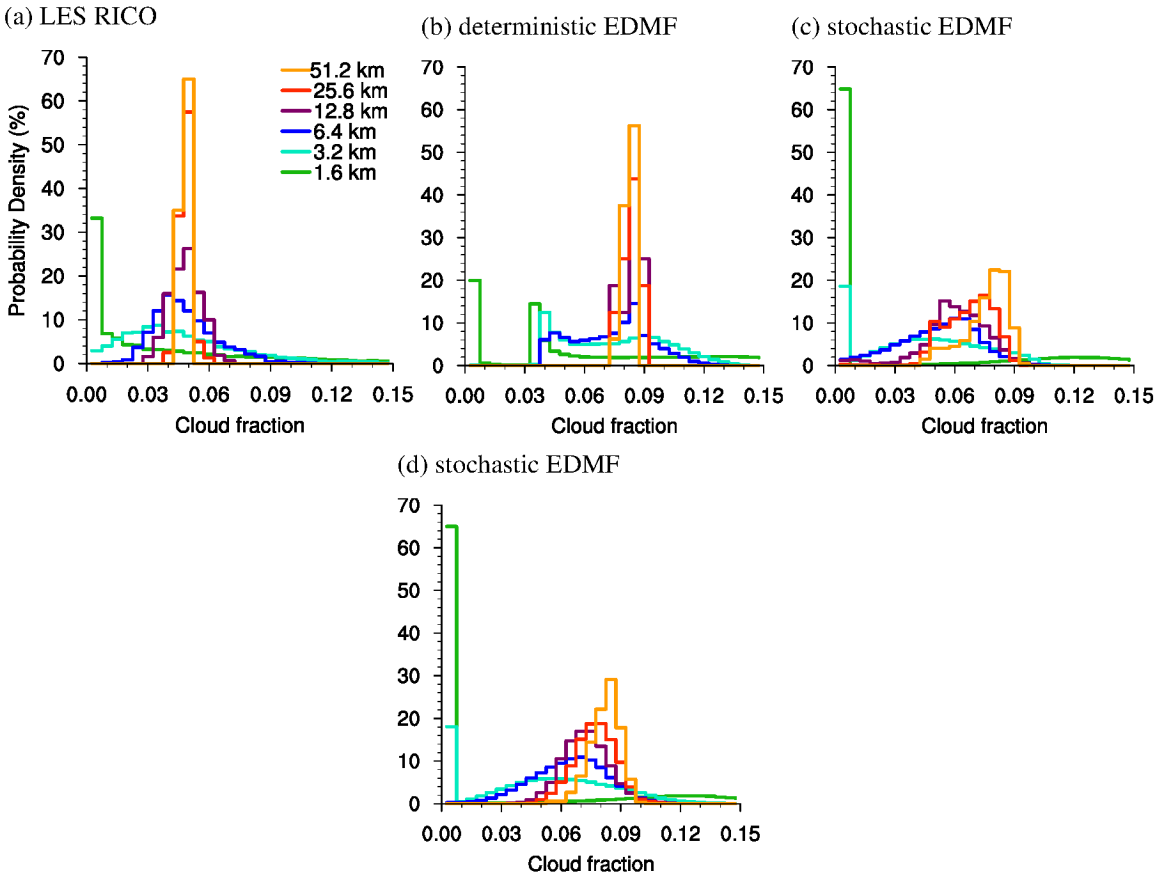

Figure 3.18: Histograms of cloud fraction above the cloud base. The coarse-grained LES RICO case histograms a) are repeated here for the convenience of the reader. The remaining plots show: b) the deterministic EDMF RICO case histograms, c) the stochastic EDMF RICO case histograms corresponding to the cloud layer vertical structure configuration without the stochastic entrainment, and d) the stochastic EDMF RICO case histograms including the semi-stochastic entrainment formulation.

fraction is reversed in the stochastic simulations (Fig. 3.18c,d) compared to the LES coarse-grained cloud fraction histograms (Fig. 3.18a). The histograms resulting from the stochastic simulations include the variability due to convective ensemble subsampling, but obviously, there is another source of variability superimposed on the stochastic variability. Similarly as in the deterministic simulations, this additional variability results from the grid-scale flow and emergence of convective circulations. Note also that the stochastic entrainment parameterization from the previous section brings in more smooth and stable shapes to the histograms (Fig. 3.18d).

3.5.4 Grid-scale dependent secondary circulations

The deterministic EDMF cloud scheme produces horizontally homogeneous thermodynamic fields on the coarse grid resolutions, from around 10 to 50 km (not shown here). In the high resolution simulations with the grid scale less than 10 km, secondary convectively induced circulations emerge and develop over time into organized convective rolls (Fig. 3.19). The timing of emergence of these circulations and their spatial scales are highly dependent on the model resolution. On the 6.4 km grid, convective circulations emerge after around 20 hours of simulation, while on the finer grids they develop sooner - short time before 20 hours in the case of the 3.2 km simulation, and after around 12 hours in the case of the 1.3 km simulation. The imposed wind and Earth's rotation dictate the direction of the organized roll structures, and the period of inertial oscillation can be recognized on the panel plot in Fig. 3.19a, as the direction of rolls changes the angle for around 45 degrees during 12 hours.

The spatial scales of convective circulations depend highly on the model resolution. On the LES model grids, convection and clouds are effectively resolved and convective organization can take place in a thermally and mechanically induced case under the constant large-scale forcing such as RICO. LES of the RICO case simulate the emergence and development of convective organization into rolls and arc structures, and even in the case when precipitation is suppressed (RICO-140), convective rolls develop and are well defined after a day of simulation time (Fig. 2.1). These rolls have a spatial scale that is controlled by the CBL depth. As the model resolution coarsens, the model grid scale becomes another dominant spatial scale, because it becomes comparable to the dominant convective scale. At these scales, where convection is no longer effectively resolved, the energy of the flow is shifted towards larger scales compared to the effectively resolved case, thus the size of the circulations developed on the model grid also has to be larger (Bryan and Rotunno, 2005; Cheng et al., 2010). This as well influences the spatial distribution of clouds, which organize along the updrafts of these secondary circulations. Cheng et al. (2010) also point out that on the gray zone scales, parameterized transport is underestimated, while the resolved-scale transport is overestimated, so that the mean transport remains equal across the model resolutions. In difference to the LES simulations of Cheng et al. (2010), in the stochastic and deterministic ICON simulations, the turbulent fluxes are almost completely subgrid, with only a negligible contribution from the resolved scales. This finding aligns well with the study of Bryan and Rotunno (2005) that explains this phenomena by the fact that the turbulent energy cascade is not explicitly resolved on the kilometer-scale grids in NWP models, and the simulated flow does not become turbulent on the grid scales coarser than approximately 100 m.

The grid-scale flow develops in a different manner in the stochastic simulations, and these flows are captured on the snapshots of liquid water content and vertical velocity taken above the cloud-base level after 24 hours of simulation (Fig. 3.20). The convective circulations are as well grid-scale dependent in these simulations and they develop immediately from the simulation start. This circulation development is supported by the stochastic fluctuations that introduce inhomogeneities into the cloud field. However, these circulations are not organized into strong roll structures which is an improvement compared to the deterministic simulations.

As expected, a high dependence on the grid scale can be found in the higher moments of convective and cloud properties, as the variance increases due to grid-scale convective structures, and skewness of the distribution changes the sign (Fig. 3.22). This obviously adds some artificial characteristics to the cloud field. In the deterministic simulations variance of the cloud liquid water mixing ratio q_c is equal to zero before the under-resolved convective structures develop (Fig. 3.22a). The emergence of convective organized structures is characterized by a strong increase in variance that takes place after

(a) 6.4 km resolution, snapshots at t = 24 h, t = 28 h, t = 32 h, and t = 36 h

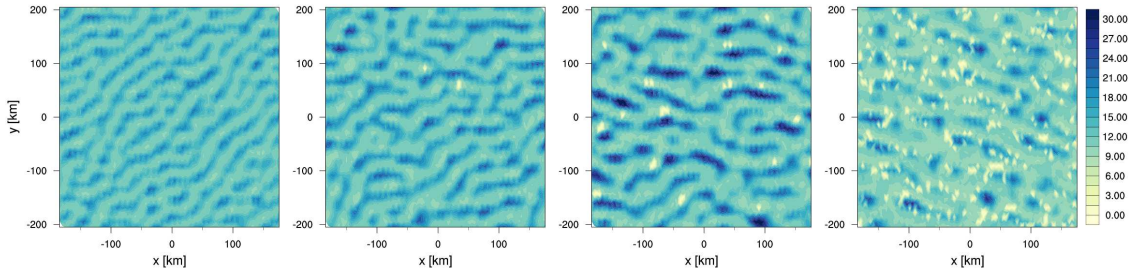

(b) 3.2 km resolution, snapshots at t = 20 h, t = 24 h, t = 28 h, and t = 32 h

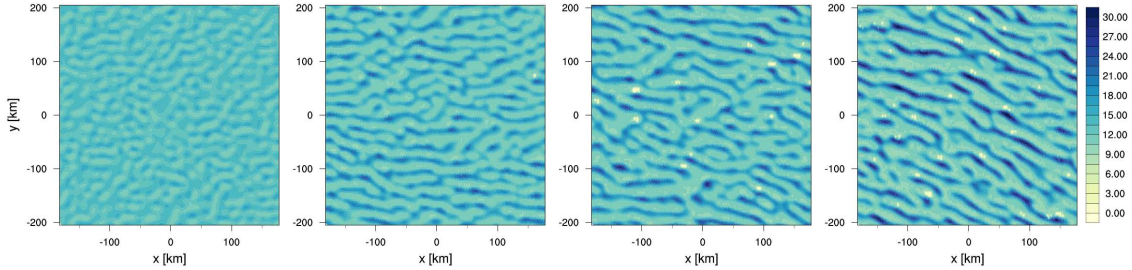

(c) 1.6 km resolution, snapshots at t = 12 h, t = 16 h, t = 20 h, and t = 24 h

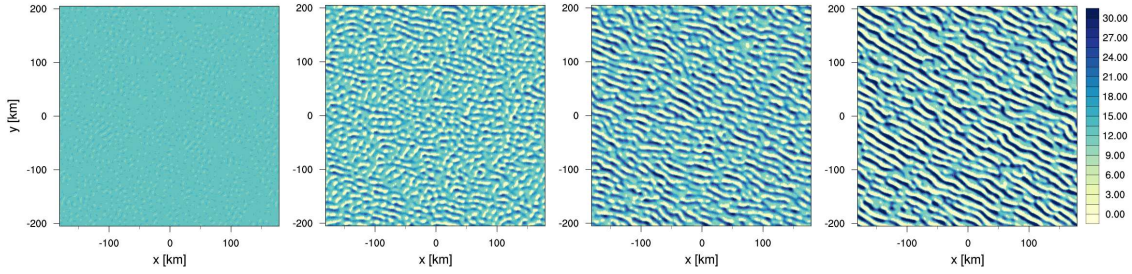

Figure 3.19: Horizontal snapshots of the RICO case cloud liquid water mixing ratio at a level above the cloud base simulated by using the deterministic EDMF scheme. The starting snapshot is at the moment when secondary circulations are initiated, which depends on the model resolution. Snapshot are taken every 4 hours.

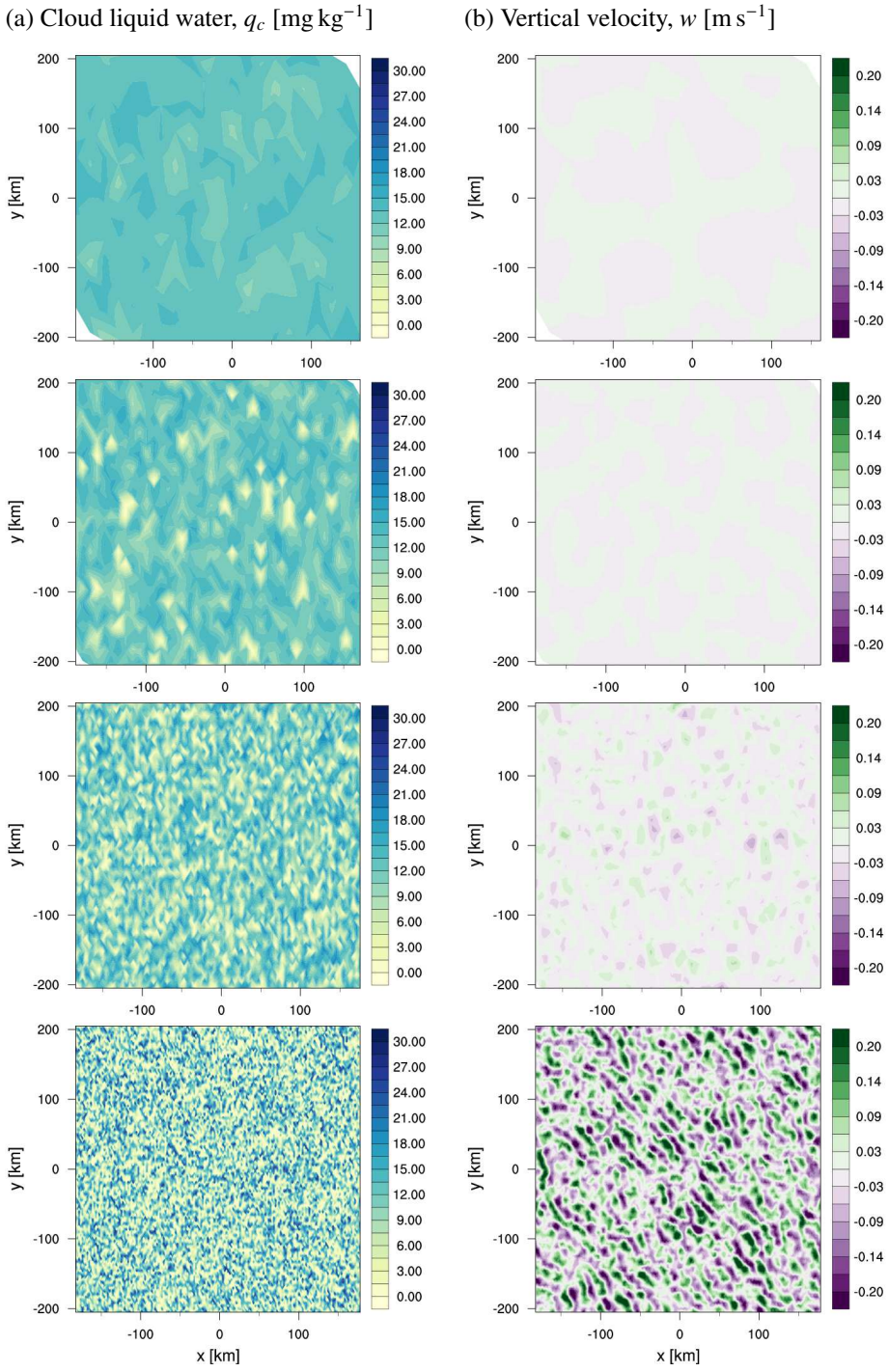

Figure 3.20: Horizontal snapshots of the RICO case cloud liquid water mixing ratio and vertical velocity at a level above the cloud base at the 24th hour of simulation using the stochastic cloud scheme. The simulation of RICO is repeated using different horizontal resolutions, from around 25.6 km (top) to around 3.2 km (bottom).

12 hours of simulation on the highest resolution grid to after 30 hours of simulation on the coarse resolution grids. The variance saturates for around half of a day after two days of simulation, but due to instability of the simulation without precipitation, it continues to increase again with time and becomes very variable until the end of simulation (Fig. 3.21). At the moment when the convective circulations emerge and develop on the model grid, the skewness of q_c in the deterministic simulations shows a peak and grows into the negative side and opposite of the skewness of q_c in the LES RICO case (Fig. 3.22b).

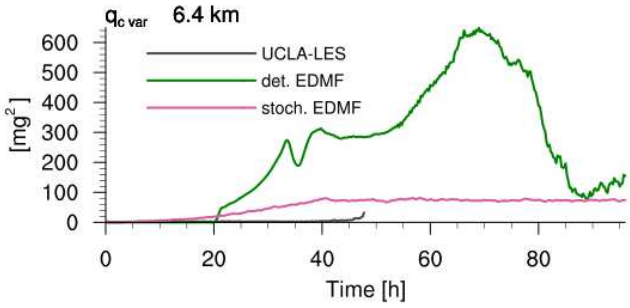

Figure 3.21: Five day long time series of the variance of cloud liquid water mixing ratio at a level above the cloud base in the deterministic EDMF (green) and stochastic EDMF RICO case (purple). The duration of the coarse-grained LES RICO case (gray) is only 48 h. After two days of simulation, the variance saturates for around half of a day, but because the simulation without precipitation is not stable, the variance continues to grow again and largely varies until the end of simulation. The abrupt drop of the variance near the end of simulation is due to the change in the cloud base height in the simulation, so the values correspond to a higher level into the cloud layer then at the start.

In the stochastic simulations of the RICO case secondary circulations also develop, even on the coarse model grids. However, these circulations have a different structure and smaller scale compared to deterministic simulations because the spurious and strong roll organization is now removed (Fig. 3.20). The stochastic cloud field still looks more realistic than the deterministic field because the stochastic variability of clouds is modelled using a physically based approach, but this variability is superimposed on the variability introduced by the grid-scale dependent convective circulations. The time series of q_c variance show that the variance is slowly growing over time by approximately same amount across the resolutions, and it is always overestimated compared to the LES RICO case q_c variance (Fig. 3.22a). After 40 hours, the variance reaches the saturation, after which the flow becomes stable (Fig. 3.21). Compared to the deterministic simulation, this variance is greatly reduced by the effects of the stochastic perturbation in the updraft area fraction, which is a significant improvement. In a similar way, the skewness of q_c is reduced and negative from the beginning of the simulations in comparison to the LES RICO case q_c skewness (Fig. 3.22b). This reduction in skewness compared to the LES RICO case q_c skewness is caused by the grid-scale dependent circulations. On the resolution finer than around 6 km, the q_c skewness of the LES simulation grows into the positive side, and the stochastic simulation behavior follows this increase. In these high resolution cases, q_c skewness resulting from the stochastic simulations changes the sign and becomes positive (Fig. 3.22b) and thus improves the distribution of subgrid convection.

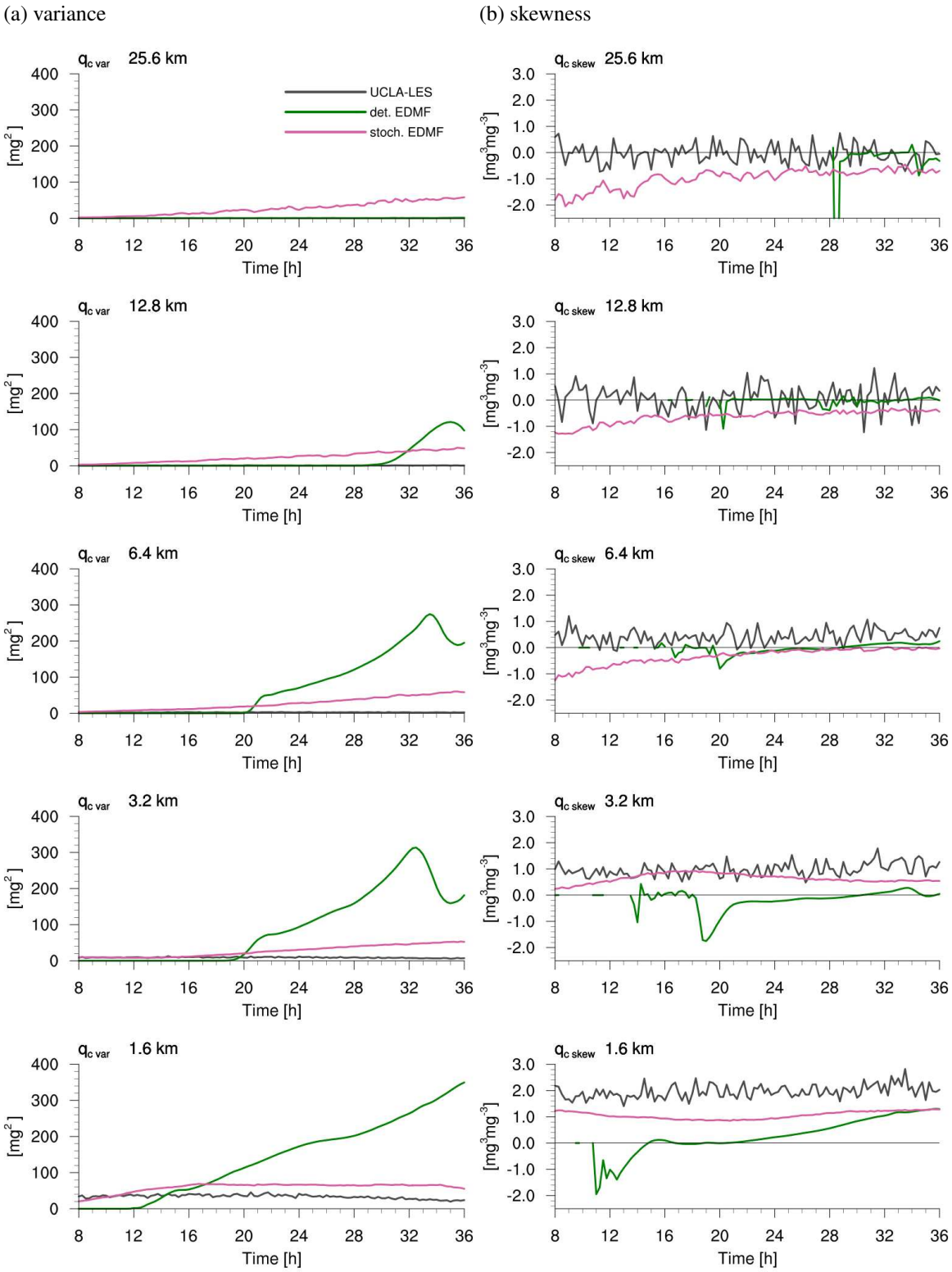

Figure 3.22: Comparison of the time series of liquid water mixing ratio variance and skewness between the coarse-grained LES RICO case (gray), deterministic EDMF (green) and stochastic EDMF (pink). These properties are calculated for a single level just above the cloud base, similar as in the previous four figures.

The results presented here indicate that the correct parameterization of variability in a convective cloud field on the gray zone grids would require prevention of the convectively induced secondary circulations that are not effectively resolved. In this case, convective organization would have to be fully parameterized, and the increase of model resolution would still show benefits for example by using high-resolution observation and land surface data. The variability in the cloud field is highly influenced by the variability in convection, which was expected in a thermally induced convective case. This suggests that a unified PLB and cloud parameterization such as EDMF is a necessity, with a more physically based link between the PBL processes than in the system with separate schemes for clouds, convection and PBL turbulence interacting only through the mean flow. From the point of view of a PBL turbulence parameterization, a 1D turbulence scheme, active only in vertical direction as conventionally used in mesoscale models, is no longer sufficient to parameterize turbulence and convection on the gray zone scales. An adequate turbulence parameterization would require a new approach to be applied on kilometer-scale grids (Fiori et al., 2010; Honnert and Valéry, 2014). The reason for this is that in the gray zone, horizontal turbulent fluxes are not negligible and horizontal scales of motion are comparable to the vertical scales of motion (Fiori et al., 2010). Furthermore, an adequate turbulence scheme would comprise a horizontal turbulent transport component that is also scale-aware and nonlocal, and with different eddy-diffusivity coefficients in horizontal and in vertical direction, because in the gray zone turbulence can not be assumed isotropic (Honnert and Valéry, 2014).

3.6 Summary and conclusions

In this chapter we considered a method to parameterize shallow cumuli in high-resolution atmospheric models across the range of horizontal resolutions. A unified parameterization of the PBL, the EDMF scheme, is employed to represent the subgrid effects of turbulence, convection and clouds of the RICO case in the idealized limited area setup of ICON. The developed stochastic parameterization provides a way to retain the validity of statistical quasi-equilibrium down to the kilometer scale of model grids in a quasi-stationary shallow convective case. The fluctuations of cloud properties around the equilibrium are modelled by a stochastic approach and the cloud field is constrained in the mean based on the physical principle that controls the development of the moist convective boundary layer.

As part of this study, the EDMF scheme is adapted to simulate the idealized RICO case over the ocean, with fixed sea surface temperature and a simple parameterization of surface fluxes, instead of using the full land/ocean surface scheme. The RICO idealized large-scale forcing is as well introduced to account for the large-scale advection, subsidence and radiation tendencies following the ICON configuration of Dipankar et al. (2015). The EDMF scheme performance and scale-dependence of the RICO case simulations are tested in multiple experiments of the same case, but on different resolutions. By analyzing these numerical tests, we studied how the deterministic EDMF scheme performs across the model resolutions, and we found that EDMF produces a robust cloud field with a small dependence on resolution. The dependence on resolution is reflected in the results mainly near the cloud layer top as a reduction of cloudiness in the high resolution simulations, and it develops as a result

of the divergence in the model grid-scale flow circulations across the range of grid resolutions. This divergence of the grid-scale flow introduces inhomogeneities in the cloud field, which then activates a different behavior of the parameterization of the cloud layer vertical structure across resolutions. So, next to the different evolution of cloud fields across resolutions, deficiencies in vertical structure parameterization on high resolution grids influence the scale-dependence of the RICO case. It is also evident that the time evolution of the RICO cloud properties stabilizes with the increase of resolution, thus, in general, the domain average properties of RICO are well reproduced in ICON.

The EDMF scheme is further developed by coupling the stochastic shallow cumulus ensemble model developed in Chapter 2 into the scheme framework, to introduce the fluctuations of the moist updraft area fraction around the statistical equilibrium. In a similar way as in the deterministic study, the resolution dependence tests were repeated to evaluate the stochastic EDMF scheme. We have found that the stochastic model produces the correct average RICO boundary layer structure and its time evolution. There is some improvement in the vertical structure of cloud layer, as the profiles resulting from stochastic simulations match the LES RICO profiles closer, and the vertical structure of the cloud layer is smoother than in the deterministic simulations. Another important effect of the stochastic scheme is the stabilization of the time series of cloud properties, and evident reduction of cloudiness with the increase of model resolution. Thus, by introducing the stochastic variability in the moist updraft area fraction we achieve the stability of the cloud system over time on all grid resolutions.

We also tested what aspects of parameterization should be reconsidered in a stochastic framework on the high resolution scales. The formulation of the cloud layer vertical structure parameterization, specifically the entrainment rate formulation, impacts the scale-dependence of the stochastic simulations. An additional semi-stochastic treatment of the cloud layer vertical structure revealed that further improvement in reproducing the cloud layer vertical profiles can be achieved, since with the correct choice of the lateral entrainment timescale distribution and adequate cloud mass flux profiles, the correct profiles of cloud fraction and cloud liquid water of RICO can be reproduced, even on the gray zone model grids. However, these tests also indicated that a separate parameterization of the momentum and thermodynamic fluxes might be necessary on the gray zone model grids. These tests provide important insights into the requirements for the correct lateral mixing and mass flux profile formulation in the future scale-aware cloud parameterizations.

In all numerical tests, variability of the RICO cloud field is quantified across a range of model resolutions and compared to the coarse-grained LES RICO case. The grid-scale flow dynamics is as well included in the analysis of the subgrid convective states distribution, and implications of the flow permitted on the model grid are assessed for the scale-aware parameterization. Convectively induced circulations develop in both deterministic and stochastic simulations, but they are of different structure and characteristics. In deterministic simulations, convection and the cloud field are strongly organized into spurious convective rolls and this organization inflates the variance of the cloud properties, and reverses and increases the skewness. In the stochastic simulations, the distribution of cloud fraction is scale-dependent and the distribution shape resembles the LES coarse-grained distribution across the range of model horizontal resolutions. The spurious organization is dissolved by the effects of the stochastic scheme, which improves the variability of the cloud field, however, the grid-scale circula-

tions are still present. The variability introduced by the grid-scale flow due to convective circulations is superimposed on the stochastic variability, so in total the variance and skewness are overestimated. However, the improvement is evident in the stochastic simulations, where the flow is stabilized, the variance is lower and the skewness is as well improved compared to the deterministic simulations.

These results confirm the point made by the previous studies of the EDMF development (Soares et al., 2004; Teixeira and Siebesma, 2000; Neggers et al., 2009; Sušelj et al., 2012), which is the necessity of developing the unified parameterizations of turbulence, convection and clouds, instead of developing the common modular model configurations where physical parameterizations update the grid-scale flow but do not communicate the information directly between the subgrid physical processes. In addition, a multi-scale approach to parameterization would require a reassessment of the parameterization approaches, so that the subgrid physical processes include a time correlation (convective memory) and spatial correlations (convective organization). The scheme developed in this thesis sets the basic requirements for a multi-scale cloud parameterization and provides a foundation for achieving the goal of a unified multi-scale PBL parameterization in future research.

Chapter 4

Conclusions

In some atmospheric modelling applications the statistical quasi-equilibrium assumption, as the main requirement for parameterizability of convection, is not satisfied. Validity of this assumption fails for two main reasons: first, spatial scales of model columns are not large enough to contain a robust number of convective elements, and second, there is no scale separation between subgrid convection and the grid-scale flow, but more importantly, there is no timescale separation in a time-varying convective environment (Williams, 2005; Yano and Plant, 2012; Davies et al., 2013). The research presented in this thesis considers the spatial-scale criterion in a quasi-stationary shallow convective case, and provides a solution to retain the assumption of statistical quasi-equilibrium across all modelled spatial scales. Moreover, the assumption that the convective mass flux is controlled by the boundary layer equilibrium would fail as a direct consequence of the failure of the statistical quasi-equilibrium assumption. Thus, the same research method presented in this thesis provides a solution to retain validity of the physical aspect of the closure assumption. Even though a quasi-stationary case is considered in this thesis and we do not address the timescale separation, it is still emphasized that the convective memory is an important component that controls the shallow cloud ensemble statistics.

The statistical ensemble framework, defined and applied to model the Rain In Cumulus over the Ocean (RICO) case in Chapter 2, provides a way to apply the parameterization closure at the system's macroscale level, while the grid cell states are governed by probabilistic laws and are carrying grid-scale dependent uncertainty. Main ingredients of the statistical ensemble applied to shallow convection are the Poisson process for counting convective elements, and a sampling process from the mixed Weibull distribution to obtain the convective intensity in a model grid column. This approach is a generalization of the deep convective ensemble of Craig and Cohen (2006) and Plant and Craig (2008) to shallow convection and is a promising framework for unification of the cloud ensemble theories.

In the following, we draw conclusions from the research conducted in this thesis, and we outline the main requirements for development of a shallow cumuli parameterization, together with some

new insights and further understanding of convective ensembles. Some important implications of the thesis results are also suggested between the conclusion statements.

4.1 What controls the cloud mass flux distribution?

The knowledge about what shapes the cloud mass flux distribution in a convective ensemble, and how the distribution parameters are influenced by the imposed forcing on the ensemble, is required to define the main pillar of the formulation of cloud parameterization schemes. From the first phase of this thesis research presented in Chapter 2, we conclude that two main factors that control the shape of the mass flux distribution in a quasi-stationary shallow cloud ensemble are the buoyancy of the cloudy air and a diversity of cloud lifetimes which we have interpreted as a local memory component.

Based on the buoyancy criterion, as the vertically integrated virtual potential temperature excess of cloudy model columns larger than 0.5 K, the shallow cloud ensemble can be split into the buoyant and nonbuoyant cloud groups (Heus and Seifert, 2013). The buoyant cloud group comprises active cumulus clouds which can be found above the level of free convection in the CBL, while the other cloud group comprises passive and forced clouds. These two cloud groups form the two modes of the cloud mass flux distribution in a shallow convective ensemble. These results could be extrapolated to interpret a deep convective cloud group as the third distribution mode that forms the right side distribution tail. In that way, this theoretical mass flux distribution model would unify the shallow and deep convective ensembles.

The mass flux distribution modes deviate from the exponential distribution shape and this deviation is governed by the diversity of cloud lifetimes. This diversity within the cumuli ensemble can be interpreted as the local memory component that drives the distribution shape further away from the exponential towards a more general Weibull distribution (see the derivation of the Weibull distribution in Appendix A.2). The resulting distribution of the cloud ensemble is a superposition of the Weibull distribution modes. The more complex the cloud ensemble is, the more power-law like the final distribution shape will be. Considerations of long-term memory effects on the statistics of a cumulus ensemble are not covered in this thesis. However, we anticipate a similar change in the distribution shape, away from an exponential and towards a power-law, due to the long-term changes in the convective environment and as well due to emergence of the cloud field organization.

4.2 Variability in a shallow convective ensemble

We have studied the fluctuations in the RICO shallow convective ensemble, by using the stochastic stand-alone model developed as a part of the thesis research. The model is based on the statistical cumulus ensemble framework and it simulates the compound distribution of convective subgrid mass fluxes, which possesses an inherent property of scale-adaptivity with the variance and skewness that increase with model resolution.

The variance of the compound distribution is controlled by the average number of convective elements and the range of the cloud-base mass flux in the model columns (Craig and Cohen, 2006). Through

the cloud-base mass flux distribution, the local cloud-scale memory affects the variance of compound distribution, which also implies that the cloud lifecycles have to be modelled explicitly to satisfy the consistency criterion in the model formulation. We prove this by performing multiple simulations using the stochastic stand-alone model. Moreover, we show that the introduction of the local memory effects into the cumulus ensemble is necessary to model the correct variance at all model resolutions.

The cloud ensemble framework that includes the memory effects into its formulation could provide more benefits in a parameterization of nonequilibrium convective cases in future research. However, a similar analysis as in this thesis could be applied to time-varying convective cases, or to transient cases, where the cumulus ensemble framework would be applied to a sequence of quasi-equilibrium states, thus maintaining the local quasi-equilibrium in a time-changing environment (e.g. as explained in Arakawa and Schubert, 1974). In that case, an additional time-dependent closure for the ensemble average mass flux and the average cloud lifetime would be necessary, while in the current model configuration these quantities are applied as constants evaluated from LES and cloud tracking.

4.3 Resolution dependence of the deterministic RICO case in ICON

In the second research phase, the eddy-diffusivity mass-flux (EDMF) scheme was employed in ICON to represent the subgrid effects of turbulence, convection and clouds of the RICO case for the range of model horizontal resolutions, from around 1 to 50 km of grid lengths. The results of these multi-resolution simulations are compared to the LES RICO case statistics. Instead of coupling it with the land surface scheme, the EDMF scheme is adapted by prescribing the constant sea surface temperature and a simple parameterization of the surface fluxes (see Appendix A.1). The large-scale advection, subsidence and radiation tendencies are applied as the constant large-scale forcing on the RICO idealized case following the ICON configuration of Dipankar et al. (2015).

In a homogeneously initialized convective case with constant and homogeneous forcing, the EDMF scheme starts with the identical performance across different model resolutions. However, as soon as the RICO case develops some spatial inhomogeneity on the high range of model resolutions (below 10 km), the differences in the average cloud profiles start to develop mainly as a reduction of cloudiness near the cloud layer top, with more reduction on the higher resolutions. The spatial inhomogeneities are a result of the convectively induced circulations that develop after a certain time period from the beginning of the simulations, with different timing and different spatial scales at different grid resolutions. This divergence of the grid-scale flow activates different behavior of the cloud layer vertical structure parameterization across different resolutions. The deterministic EDMF cloud layer vertical structure parameterization breaks down on the grid lengths of approximately 10 km and less, so the deficiencies in vertical structure parameterization in EDMF influence the scale-dependence of the RICO case only on high resolution grids. Another aspect of the RICO case scale-dependence is an evident stabilization of the time series of the RICO cloud properties with the increase of resolution. This is again caused by the grid-scale circulations that are removing the convective instability more efficiently than EDMF is independently capable of.

4.4 Stochastic EDMF scheme in ICON

The stochastic shallow cumulus ensemble model is coupled to the EDMF scheme in ICON to introduce the fluctuations of the moist updraft area fraction around the statistical equilibrium into the representation of the RICO cumulus ensemble. We have found that the stochastic model produces the correct average RICO boundary layer structure and its time evolution (Section 3.5.2). The vertical structure of the cloud layer is improved as the profiles resulting from stochastic simulations match the LES RICO profiles closer, especially on the high resolution grids, and the vertical structure of the cloud layer is smoother than in the deterministic simulations. This improvement results from relaxation of the statistical equilibrium assumption and random sampling of the convective subensembles.

The parameterization of lateral mixing remains one of the most uncertain components of the parameterization scheme in this study as well as in the previous parameterization studies described in the Introduction, Section 1.2.2. The formulation of the cloud layer vertical structure, especially the entrainment rate formulation, is very sensitive to small changes in the value of key parameters, which has a negative impact on the resolution dependence of the stochastic simulations. Additional tests of the cloud layer vertical structure were undertaken to reveal that the improvement in the simulated RICO case cloud vertical profiles can be achieved by applying an adequate formulation of the mass flux vertical structure combined with a finely tuned lateral entrainment formulation. Thus, in a similar way in which the multi-mass-flux approach (Neggers, 2015) reduces the excessive cloud liquid water in the EDMF framework, the stochastic cloud ensemble subsampling scheme with a refined vertical structure parameterization is as well capable to provide the correct liquid water and cloud fraction profiles. However, further research and parameterization development are still necessary to achieve the scale-aware lateral entrainment formulation in the stochastic EDMF scheme developed in Chapter 3. An alternative approach to achieve the most efficient and scale-aware parameterization that would be able to reproduce the correct vertical cloud layer structure, would be to combine a multi-mass-flux cloud parameterization with the stochastic subensemble sampling method developed in this thesis.

We have also demonstrated in Section 3.5.2 that by introducing the stochastic fluctuations in the moist updraft area fraction, the stability of the cloud system over time is achieved on all grid resolutions. This improvement results from the fluctuations that introduce spatial inhomogeneity into the cloud field immediately from the beginning of the simulation and help the grid-scale circulations to develop even on coarse grids.

4.5 Implications for convection in meso-γ-scale models

Atmospheric meso-γ scales fall into the convective gray zone, which is a range of horizontal model resolutions where convection is not effectively resolved. In the RICO convective case, thermally forced at the lower boundary, convective circulations develop on the model grid in both deterministic and stochastic simulations performed using the ICON model. The spatial length scale and intensity of these circulations are controlled by the model grid resolution, and thus cannot be considered realistic and are not comparable with the LES RICO convective circulations. Furthermore, deterministic and

stochastic RICO case simulations in ICON show a different behavior and structure of the grid-scale flow circulations.

Convection developed on the gray zone grids highly affects the distribution of cloud properties, like liquid water content and cloud fraction. The grid-scale circulations inflate the variance and change the sign of the distribution skewness compared to the LES RICO case, so in the stochastic RICO simulations the gray zone variability is superimposed on the stochastic variability. On the other side, in deterministic simulations, convection and the cloud field are strongly organized into spurious convective rolls and this type of organization changes the variance and skewness of the convective subgrid states distribution even further.

The stochastic parameterization improves the representation of the RICO case in ICON by dissolving the spurious gray zone organization and thus improving the measure of convective variability. By removing the spurious organization, the variance of subgrid cloud distribution is vastly reduced compared to the deterministic simulations and the skewness is as well improved. As a result of this effect, the distribution of subgrid cloud properties resembles the coarse-grained LES RICO distribution and its scale-dependence much closer compared to the deterministic case distribution at all tested resolutions. And finally, the stochastic fluctuations stabilize the time evolution of the RICO cloud properties at all tested resolutions. However, even though the stochastic scheme solves the gray zone problem for a cloud ensemble by subsampling the total cloud number, it does not provide a mechanism to solve the gray zone turbulence and convection problem, and improve the under-resolved convective grid-scale circulations. The under-resolved grid-scale circulations are still present at all model horizontal resolutions in the stochastic RICO simulations.

Because turbulence and convection highly affect the cloud field distribution, cloud parameterization should be unified with the turbulence and dry convection parameterization within a single parameterization scheme instead of approaching the parameterization in a modular manner. Under-resolved convection in the gray zone can lead to severe model biases in cloudiness and precipitation amounts (e.g. Lean et al., 2008; Roberts and Lean, 2008). Thus, the unified parameterization of a cloudy CBL should work towards preventing the under-resolved circulations and parameterizing the effect of turbulence and convection completely. How to approach the development of such a parameterization for the gray zone is not an easy solvable and fully understood problem, but there are some indications that a gray zone turbulence and convection parameterization should be three-dimensional, anisotropic and nonlocal in horizontal as well as in the vertical direction (Honnert and Valéry, 2014), or the LES type schemes should be used to bridge the gap between the mesoscales and the LES resolution scales (Fiori et al., 2010; Bhattacharya, 2014), instead of simply applying one-dimensional vertical turbulent mixing schemes commonly used in NWP models nowadays.

4.6 A consistent and the least complex model configuration

In this concluding section, we will combine the results from all conducted simulations to infer what is the least complex but still sufficient and consistent parameterization formulation to reproduce the RICO thermodynamic structure, its time evolution and variability.

In the first phase of the thesis research, we concluded that there are two possible consistent stochastic cumulus ensemble formulations: one that does not include the local memory component and the other that includes the memory component. The question of consistency comes into play when choosing the combination of the stochastic model components, the mass flux distribution function and the level of diversity in cloud lifetimes and cloud lifecycles. The first choice combines the exponential distribution function for the cloud mass fluxes and constant cloud lifetimes in a stochastic ensemble, without modelling the cloud lifecycles explicitly and thus keeping the cloud properties constant during the cloud lifetime. The second consistent option combines the Weibull distribution function to model the cloud mass fluxes in the ensemble, and cloud lifetimes that change across the ensemble and depend on the cloud convective intensity. In this case, the cloud lifecycles are modelled explicitly. An important implication of these choices is that it is necessary to discover and understand the physical mechanisms that lead to the distribution function used in a model in order to avoid the inconsistencies in model formulation. These inconsistencies can sometimes be severe and in some cases the increased complexity of the model, even though it represents the cloud ensemble more accurately, does not lead to an improved result but instead degrades the model performance, as we showed in the Chapter 2. Furthermore, we proved that the second option, the model formulation that includes the local memory component, is necessary to represent the variance of subgrid cloud properties correctly. It was also shown that the simplicity in some aspects of the cumulus ensemble can be retained, such as using the average vertical velocity instead of representing its stochastic variability among the clouds, or the deterministic power-law relation between the cloud mass flux and cloud lifetime, instead of random sampling of the joint PDF which is indeed highly scattered. The compound distribution of subgrid convective states, as the main result from the stochastic modelling of the RICO cumulus ensemble, is robust and insensitive to the randomness of local cloud properties other than the cloud mass flux and the cloud size.

The stochastic shallow cumulus ensemble developed in this thesis is a generalization of the deep convective ensemble theory of Craig and Cohen (2006), using a formulation that attempts to unify the stochastic ensembles of shallow and deep convective clouds depending on two parameters: ensemble average cloud lifetime $\langle\tau\rangle$ and the ensemble average cloud mass flux $\langle m\rangle$. Thus, the same framework would be sufficient to model multiple cloud types, based on these two parameters and based on the complete mass flux distribution that represents multiple cloud types (a three-mode distribution already discussed in Section 4.1). The shape of the cloud mass flux distribution is controlled by the ensemble memory component, thus it is also possible to relate the power-law exponent β in the cloud lifetime equation to the mass flux distribution shape parameter k (see Appendix A.2). These parameters and the mass flux distribution function are possibly controlled by the synoptic situation and by the changes in the forcing imposed by the environment onto the ensemble. To develop the stochastic framework further, it would be necessary to develop a closure for these parameters based on the large-scale processes controlling the atmospheric boundary layer and the transition to deep convection.

When implemented into ICON by coupling it with the EDMF scheme, the stochastic cloud ensemble provides a tool to answer the questions asked in Section 1.2.1: Is a spectral parameterization of clouds necessary or would a bulk scheme suffice to model the RICO case? In the early work of (Betts, 1975), a bulk approach to parameterize the BOMEX shallow cumuli ensemble was successful and sufficient

to model the thermodynamic structure of that case. However, this does not imply that the bulk approach should be sufficient for a more complex case, such as RICO. This was already indicated in the previous parameterization studies (Neggers, 2009). So, in this thesis we have confirmed that a multi-mass-flux approach or a stochastic cumulus ensemble model with an adequate lateral entrainment parameterization has to be developed to represent the correct RICO cloud water content and cloud fraction (see also Neggers, 2015). However, in order to apply the multi-mass-flux parameterization across the convective gray zone regimes, it is also necessary to model the cumulus cloud ensemble by randomly subsampling the subgrid convective states. Thus, we conclude that a hybrid subensemble multi-mass-flux approach would be the least complex and sufficient approach necessary to model the RICO case properly.

The second question concerned a single cloud type model and whether it can represent the cloudy layers well or multi-cloud-type models are necessary. Even though we do not address this question in this thesis, because our analysis is limited to a single convective case that does not include all convective cloud types, we provide the formulation of a stochastic ensemble that has a great potential to address this question in future work.

The answer to the third question, i.e. whether to develop a unified or a separate scheme for the subcloud and cloud layers, follows from this thesis research as an obvious choice of a unified model, because forced and active cumulus clouds are rooted in the subcloud updrafts. The EDMF scheme used in this thesis unifies the subcloud layer updrafts with the clouds that they initiate. Based on the gained knowledge, we suggest that all parameterization schemes should be developed to unify all relevant CBL processes within a single parameterization scheme, in a similar way as the EDMF parameterization is formulated.

4.7 Overall concluding remarks

A scale-aware shallow convection parameterization that represents the average cumulus ensemble properties and the convective fluctuations around the statistical equilibrium comprises a deterministic component, a stochastic component and the local cloud memory component. These three components change in their contributions to the subgrid cloud fraction, cloud liquid water and mixing tendencies depending on the resolution of the model. The developed approach introduces a stochastic cloud ensemble into the parameterization formulation and is more complex than a bulk scheme, but it is still less complex than a full spectral scheme. Our results support the recent trend in the parameterization development community towards a unified parameterization of turbulence, convection and clouds, but also towards three-dimensional, and spatially and temporally nonlocal approaches.

The stochastic parameterization developed here provides a method to represent the fluctuations in a convective ensemble, but still retains the constraint on the ensemble average realization so that the results of modelling are reproducible on the macro-scale, while quantifying the subgrid uncertainty at the level of a single realization. An implication of such an approach to parameterization of shallow clouds for the ensemble modelling is that the uncertainty due to the model physics could be represented using this approach to improve the ensemble spread, while not degrading the average model

outcome, and to simulate the model error growth and upscale propagation, in a similar way as in the deep convective cases of Craig and Cohen (2006), Plant and Craig (2008), and Selz and Craig (2015).

Appendices

A.1 RICO case setup

The LES RICO case configuration is presented here, as defined in van Zanten et al. (2011) and can be found as well on the web address: `http://www.knmi.nl/samenw/rico/index.html`.

Initial profiles

The initial profiles of potential temperature θ, specific humidity q_v, and wind components u and v are constructed as linear fits of the measurement data from radiosondes during the RICO field study in the period from 16 December 2004 to 8 January 2005. It is assumed that there is no liquid water at the initial time $q_l = 0$, so that $\theta = \theta_l$ and $q_v = q_t$. Location of the RICO case domain center is at 18.0° N and 61.5° W.

Zonal wind u [m/s]

$z > 0 \quad -9.9 + 2 \times 10^{-3}\, z$

Meridional wind v [m/s]

$z > 0 \quad -3.8$

Total water mixing ratio $\mathbf{q_t}$ [g/kg]

$0 < z < 740 \quad 16.0 + (13.8 - 16.0)/740\, z$

$740 < z < 3260 \quad 13.8 + (2.4 - 13.8)/(3260 - 740)\, (z - 740)$

$z > 3260 \quad 2.4 + (1.8 - 2.4)/(4000 - 3260)\, (z - 3260)$

Liquid water potential temperature $\theta_\mathbf{l}$ [K]

$0 < z < 740 \quad 297.9$

$z > 740 \quad 297.9 + (317.0 - 297.9)/(4000 - 740)\, (z - 740)$

Surface conditions

The surface turbulent fluxes of heat, moisture and momentum are parameterized using the bulk aerodynamic formulation:

$$\overline{w'\theta'_l} = -C_h\,|U|\,\left(\theta_l - SST\left(\frac{p_0}{p}\right)^{Rd/c_p}\right)$$

$$\overline{w'q'_t} = -C_q\,|U|\,\left(q_t - q_{sat}|_{z=0}\right)$$

$$\overline{u'w'} = -C_m\,|U|\,u$$

$$\overline{v'w'} = -C_m\,|U|\,v$$

where $C_h = 0.001094$, $C_q = 0.001133$, $C_m = 0.001229$, $Rd = 287$ JK^{-1}kg^{-2} is the gas constant of dry air and $c_p = 1004$ JK^{-1}kg^{-1} is the specific heat of dry air at constant pressure. The sea-surface temperature is prescribed as a constant $SST = 299.8$ K, and the surface pressure is set to $p_s = 1015.4$ mb. The sea surface potential temperature is $\theta_0 = 298.5$ K with a reference pressure of 1000 mb. The mean wind velocity $|U|$ is defined by averaging the lowest model level wind intensity.

Large-scale forcing

The vertical profiles of the subsidence rate and temperature and moisture tendencies due to horizontal advection are prescribed as the constant large-scale forcing. The large-scale cooling combines the radiative and advective cooling, while the effects of subsidence are applied only on the thermodynamic fields q_t and θ_l. The geostrophic winds u_g and v_g are as well prescribed as constant tendencies.

Large-scale subsidence w [m/s]:

$0 < z < 2260 \quad -0.005/2100\,z$

$z > 2260 \quad -0.005$

Large-scale horizontal θ_l advection combined with radiative cooling rate [K/s]:

$z > 0 \quad -2.5/86400$

Large-scale horizontal q_t advection [g/kg/s]:

$0 < z < 2980 \quad -1.0/86400 + (1.3456/86400)\,z/2980$

$z > 2980 \quad 4 \times 10^{-6}$

Geostrophic zonal wind u_g [m/s]:

$z > 0 \quad -9.9 + 2.0 \times 10^{-3} z$

Geostrophic meridional wind v_g [m/s]:

$z > 0 \quad -3.8$

A.2 Survival analysis of a stationary cloud ensemble

To study the cloud lifecycles and the role they play in shaping the distribution of cloud properties, we use a method from the survival analysis. In this appendix, we relate the individual cloud mass flux to the cloud lifetime and derive the survival function of a shallow cloud population. This function is then used to define the distribution of the cloud mass flux and to derive the link between the distribution shape parameter and the exponent of the cloud lifetime relation. Thus, this analysis can be considered as a closure for the distribution shape parameter in a stationary cumulus case.

First, we assume that there is a population of N shallow cumulus clouds that are initialized at the same time and that have different sizes and lifetimes $\tau_i, i = 1, N$. A "stress" is introduced to the system and is depleting the individual clouds by the average rate μ_r. This depleting stress can be any process counteracting the convection and cloud development. In a stationary convective case the stress is corresponding to the turbulent mixing and dilution of clouds due to entrainment and by the influence of clouds on their environment by detrainment. This stress has an effect distributed over the individual clouds depending on the cloud horizontal area or cloud mass flux m, so that by rule, larger clouds can live longer: $\tau_i = \alpha m_i^{\beta}$, where $i = 1, N$, and α and β are the fitting parameters. This relation can be inferred from LES (Chapter 2).

Different cloud populations can have a different average cloud lifetime $\langle\tau\rangle$ and average cloud mass flux $\langle m\rangle$. For every set of the parameters $\langle\tau\rangle$ and $\langle m\rangle$ there is a reference cloud depleting rate μ_r. In such population of clouds, a change in the number of clouds during the time happens following the equation:

$$\frac{dN}{d\tau} = -N\mu_\tau \frac{\langle\tau\rangle}{\tau}, \tag{A.1}$$

or, assuming a power-law relation for the normalized cloud lifetimes $\tau/\langle\tau\rangle = (m/\langle m\rangle)^{\beta}$ following:

$$\frac{dN}{N} = -\mu_\tau \frac{\langle\tau\rangle}{\tau} d\tau. \tag{A.2}$$

Substituting and solving for m we get:

$$lnN = -\mu_\tau \langle m\rangle^{\beta} \int m^{-\beta} dm, \tag{A.3}$$

$$lnN = -\mu_\tau \langle m\rangle^{\beta} \frac{m^{1-\beta}}{1-\beta}, \tag{A.4}$$

$$N = exp\left[-\mu_\tau \langle m\rangle^{\beta} \frac{m^{1-\beta}}{1-\beta}\right]. \tag{A.5}$$

This expression is the survival function of Weibull distribution with the shape parameter $k = 1 - \beta$ and a scale parameter λ if $\mu_\tau \langle m\rangle^{1-k}/k = 1/\lambda^k$. The survival function describes the probability that the element of a system will survive beyond a specified time, or in our case it is a probability that the cloud will survive beyond the point of developing mass flux m. So, the survival function of a Weibull

distributed population can be written as:

$$N = exp\left[-\left(\frac{m}{\lambda}\right)^k\right] \tag{A.6}$$

The expected value of the Weibull distribution is $\langle m\rangle = \lambda\Gamma[1 + 1/k]$, while the expected value of the transformed distribution is $\langle\tau\rangle = \lambda^{1-k}\Gamma[1/k]$, thus, we find that the average rate of cloud depletion is equall to:

$$\mu_\tau = \frac{\langle\tau\rangle}{\langle m\rangle^{2-k}}. \tag{A.7}$$

Following this formulation, the shape parameter k and the lifetime exponent β are related as $k = 1-\beta$. In the case of a single-parameter exponential distribution $k = 1$ and $\beta = 0$, i.e. lifetime is constant and independent on the cloud mass flux.

Second parameter α from relation $\tau = \alpha m^\beta$ equals $\alpha = \langle\tau\rangle\langle m\rangle^{-\beta} = \langle\tau\rangle\langle m\rangle^{k-1}$.

Now we set up a theoretical model of the dependence of the shape parameter k on the system characteristic time scale $\langle\tau\rangle$. In a stationary case, the characteristic time is the average cloud lifetime $\langle\tau\rangle$.

As it is stated in Chapter 2, the total number of clouds in a domain $N(t)$ can be estimated by integrating the instantaneous distribution $n(m', t)$ with respect to the instantaneous mass flux m', and here we repeat the equation:

$$N(t) = \int_0^\infty n(m', t)dm', \tag{A.8}$$

where m' is the instantaneous cloud mass flux. The cloud rate distribution of cloud mass flux $g(m)$ relates to the instantaneous distribution $n(m')$ through the information about the cloud lifetime $\tau(m)$. So, in the ensemble average limit, we can assume:

$$\langle g(m)\rangle = \frac{\langle n(m)\rangle}{\langle\tau(m)\rangle}\,. \tag{A.9}$$

We consider here only the active cloud group and approximate the cloud rate distribution of mass flux with the Weibull function:

$$g(m) = G\frac{k}{\lambda^k}m^{k-1}e^{-(m/\lambda)^k} \tag{A.10}$$

with scale parameter λ and shape parameter k, related to the average mass flux per cloud as $\langle m\rangle = \lambda\ \Gamma(1 + \frac{1}{k})$. The cloud generating rate G, as the number of generated clouds per second in a given area, is the intensity parameter of the Poisson distribution.

The ensemble average number of clouds in a domain can be written as:

$$\langle N\rangle = \int_0^\infty \langle\tau(m)\rangle\ \langle g(m)\rangle dm. \tag{A.11}$$

A power law relation is assumed for the cloud lifetime dependence on the cloud mass flux as inferred from LES in Chapter 2: $\tau = \alpha m^\beta$. After substitution and integration we get an expression for the

ensemble mean number of clouds:

$$\langle N \rangle = G\alpha\, \lambda^{\beta}\, \Gamma\left(1 + \frac{\beta_i}{k}\right). \tag{A.12}$$

Substituting $\alpha = \langle\tau\rangle\langle m\rangle^{-\beta} = \langle\tau\rangle\langle m\rangle^{k-1}$ into Eq. (A.12) we get:

$$\frac{\langle N \rangle}{G\langle\tau\rangle} = \Gamma\left(\frac{1}{k}\right)\Gamma\left(1 + \frac{1}{k}\right)^{k-1}. \tag{A.13}$$

In the case of an exponential distribution $k = 1$ and Eq. (A.13) reduces to $\frac{\langle N \rangle}{G\langle\tau\rangle} = 1$. This will be our starting point to constrain the system. If the average number of clouds is $\langle N \rangle = 1000$, and if we choose a typical value for the cloud lifetime $\langle\tau\rangle = 600$ s, we get $G = 1.66\dot{6}$. Now we keep $\langle N \rangle$ and G constant because the convective case is stationary, and change $\langle\tau\rangle$ to find out how the distribution shape k depends on the lifetime. In order to solve this equation, we need to approximate the gamma function expression on the right hand side of Eq. A.13. It turns out that this function shows a simple shape that can be fitted to a polynomial expression:

$$k = c_0 + c_1 \cdot \frac{\langle N \rangle}{G\langle\tau\rangle} + c_2 \cdot \frac{\langle N \rangle^{2}}{G\langle\tau\rangle} + c_3 \cdot \frac{\langle N \rangle^{3}}{G\langle\tau\rangle} \tag{A.14}$$

$$c_0 = -0.3406722,\ c_1 = 0.4097458,\ c_2 = 1.513103,\ c_3 = -0.583738 \tag{A.15}$$

Because our case is stationary so that the cloud generating rate is $G = const$, the distribution shape parameter k is determined by the average cloud lifetime $\langle\tau\rangle$ (Fig: A.1).

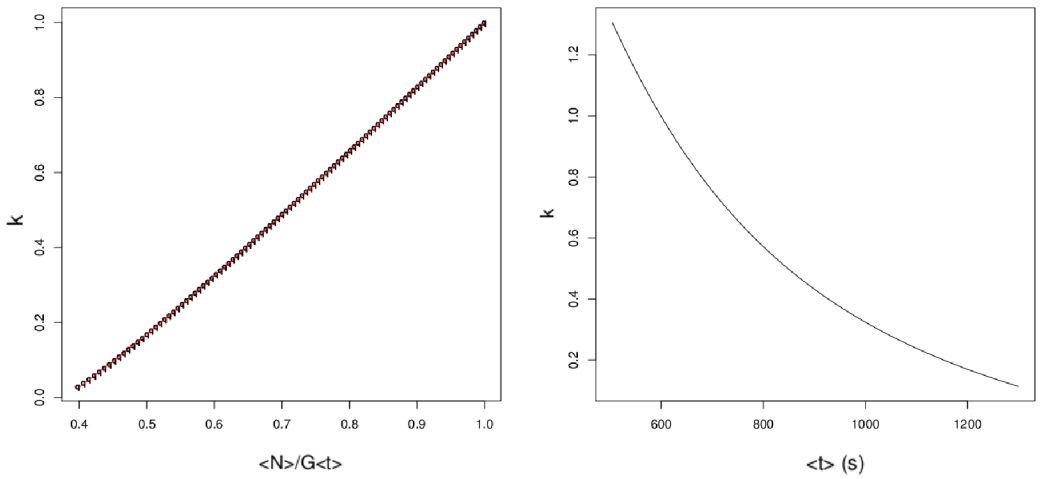

Figure A.1: a) The approximation of Eq. A.13. b) Dependency of the distribution shape k on the average cloud lifetime $\langle\tau\rangle$ in a stationary case.

References

Arakawa, A. (2004). The cumulus parameterization problem: past, present, and future. *J. Climate*, 17:2493–2525.

Arakawa, A. and Jung, J.-H. (2011). Multiscale modeling of the moist-convective atmosphere - a review. *Atmos. Res.*, 102(3):263–285.

Arakawa, A. and Schubert, W. H. (1974). Interaction of a cumulus cloud ensemble with the large-scale environment, Part I. *J. Atmos. Sci.*, 31:674–701.

Baker, L. H., Rudd, A. C., Migliorini, S., and Bannister, R. N. (2014). Representation of model error in a convective-scale ensemble prediction system. *Nonlinear Proc. Geoph.*, 21:19–39.

Baldauf, M., Seifert, A., Förstner, J., Majewski, D., Raschendorfer, M., and Reinhardt, T. (2011). Operational convective-scale numerical weather prediction with the COSMO model: Description and sensitivities. *Mon. Weather Rev.*, 139:3887–3905.

Bechtold, P., Bazile, E., Guichard, F., Mascart, P., and Richard, E. (2001). A mass-flux convection scheme for regional and global models. *Q. J. Roy. Meteor. Soc.*, 127:869–886.

Bengtsson, L., Körnich, H., Källén, E., and Svensson, G. (2011). Large-scale dynamical response to subgrid-scale organization provided by cellular automata. *J. Atmos. Sci.*, 68:3132–3144.

Bengtsson, L., Steinheimer, M., Bechtold, P., and Geleyn, J.-F. (2013). A stochastic parametrization for deep convection using cellular automata. *Q. J. Roy. Meteor. Soc.*, 139:1533–1543.

Berner, J., Fossell, K. R., Ha, S.-Y., Hacker, J. P., and Snyder, C. (2015). Increasing the skill of probabilistic forecasts: Understanding performance improvements from model-error representations. *Mon. Weather Rev.*, 143:1295–1320.

Berner, J., Jung, T., and Palmer, T. N. (2012). Systematic model error: The impact of increased horizontal resolution versus improved stochastic and deterministic parameterizations. *J. Climate*, 25:4946–4962.

Betts, A. K. (1973). Non-precipitating convection and its parameterization. *Q. J. Roy. Meteor. Soc.*, 99:178–196.

Betts, A. K. (1975). Parametric interpretation of trade-wind cumulus budget studies. *J. Atmos. Sci.*, 32:1934–1945.

Betts, A. K. (1976). Modeling subcloud layer structure and interaction with shallow cumulus layer. *J. Atmos. Sci.*, 33:2363–2382.

Betts, A. K. and Miller, M. J. (1986). A new convective adjustment scheme. Part II: Single column tests using GATE wave, BOMEX, ATEX and arctic air-mass data sets. *Q. J. Roy. Meteor. Soc.*, 112:693–709.

Bhattacharya, R. (2014). *A two Turbulence Kinetic Energy Model for the Scale Adaptive Treatment of the Planetary Boundary Layers*. PhD thesis, International Max Planck Research School on Earth System Modelling (IMPRS-ESM), Max Planck Institute for Meteorology (MPI-M).

Bony, S. and Dufresne, J.-L. (2005). Marine boundary layer clouds at the heart of tropical cloud feedback uncertainties in climate models. *Geophys. Res. Lett.*, 32(20). L20806.

Bony, S., Stevens, B., Frierson, D. M. W., Jakob, C., Kageyama, M., Pincus, R., Shepherd, T. G., Sherwood, S. C., Siebesma, A. P., Sobel, A. H., Watanabe, M., and Webb, M. J. (2015). Clouds, circulation and climate sensitivity. *Nature Geoscience*, 8:261–268.

Bouttier, F., Vié, B., Nuissier, O., and Raynaud, L. (2012). Impact of stochastic physics in a convection-permitting ensemble. *Mon. Weather Rev.*, 140:3706–3721.

Bowler, N. E., Arribas, A., Mylne, K. R., Robertson, K. B., and Beare, S. E. (2008). The MOGREPS short-range ensemble prediction system. *Q. J. Roy. Meteor. Soc.*, 134:703–722.

Bretherton, C. S., McCaa, J. R., and Grenier, H. (2004). A new parameterization for shallow cumulus convection and its application to marine subtropical cloud-topped boundary layers. Part I: Description and 1D results. *Mon. Weather Rev.*, 132:864–882.

Bright, D. R. and Mullen, S. L. (2002). Short-range ensemble forecasts of precipitation during the southwest monsoon. *Weather Forecast.*, 17:1080–1100.

Bryan, G. H. (2005). Spurious convective organization in simulated squall lines owing to moist absolutely unstable layers. *Mon. Weather Rev.*, 133:1978–1997.

Bryan, G. H. and Rotunno, R. (2005). Statistical convergence in simulated moist absolutely unstable layers. *Preprints, 11th Conf. on Mesoscale Processes, Albuquerque, NM, Amer. Meteor. Soc.*, 1M.6.

Bryan, G. H., Wyngaard, J. C., and Fritsch, J. M. (2003). Resolution requirements for the simulation of deep moist convection. *Mon. Weather Rev.*, 131:2394–2416.

Buizza, R., Miller, M., and Palmer, T. N. (1999). Stochastic representation of model uncertainties in the ECMWF ensemble prediction system. *Q. J. Roy. Meteor. Soc.*, 125:2887–2908.

Chabrier, G. (2003). Galactic stellar and substellar initial mass function. *Publ. Astron. Soc. Pac.*, 115:763–795.

Cheinet, S. (2004). A multiple mass flux parameterization for the surface-generated convection. Part II: Cloudy cores. *J. Atmos. Sci.*, 61:1093–1113.

Cheng, A., Xu, K.-M., and Stevens, B. (2010). Effects of resolution on the simulation of boundary-layer clouds and the partition of kinetic energy to subgrid scales. *J. Adv. Model. Earth Syst.*, 2, 3:doi:10.3894/JAMES.2010.2.3.

Ching, J., Rotunno, R., LeMone, M., Martilli, A., Kosovic, B., Jimenez, P. A., and Dudhia, J. (2014). Convectively induced secondary circulations in fine-grid mesoscale numerical weather prediction models. *Mon. Weather Rev.*, 142:3284–3302.

Clark, A. J., Gallus, W. A., Xue, M., and Kong, F. (2009). A comparison of precipitation forecast skill between small convection-allowing and large convection-parameterizing ensembles. *Weather Forecast.*, 24:1121–1140.

Clark, A. J., Kain, J. S., Stensrud, D. J., Xue, M., Kong, F., Coniglio, M. C., Thomas, K. W., Wang, Y., Brewster, K., Gao, J., Wang, X., Weiss, S. J., and Du, J. (2011). Probabilistic precipitation forecast skill as a function of ensemble size and spatial scale in a convection-allowing ensemble. *Mon. Weather Rev.*, 139:1410–1418.

Cohen, B. G. and Craig, G. C. (2006). Fluctuations in an equilibrium convective ensemble, Part II: Numerical experiments. *J. Atmos. Sci.*, 63:2005–2015.

Craig, G. C. and Cohen, B. G. (2006). Fluctuations in an equilibrium convective ensemble, Part I: Theoretical formulation. *J. Atmos. Sci.*, 63:1996–2004.

Davies, L., Plant, R. S., and Derbyshire, S. H. (2013). Departures from convective equilibrium with a rapidly varying surface forcing. *Q. J. Roy. Meteor. Soc.*, 139:1731–1746.

Dawe, J. T. and Austin, P. H. (2013). Direct entrainment and detrainment rate distributions of individual shallow cumulus clouds in an LES. *Atmos. Chem. Phys.*, 13:7795–7811.

de Roode, S. R., Siebesma, A. P., Jonker, H. J. J., and de Voogd, Y. (2012). Parameterization of the vertical velocity equation for shallow cumulus clouds. *Mon. Weather Rev.*, 140:2424–2436.

de Rooy, W. C. and Siebesma, A. P. (2008). A simple parameterization for detrainment in shallow cumulus. *Mon. Weather Rev.*, 136:560–576.

de Rooy, W. C. and Siebesma, A. P. (2010). Analytical expressions for entrainment and detrainment in cumulus convection. *Q. J. Roy. Meteor. Soc.*, 136:1216–1227.

Deng, A., Seaman, N. L., and Kain, J. S. (2003). A shallow-convection parameterization for mesoscale models. Part I: Submodel description and preliminary applications. *J. Atmos. Sci.*, 60:34–56.

Dipankar, A., Stevens, B., Heinze, R., Moseley, C., Zängl, G., and Giorgetta, M. A. (2015). A large eddy simulation version of ICON (ICOsahedral Nonhydrostatic): Model description and validation. *submitted to J. Adv. Model. Earth Syst.*

Done, J., Davis, C. A., and Weisman, M. (2004). The next generation of NWP: explicit forecasts of convection using the weather research and forecasting (WRF) model. *Atmosph. Sci. Lett.*, 5:110–117.

Dorrestijn, J., Crommelin, D. T., Siebesma, A. P., and Jonker, H. J. J. (2013). Stochastic parameterization of shallow cumulus convection estimated from high-resolution model data. *Theor. Comp. Fluid Dyn.*, 27:133–148.

Esbensen, S. (1978). Bulk thermodynamic effects and properties of small tropical cumuli. *J. Atmos. Sci.*, 35:826–837.

Fiori, E., Parodi, A., and Siccardi, F. (2010). Turbulence closure parameterization and grid spacing effects in simulated supercell storms. *J. Atmos. Sci.*, 67:3870–3890.

Frenkel, Y., Majda, A. J., and Khouider, B. (2012). Using the stochastic multicloud model to improve tropical convective parameterization: A paradigm example. *J. Atmos. Sci.*, 69:1080–1105.

Gebhardt, C., Theis, S., Krahe, P., and Renner, V. (2008). Experimental ensemble forecasts of precipitation based on a convection-resolving model. *Atmosph. Sci. Lett.*, 9:67–72.

Gebhardt, C., Theis, S. E., and Paulat, M., e. a. (2011). Uncertainties in COSMO-DE precipitation forecasts introduced by model perturbations and variation of lateral boundaries. *Atmos. Res.*, 100:168–177.

Giorgi, F. and Marinucci, M. R. (1996). A investigation of the sensitivity of simulated precipitation to model resolution and its implications for climate studies. *Mon. Weather Rev.*, 124:148–166.

Gray, W. M. (1973). Cumulus convection and larger scale circulations I. Broadscale and mesoscale considerations. *Mon. Weather Rev.*, 101:839–855.

Gregory, D. and Rowntree, P. R. (1990). A mass flux convection scheme with representation of cloud ensemble characteristics and stability-dependent closure. *Mon. Weather Rev.*, 118:1483–1506.

Herbort, F. and Etling, D. (2011). Post-frontal shower cells in the COSMO-DE model. A comparison with radar measurements. *Meteorol. Z.*, 20:217–226.

Heus, T. and Seifert, A. (2013). Automated tracking of shallow cumulus clouds in large domain, long duration large eddy simulations. *Geosci. Model Dev.*, 6:1261–1273.

Hohenegger, C., Lüthi, D., and Schär, C. (2006). Predictability mysteries in cloud-resolving models. *Mon. Weather Rev.*, 134:2095–2107.

Holland, J. Z. and Rasmusson, E. M. (1973). Measurements of the atmospheric mass, energy, and momentum budgets over a 500-kilometer square of tropical ocean. *Mon. Weather Rev.*, 101:44–55.

Holtslag, A. A. M. and Boville, B. (1993). Local versus nonlocal boundary-layer diffusion in a global climate model. *J. Climate*, 6:1825–1842.

Honnert, R., Masson, V., and Couvreux, F. (2011). A diagnostic for evaluating the representation of turbulence in atmospheric models at the kilometric scale. *J. Atmos. Sci.*, 68:3112–3131.

Honnert, R. and Valéry, M. (2014). What is the smallest physically acceptable scale for 1D turbulence schemes? *Front. Earth Sci.*, 2(00027).

Jaynes, E. T. (1957). Information theory and statistical mechanics. *Phys. Rev.*, 106:620–630.

Jones, T. R. and Randall, D. A. (2011). Quantifying the limits of convective parameterizations. *J. Geophys. Res.*, 116:D08210.

Jung, J.-H. and Arakawa, A. (2004). The resolution dependence of model physics: illustrations from nonhydrostatic model experiments. *J. Atmos. Sci.*, 61:88–102.

Kain, J. S. and Fritsch, J. M. (1990). A one-dimensional entraining/detraining plume model and its application in convective parameterization. *J. Atmos. Sci.*, 47:2784–2802.

Keane, R. J. and Plant, R. S. (2012). Large-scale length and time-scales for use with stochastic convective parameterization. *Q. J. Roy. Meteor. Soc.*, 138:1150–1164.

Khouider, B., Biello, J., and Majda, A. (2010). A stochastic multicloud model for tropical convection. *Commun. Math. Sci.*, 8:187–216.

Kiehl, J. T. and Williamson, D. L. (1991). Dependence of cloud amount on horizontal resolution in the national center for atmospheric research community climate model. *J. Geophys. Res.*, 96(D6):10955–10980.

Knippertz, P., Trentmann, J., and Seifert, A. (2009). High-resolution simulations of convective cold pools over the northwestern sahara. *J. Geophys. Res.-Atmos.*, 114(D8). D08110.

Köhler, M., Ahlgrimm, M., and Beljaars, A. (2011). Unified treatment of dry convective and stratocumulus-topped boundary layers in the ECMWF model. *Q. J. Roy. Meteor. Soc.*, 137:43–57.

Kong, F., Droegemeier, K. K., and Hickmon, N. L. (2007). Multiresolution ensemble forecasts of an observed tornadic thunderstorm system. Part II: storm-scale experiments. *Mon. Weather Rev.*, 135:759–782.

Lappen, C.-L. and Randall, D. A. (2001). Toward a unified parameterization of the boundary layer and moist convection. Part I: A new type of mass-flux model. *J. Atmos. Sci.*, 58:2021–2036.

Lappen, C.-L. and Schumacher, C. (2014). The role of tilted heating in the evolution of the MJO. *J. Geophys. Res.-Atmos.*, 119:2966–2989.

Lean, H. W., Clark, P. A., Dixon, M., Roberts, N. M., Fitch, A., Forbes, R., and Halliwell, C. (2008). Characteristics of high-resolution versions of the Met Office unified model for forecasting convection over the United Kingdom. *Mon. Weather Rev.*, 136:3408–3424.

Leith, C. E. (1971). Atmospheric predictability and two-dimensional turbulence. *J. Atmos. Sci.*, 28:145–161.

LeMone, M. A., Chen, F., Tewari, M., Dudhia, J., Geerts, B., Miao, Q., Coulter, R. L., and Grossman, R. L. (2010). Simulating the IHOP_2002 fair-weather CBL with the WRF-ARW-NOAH modeling system. Part II: Structures from a few kilometers to 100 km across. *Mon. Weather Rev.*, 138:745–764.

Li, C., Jia, X., Ling, J., Zhou, W., and Zhang, C. (2009). Sensitivity of MJO simulations to diabatic heating profiles. *Clim. Dynam.*, 32(2–3):167–187.

Lin, J. W.-B. and Neelin, J. D. (2000). Influence of a stochastic moist convective parameterization on tropical climate variability. *Geophys. Res. Lett.*, 27:3691–3694.

Lin, J. W.-B. and Neelin, J. D. (2002). Considerations for stochastic convective parameterization. *J. Atmos. Sci.*, 59:959–975.

Lorenz, E. N. (1969). The predictability of a flow which possesses many scales of motion. *Tellus*, 21:289–307.

Mass, C. F., Ovens, D., Westrick, K., and Colle, B. A. (2002). Does increasing horizontal resolution produce more skillful forecasts? *B. Am. Meteorol. Soc.*, 83:407–430.

Medeiros, B., Stevens, B., Held, I. M., Zhao, M., Williamson, D. L., Olson, J. G., and Bretherton, C. S. (2008). Aquaplanets, climate sensitivity, and low cloud. *J. Climate*, 21:4974–4991.

Migliorini, S., Dixon, M., Bannister, R., and Ballard, S. (2011). Ensemble prediction for nowcasting with a convection-permitting model – I: Description of the system and the impact of radar-derived surface precipitation rates. *Tellus A*, 63:468–496.

Nastrom, G. D. and Gage, K. S. (1985). A climatology of atmospheric wavenumber spectra of wind and temperature observed by commercial aircraft. *J. Atmos. Sci.*, 42:950–960.

Neggers, R. A. J. (2009). A dual mass flux framework for boundary layer convection. Part II: Clouds. *J. Atmos. Sci.*, 66:1489–1506.

Neggers, R. A. J. (2015). Exploring bin-macrophysics models for moist convective transport and clouds. *In preparation*.

Neggers, R. A. J., Köhler, M., and Beljaars, A. C. M. (2009). A dual mass flux framework for boundary layer convection. Part I: Transport. *J. Atmos. Sci.*, 66:1465–1487.

Neggers, R. A. J., Neelin, J. D., and Stevens, B. (2007a). Impact mechanisms of shallow cumulus convection on tropical climate dynamics. *J. Climate*, 20:2623–2642.

Neggers, R. A. J., Siebesma, A. P., and Jonker, H. J. J. (2002). A multiparcel model for shallow cumulus convection. *J. Atmos. Sci.*, 59:1655–1668.

Neggers, R. A. J., Stevens, B., and Neelin, J. (2006). A simple equilibrium model for shallow-cumulus-topped mixed layers. *Theor. Comp. Fluid Dyn.*, 20(5–6):305–322.

Neggers, R. A. J., Stevens, B., and Neelin, J. D. (2007b). Variance scaling in shallow-cumulus-topped mixed layers. *Q. J. Roy. Meteor. Soc.*, 133:1629–1641.

Palmer, T. N. (2001). A nonlinear dynamical perspective on model error: A proposal for non-local stochastic-dynamic parametrization in weather and climate prediction models. *Q. J. Roy. Meteor. Soc.*, 127:279–304.

Palmer, T. N., Shutts, G. J., Hagedorn, R., Doblas-Reyes, F. J., Jung, T., and Leutbecher, M. (2005). Representing model uncertainty in weather and climate prediction. *Annu. Rev. Earth Pl. Sc.*, 33:163–193.

Pan, D.-M. and Randall, D. D. A. (1998). A cumulus parameterization with a prognostic closure. *Q. J. Roy. Meteor. Soc.*, 124:949–981.

Petch, J. C. (2006). Sensitivity studies of developing convection in a cloud-resolving model. *Q. J. Roy. Meteor. Soc.*, 132:345–358.

Pinsky, M. A. and Karlin, S. (2011). *An Introduction to Stochastic Modeling*. Academic Press, Elsevier, 4th edition.

Piotrowski, Z. P., Smolarkiewicz, P. K., Malinowski, S. P., and Wyszogrodzki, A. A. (2009). On numerical realizability of thermal convection. *J. Comput. Phys.*, 228:6268–6290.

Plant, R. S. and Craig, G. C. (2008). A stochastic parameterization for deep convection based on equilibrium statistics. *J. Atmos. Sci.*, 65:87–105.

Pope, V. and Stratton, R. (2002). The processes governing horizontal resolution sensitivity in a climate model. *Clim. Dynam.*, 19:211–236.

R Development Core Team (2013). *R: A Language and Environment for Statistical Computing*. R Foundation for Statistical Computing, Vienna, Austria. Available at: `http://www.R-project.org`.

Rauber, R. M., OchsIII, H. T., Di Girolamo, L., Göke, S., Snodgrass, E., Stevens, B., Knight, C., Jensen, J. B., Lenschow, D. H., Rilling, R. A., Rogers, D. C., Stith, J. L., Albrecht, B. A., Zuidema, P., Blyth, A. M., Fairall, C. W., Brewer, W. A., Tucker, S., Lasher-Trapp, S. G., Mayol-Bracero, O. L., Vali, G., Geerts, B., Anderson, J. R., Baker, B. A., Lawson, R. P., Bandy, A. R., Thornton, D. C., Burnet, E., Brenguier, J.-L., Gomes, L., Brown, P. R. A., Chuang, P., Cotton, W. R., Gerber, H., Heikes, B. G., Hudson, J. G., Kollias, P., Krueger, S. K., Nuijens, L., O'Sullivan, D. W., Siebesma, A. P., and Twohy, C. H. (2007). Rain in shallow cumulus over the ocean: the RICO campaign. *B. Am. Meteorol. Soc.*, 88:1912–1928.

Raymond, D. J. and Blyth, A. M. (1986). A stochastic mixing model for nonprecipitating cumulus clouds. *J. Atmos. Sci.*, 43:2708–2718.

Roberts, N. M. and Lean, H. W. (2008). Scale-selective verification of rainfall accumulations from high-resolution forecasts of convective events. *Mon. Weather Rev.*, 136:78–97.

Romine, G. S., Schwartz, C. S., Berner, J., Fossell, K. R., Snyder, C., Anderson, J. L., and Weisman, M. L. (2014). Representing forecast error in a convection-permitting ensemble system. *Mon. Weather Rev.*, 142:4519–4541.

Romps, D. M. and Kuang, Z. (2010). Nature versus nurture in shallow convection. *J. Atmos. Sci.*, 67:1655–1666.

Schumann, U. and Moeng, C.-H. (1991). Plume budgets in clear and cloudy convective boundary layers. *J. Atmos. Sci.*, 48:1758–1770.

Seifert, A. and Beheng, K. D. (2001). A double-moment parameterization for simulating autoconversion, accretion and selfcollection. *Atmos. Res.*, 59–60:265–281.

Seifert, A. and Heus, T. (2013). Large-eddy simulation of organized precipitating trade wind cumulus clouds. *Atmos. Chem. Phys.*, 13:5631–5645.

Selz, T. and Craig, G. C. (2015). Upscale error growth in a high-resolution simulation of a summertime weather event over europe. *Mon. Weather Rev.*, 143:813–827.

Shutts, G. (2005). A kinetic energy backscatter algorithm for use in ensemble prediction systems. *Q. J. Roy. Meteor. Soc.*, 131:3079–3102.

Shutts, G. J. and Palmer, T. N. (2007). Convective forcing fluctuations in a cloud-resolving model: relevance to the stochastic parameterization problem. *J. Climate*, 20:187–202.

Siebesma, A. P. and Cuijpers, J. W. M. (1995). Evaluation of parametric assumptions for shallow cumulus convection. *J. Atmos. Sci.*, 52:650–666.

Siebesma, A. P., Soares, P. M. M., and Teixeira, J. (2007). A combined eddy-diffusivity mass-flux approach for the convective boundary layer. *J. Atmos. Sci.*, 64:1230–1248.

Skamarock, W. C., Klemp, J. B., Duda, M. G., Fowler, L. D., Park, S.-H., and Ringler, T. D. (2012). A multiscale nonhydrostatic atmospheric model using centroidal Voronoi tesselations and C-grid staggering. *Mon. Weather Rev.*, 140:3090–3105.

Soares, P. M. M., Miranda, P. M. A., Siebesma, A. P., and Teixeira, J. (2004). An eddy-diffusivity/mass-flux parametrization for dry and shallow cumulus convection. *Q. J. Roy. Meteor. Soc.*, 130:3365–3383.

Speer, M. S. and Leslie, L. M. (2002). The prediction of two cases of severe convection: implications for forecast guidance. *Meteorol. Atmos. Phys.*, 80:165–175.

Steppeler, J., Doms, G., Schättler, U., Bitzer, H. W., Gassmann, A., Damrath, U., and Gregoric, G. (2003). Meso-gamma scale forecasts using the nonhydrostatic model LM. *Meteorol. Atmos. Phys.*, 82:75–96.

Stevens, B. (2010). Introduction to UCLA-LES, version 3.2.1. *available at:* `https://gitorious.org/uclales`. (last access: 12 August 2014).

Stevens, B., Moeng, C.-H., Ackerman, A. S., Bretherton, C. S., Chlond, A., de Roode, S., Edwards, J., Golaz, J.-C., Jiang, H., Khairoutdinov, M., Kirkpatrick, M. P., Lewellen, D. C., Lock, A., Müller, F., Stevens, D. E., Whelan, E., and Zhu, P. (2005). Evaluation of large-eddy simulations via observations of nocturnal marine stratocumulus. *Mon. Weather Rev.*, 133:1443–1462.

Stevens, B., Moeng, C.-H., and Sullivan, P. P. (1999). Large-eddy simulations of radiatively driven convection: sensitivities to the representation of small scales. *J. Atmos. Sci.*, 56:3963–3984.

Stevens, B. and Seifert, A. (2008). Understanding macrophysical outcomes of microphysical choices in simluations of shallow cumulus convection. *J. Meteorol. Soc. Jpn.*, 86A:143–162.

Stirling, A. J. and Petch, J. C. (2004). The impacts of spatial variability on the development of convection. *Q. J. Roy. Meteor. Soc.*, 130:3189–3206.

Stull, R. B. (1985). A fair-weather cumulus cloud classification scheme for mixed-layer studies. *J. Clim. Appl. Meteorol.*, 24:49–56.

Sušelj, K., Teixeira, J., and Chung, D. (2013). A unified model for moist convective boundary layers based on a stochastic eddy-diffusivity/mass-flux parameterization. *J. Atmos. Sci.*, 70:1929–1953.

Sušelj, K., Teixeira, J., and Matheou, G. (2012). Eddy diffusivity/mass flux and shallow cumulus boundary layer: An updraft PDF multiple mass flux scheme. *J. Atmos. Sci.*, 69:1513–1533.

Takemi, T. and Rotunno, R. (2003). The effects of subgrid model mixing and numerical filtering in simulations of mesoscale cloud systems. *Mon. Weather Rev.*, 131:2085–2101.

Tan, Z.-M., Zhang, F., Rotunno, R., and Snyder, C. (2004). Mesoscale predictability of moist baroclinic waves: experiments with parameterized convection. *J. Atmos. Sci.*, 61:1794–1804.

Teixeira, J. and Reynolds, C. A. (2008). Stochastic nature of physical parameterizations in ensemble prediction: A stochastic convection approach. *Mon. Weather Rev.*, 136:483–496.

Teixeira, J. and Siebesma, A. P. (2000). A mass-flux/K-diffusion approach to the parameterization of the convective boundary layer: global model results. In *Proceedings of the 14th symposium on Boundary Layers and Turbulence*, pages 231–234, Aspen.

Tiedtke, M. (1989). A comprehensive mass flux scheme for cumulus parameterization in large-scale models. *Mon. Weather Rev.*, 117:1779–1800.

Tiedtke, M., Heckley, W. A., and Slingo, J. (1988). Tropical forecasting at ECMWF: The influence of physical parametrization on the mean structure of forecasts and analyses. *Q. J. Roy. Meteor. Soc.*, 114:639–664.

Tomita, H. and Satoh, M. (2004). A new dynamical framework of nonhydrostatic global model using the icosahedral grid. *Fluid Dyn. Res.*, 34:357–400.

Torn, R. D. and Davis, C. A. (2012). The influence of shallow convection on tropical cyclone track forecasts. *Mon. Weather Rev.*, 140:2188–2197.

Troen, I. B. and Mahrt, L. (1986). A simple model of the atmospheric boundary layer; sensitivity to surface evaporation. *Bound.-Lay. Meteorol.*, 37:129–148.

van Stratum, B. J. H., Vilá–Guerau de Arellano, J., van Heerwaarden, C. C., and Ouwersloot, H. G. (2014). Subcloud-layer feedbacks driven by the mass flux of shallow cumulus convection over land. *J. Atmos. Sci.*, 71:881–895.

van Zanten, M. C., Stevens, B., Nuijens, L., Siebesma, A. P., Ackerman, A. S., Burnet, F., Cheng, A., Couvreux, F., Jiang, H., Khairoutdinov, M., Kogan, Y., Lewellen, D. C., Mechem, D., Nakamura, K., Noda, A., Shipway, B. J., Slawinska, J., Wang, S., and Wyszogrodzki, A. (2011). Controls on precipitation and cloudiness in simulations of trade-wind cumulus as observed during RICO. *J. Adv. Model. Earth Syst.*, 3:M06001.

von Salzen, K. and McFarlane, N. A. (2002). Parameterization of the bulk effects of lateral and cloud-top entrainment in transient shallow cumulus clouds. *J. Atmos. Sci.*, 59:1405–1430.

von Salzen, K., McFarlane, N. A., and Lazare, M. (2005). The role of shallow convection in the water and energy cycles of the atmosphere. *Clim. Dynam.*, 25(7-8):671–688.

Weisman, M. L., Skamarock, W. C., and Klemp, J. B. (1997). The resolution dependence of explicitly modeled convective systems. *Mon. Weather Rev.*, 125:527–548.

Wilks, D. S. (2006). *Statistical Methods in the Atmospheric Sciences, in: International Geophysics Series*, volume 91. Academic Press, 2nd edition.

Williams, P. D. (2005). Modelling climate change: the role of unresolved processes. *Philos. T. Roy. Soc. A*, 363:2931–2946.

Williamson, D. L. (1999). Convergence of atmospheric simulations with increasing horizontal resolution and fixed forcing scales. *Tellus*, 51A:663–673.

Wouters, J. and Lucarini, V. (2012). Disentangling multi–level systems: averaging, correlations and memory. *J. Stat. Mech.*, 2012(3):P03003.

Wouters, J. and Lucarini, V. (2013). Multi–level dynamical systems: Connecting the Ruelle response theory and the Mori–Zwanzig approach. *J. Stat. Phys.*, 151(5):850–860.

Wyant, M. C., Bretherton, C. S., Bacmeister, J. T., Kiehl, J. T., Held, I. M., Zhao, M., Klein, S. A., and Soden, B. J. (2006). A comparison of low-latitude cloud properties and their response to climate change in three AGCMs sorted into regimes using mid-tropospheric vertical velocity. *Clim. Dynam.*, 27(2–3):261–279.

Wyngaard, J. C. (2004). Toward numerical modeling in the "terra incognita". *J. Atmos. Sci.*, 61:1816–1826.

Xu, K.-M., Arakawa, A., and Krueger, S. K. (1992). The macroscopic behavior of cumulus ensembles simulated by a cumulus ensemble model. *J. Atmos. Sci.*, 49:2402–2420.

Yanai, M., Esbensen, S., and Chu, J.-H. (1973). Determination of bulk properties of tropical cloud clusters from large-scale heat and moisture budgets. *J. Atmos. Sci.*, 30:611–627.

Yano, J.-I. and Plant, R. S. (2012). Convective quasi-equilibrium. *Rev. Geophys.*, 50(4). RG4004.

Zängl, G., Reinert, D., Rípodas, P., and Baldauf, M. (2015). The ICON (ICOsahedral Non-hydrostatic) modelling framework of DWD and MPI-M: Description of the non-hydrostatic dynamical core. *Q. J. Roy. Meteor. Soc.*, 141:563–579.

Zhang, F., Odins, A. M., and Nielsen-Gammon, J. W. (2006). Mesoscale predictability of an extreme warm-season precipitation event. *Weather Forecast.*, 21:149–166.

Zhang, F., Snyder, C., and Rotunno, R. (2003). Effects of moist convection on mesoscale predictability. *J. Atmos. Sci.*, 60:1173–1185.

Zhang, G. J. and Mu, M. (2005). Simulation of the Madden–Julian oscillation in the NCAR CCM3 using a revised Zhang–McFarlane convection parameterization scheme. *J. Climate*, 18:4046–4064.

Zhang, G. J. and Song, X. L. (2009). Interaction of deep and shallow convection is key to Madden–Julian oscillation simulation. *Geophys. Res. Lett.*, 36(9). L09708.

Zhou, B., Simon, J. S., and Chow, F. K. (2014). The convective boundary layer in the terra incognita. *J. Atmos. Sci.*, 71:2545–2563.

Zhu, H. and Smith, R. K. (2002). The importance of three physical processes in a minimal three-dimensional tropical cyclone model. *J. Atmos. Sci.*, 59:1825–1840.

Zhu, P. and Bretherton, C. S. (2004). A simulation study of shallow moist convection and its impact on the atmospheric boundary layer. *Mon. Weather Rev.*, 132:2391–2409.

Acronyms

CA	Cellular Automaton
CAPE	Convective Available Potential Energy
CBL	Convective Boundary Layer
CMC	Conditional Markov Chain
CRM	Cloud Resolving Model
BOMEX	Barbados Oceanographic and Meteorological Experiment
DWD	Deutscher Wetterdienst (German Weather Service)
ECMWF	European Centre for Medium-Range Weather Forcasts
EDMF	Eddy-Diffusivity Mass-Flux
EDMF-DualM	Eddy-Diffusivity Mass-Flux - Dual-Mass-Flux
EPS	Ensemble Prediction System
GCM	Global Circulation Model
GCSS	Global Energy and Water Cycle Experiment Cloud System Study
GEWEX	Global Energy and Water Cycle Experiment
ICON	Icosahedral Nonhydrostatic General Circulation Model
ITCZ	Inter Tropical Convergence Zone
LCL	Lifting Condensation Level
LFC	Level of Free Convection
LES	Large-Eddy Simulation
MJO	Madden-Julian Oscillation
MPI-M	Max Planck Institute for Meteorology
NWP	Numerical Weather Prediction
PBL	Planetary Boundary Layer
PC-2008	Plant and Craig (2008)
PDF	Probability Density Function
RICO	Rain In Cumulus over the Ocean
RICO-GCSS	Rain In Cumulus over the Ocean - Global Energy and Water Cycle Experiment Cloud System Study
RICO-140	Rain In Cumulus over the Ocean - $N_c = 140$ cm^{-3}
RP	Random Parameters
SPPT	Stochastic Perturbed Parametrization Tendency
UCLA-LES	University of California Los Angeles - Large-Eddy Simulation

List of Figures

List of Tables

Acknowledgements

I wish to express my sincere thanks to my advisor Axel Seifert for such a great idea for my research project, and for his guidance and advice that enriched and supported my thesis research. I would also like to thank Valerio Lucarini for his support and encouragement from the beginning of my work on this thesis, and for taking the major role in the final stages of my dissertation. My gratitude goes as well to my co-advisors Bjorn Stevens and Cathy Hohenegger who greatly assisted and encouraged my research, and to the evaluation committee members Jörn Behrens and Gualtiero Badin who kindly accepted to take a part in the thesis evaluation.

I am extremely thankful to Thijs Heus, Anurag Dipankar and Martin Köhler for sharing their expertise and knowledge and for their help and support during the challenging phases of my research. I am also grateful to George C. Craig and Robert S. Plant first, for developing the framework of deep-convection parameterization that served as a starting point of my research, and second, for their encouraging and inspiring comments on the first phase of my research. For similar reasons, I'm thankful to Roel Neggers, for his advice about the EDMF parameterization, which was of great help to me during the model development.

A great Thanks! goes to my Herz research group on Clouds and Convection, for all the interesting and inspiring discussions during these years. Thank you Linda, Lorenzo, Cheska, Malte, Ritthik, Vera, Verena and Vivek! I take this opportunity to express gratitude to all of the IMPRS school staff for their help and guidance. Thank you Antje Weitz, Cornelia Kampmann, and Wiebke Böhm for making my PhD research an enjoyable experience. Thank you Christina Rieckers and Angela Gruber for countless number of occasions when I asked for your help with administrative issues.

And of course, my dear officemates Ann Kristin and Matthias, thank you for sharing the office and long chats with me during the working hours! My dear colleagues and friends Antonija, Chiel, Bart and Josiane, thank you for being so wonderful, especially during the writing period of my thesis. Thank you for proofreading and commenting on my writing. Also, thanks to Christopher Moseley for his constructive suggestions that improved my thesis text.

Finally, I would like to thank my dear family for the unlimited encouragement and support, and a special and great thanks goes to my husband Vladimir for his understanding and love during the past few years. His support and encouragement made this thesis possible.

I express my gratitude to all, who directly or indirectly influenced my research during the last four years.

Thank you!

List of publications:

Sakradzija, M., Seifert, A., and Heus, T.: Fluctuations in a quasi-stationary shallow cumulus cloud ensemble, Nonlin. Processes Geophys., 22, 65-85, doi:10.5194/npg-22-65-2015, 2015.

Sakradzija, M., Seifert, A.: An approach to parameterize shallow convection across scales, in preparation, 2015.

Eidesstattliche Versicherung
Declaration on Oath

Hiermit erkläre ich an Eides statt, dass ich die vorliegende Dissertationsschrift selbst verfasst und keine anderen als die angegebenen Quellen und Hilfsmittel benutzt habe.

I hereby declare, on oath, that I have written the present dissertation by myself and have not used other than the acknowledged resources and aids.

Hamburg, den May 12, 2015

_____

Mirjana Sakradžija

Hinweis / Reference

Die gesamten Veröffentlichungen in der Publikationsreihe des MPI-M
„Berichte zur Erdsystemforschung / Reports on Earth System Science“,
ISSN 1614-1199

sind über die Internetseiten des Max-Planck-Instituts für Meteorologie erhältlich:
http://www.mpimet.mpg.de/wissenschaft/publikationen.html

All the publications in the series of the MPI -M
„Berichte zur Erdsystemforschung / Reports on Earth System Science“,
ISSN 1614-1199

are available on the website of the Max Planck Institute for Meteorology:
http://www.mpimet.mpg.de/wissenschaft/publikationen.html